

# THÈSE POUR OBTENIR LE GRADE DE DOCTEUR DE L'UNIVERSITÉ DE MONTPELLIER

En informatique

École doctorale I2S

Unité de recherche LIRMM

## Génération procédurale d'environnements sous-marins

Présentée par Marc HARTLEY  
le [XX mois année]

Sous la direction de Christophe FIORIO, Noura FARAJ  
et Karen GODARY-DEJEAN

Devant le jury composé de

[Prénom NOM, Titre, Affiliation]  
[Prénom NOM, Titre, Affiliation]

[Statut jury]  
[Statut jury]





---

## Contents

---

<b>Table of Contents</b>	<b>vi</b>
<b>1 Introduction</b>	<b>1</b>
1.1 Prototype creation . . . . .	2
1.2 Contributions and outlines . . . . .	2
1.2.1 Semantics . . . . .	3
1.2.2 Modeling . . . . .	3
1.2.3 Amplification . . . . .	3
<b>2 State of the art</b>	<b>5</b>
2.1 Procedural generation . . . . .	6
2.1.1 Definition . . . . .	6
2.1.2 History . . . . .	7
2.1.3 Models represented . . . . .	8
2.1.4 User interaction . . . . .	9
2.2 Terrain representation . . . . .	12
2.2.1 2.5D terrains . . . . .	12
2.2.2 3D terrains . . . . .	13
2.2.3 Other models . . . . .	13
2.2.4 Underwater landscapes . . . . .	13
2.2.5 Fluid simulations . . . . .	15
2.3 Coral reefs (biological aspects) . . . . .	16
2.3.1 Historical Discovery of Coral Reefs . . . . .	16
2.3.2 Coral Reef Structure and Formation . . . . .	17
2.3.3 Importance in Biodiversity . . . . .	17
2.3.4 Threats to coral reefs . . . . .	18
2.3.5 Conservation efforts . . . . .	18
2.3.6 Future Research and Monitoring . . . . .	19
2.4 Implicit terrains with materials . . . . .	19
2.4.1 Material density . . . . .	19
2.4.2 Scalar functions . . . . .	19
2.4.3 Blending functions . . . . .	20
2.4.4 Placement functions . . . . .	20
2.4.5 Material usage . . . . .	20

<b>I Semantic Representation</b>	<b>21</b>
<b>3 Generation de terrain sémantique</b>	<b>25</b>
3.1 Introduction . . . . .	26
3.2 Related works . . . . .	27
3.3 Overview . . . . .	28
3.3.1 Environmental attributes . . . . .	29
3.3.2 Semantic Terrain Entity . . . . .	30
3.3.3 Environmental modifiers . . . . .	30
3.4 Placing Semantic Terrain Entities in an environment . . . . .	30
3.4.1 Fitness function . . . . .	31
3.4.2 Skeleton fitting function . . . . .	32
3.5 Life cycle of Semantic Terrain Entity . . . . .	32
3.5.1 Hard constraints vs. soft constraints . . . . .	33
3.6 Communication between Semantic Terrain Entity . . . . .	33
3.6.1 Problem of direct communication . . . . .	33
3.6.2 Natural process (or cellular automata) . . . . .	33
3.7 Environment stability . . . . .	33
3.7.1 Dynamic system vs. stable system . . . . .	33
3.7.2 Dying . . . . .	33
3.8 Environmental attributes and environmental modifiers . . . . .	33
3.8.1 Influence on water currents . . . . .	34
3.9 Physics simulation . . . . .	35
3.9.1 Heights of Semantic Terrain Entity . . . . .	35
3.9.2 Combining heights . . . . .	35
3.10 User interaction . . . . .	35
3.10.1 Direct interactions on the Semantic Terrain Entities . . . . .	35
3.10.2 Indirect interaction of Semantic Terrain Entities . . . . .	36
3.11 Results . . . . .	38
3.12 Conclusion . . . . .	40
<b>II Modelisation</b>	<b>43</b>
<b>4 Graphical representation of environmental objects</b>	<b>47</b>
<b>5 Automatic Generation of Coral Islands</b>	<b>49</b>
5.1 Introduction . . . . .	49
5.1.1 Multiple theories . . . . .	50
5.1.2 Darwinian theory . . . . .	52
5.1.3 Overview . . . . .	52
5.2 Related works . . . . .	52
5.3 Example generation . . . . .	53
5.3.1 Closed form of coral growth . . . . .	54
5.3.2 Labeling of the map . . . . .	54
5.3.3 Automation . . . . .	54
5.4 cGAN . . . . .	54
5.4.1 Definition of cGAN . . . . .	54
5.4.2 Why cGAN? . . . . .	55
5.4.3 Training . . . . .	55

5.4.4	Model usage . . . . .	55
<b>6</b>	<b>Generation of karst networks</b>	<b>57</b>
6.1	Introduction . . . . .	57
6.2	Related works . . . . .	59
6.3	Space colonization . . . . .	59
6.4	Our method . . . . .	59
6.5	Modeling . . . . .	60
6.6	User Control . . . . .	60
6.7	Results . . . . .	60
6.8	Conclusion . . . . .	60
<b>III</b>	<b>Erosion Simulation</b>	<b>61</b>
<b>7</b>	<b>Érosion par particules</b>	<b>65</b>
7.1	Introduction . . . . .	66
7.2	State of the art . . . . .	67
7.2.1	Terrain Representations . . . . .	67
7.2.2	Erosion Processes . . . . .	68
7.3	Particle erosion . . . . .	68
7.3.1	Overview . . . . .	69
7.3.2	Erosion process . . . . .	69
7.3.3	Transport . . . . .	70
7.4	Our erosion method . . . . .	72
7.4.1	Application on height fields . . . . .	73
7.4.2	Application on layered terrains . . . . .	73
7.4.3	Application on implicit terrains . . . . .	74
7.4.4	Application on voxel grids . . . . .	75
7.5	Results . . . . .	76
7.6	Comparisons . . . . .	79
7.7	Discussion . . . . .	81
7.8	Conclusion . . . . .	82
<b>IV</b>		<b>85</b>
<b>Conclusion</b>		<b>87</b>
<b>References</b>		<b>87</b>
<b>Glossary</b>		<b>95</b>
<b>Acronyms</b>		<b>97</b>
<b>Appendices</b>		<b>99</b>
<b>Data structures</b>		<b>101</b>
.1	3D grids . . . . .	101

<b>Geometry</b>	<b>103</b>
.2 Points . . . . .	103
.3 Curves . . . . .	103
<b>Snake - Modèle de contour actif</b>	<b>105</b>
<b>Computation of a metaball</b>	<b>107</b>

## Abstract

This thesis, entitled "*Procedural terrain generation for underwater environments*", focuses on the topic of procedural terrain generation in underwater environments. Terrain generation is still an open research area in computer graphics because, with the emergence of simulation, rendering, and interaction techniques, the entire field is experiencing increased collaboration with terrain experts. Bringing the physical world into a computer and allowing users to see and manipulate this virtual world helps to better understand it and to bring together numerous experts, gradually breaking down the boundaries of scientific disciplines. Terrain science brings together, in almost a direct manner, geologists, oceanologists, physicists, meteorologists, biologists, roboticists, computer scientists, artists, and more. We focused our work on the inclusion of the user in the generation process through fast and controllable algorithms.

This thesis is divided into three parts, guiding the user from the design of a landscape to its finalization, step by step. Firstly, we will propose a formalization of terrain designing, allowing for the conception of environments in a semantic sense, abstracting away from geometry and data structures.

Secondly, we will see how to give 3D form to these environments. We will propose new algorithms for the generation and modeling of coral islands and karst networks.

In the third part, we will focus on adding realism to 3D terrains through physical simulations of erosion processes. We will demonstrate a flexible and controllable method to imitate the long-term effects of water and wind on both terrestrial and marine landscapes.

**Keywords:** terrain representation, procedural generation, physical simulations, user interaction

## Résumé



# CHAPTER 1

---

## Introduction

---

- ...

- Active domain for the last 50 years
- Computer graphics more and more prominent
- Need to be always faster, realistic, automatic
- Terrain generation affected the same way
- Our focus on one branch: the landscape
- Useful domain for:
  - \*\* Biology
  - \*\* Geology
  - \*\* Robotics
  - \*\* But also entertaining industries
    - \*\*\* Video games
    - \*\*\* Cinema
  - Because helps understanding rules and observing hypotheses
  - Novelty is the underwater aspect
  - Useful for:
    - \*\* Marine biology
    - \*\* Oceanology
    - \*\* Underwater robotics
    - \*\* And by extension, new fields of entertaining industries:
      - \*\*\* Video games
      - \*\*\* Cinema
    - Big challenges:
      - \*\* Balance between automation and user desires
      - \*\* Isolation of variables
      - \*\* Scaling
    - 3 main ways to generate worlds:
      - \*\* Simulations
      - \*\* User interaction/modeling
      - \*\* Procedural modeling
      - \*\*\* This one is tricky, maybe "automatic generation"
      - \*\*\* I mean: "Content creation using functions, independent of the user actions" (eg. using

Perlin noise for a terrain, random noise for a rock modeling, specific texture generation, etc...)

- Main question:

\*\* "How to efficiently guide the user in the creation of virtual content along the production process line to keep as much control on the final product?"

\*\*\* "Guiding" as opposed to "replace": I believe no machine can know better than a human what he wants

\*\*\* "Production process line": we are presenting algorithms that can be used in a pipeline

\*\*\*\* We want each component of the thesis to be as flexible as possible to the user workspace:

\*\*\*\*\* Any terrain representation

\*\*\*\*\* Any fluid solver

\*\*\*\*\* Any landscape type

\*\*\*\*\* Any hardware

\*\*\*\*\* Any objective (real-time rendering, realistic, animated, etc...)

\*\*\* "As much control": \*\*\*\* Each result should feel unique

\*\*\*\* Each result should be expected by the user

\*\*\*\* Each result should be explainable

\*\*\*\* Each result should be correctible(?) -> without having to restart everything

- ...

## 1.1 Prototype creation

- C++23 and Qt5.12

- OpenGL 4.6 and GLSL

- Marching Cubes on geometry shader

- \*\* Bad idea, but justify why

- Renderings:

- \*\* With the prototype:

- \*\*\* Marching Cubes on geometry shader

- \*\*\* Triplanar texture

- \*\*\* Real-time results

- \*\*\* Textures based on materials

- \*\* With Unreal Engine 5:

- \*\*\* Static meshes

- \*\*\* Added procedural vegetation with plugin [PLUGIN NAME] and ocean with [PLUGIN NAME]

- \*\* With Blender 4.1:

- \*\*\* Static meshes

- \*\*\* Easier script usage

- ...

## 1.2 Contributions and outlines

- Chronological order of terrain generation

- Proposes an abstract representation halfway between computing and terrain expertise

- \*\* Offering a generalization of the desired landscape type (underwater, but also terrestrial)

- Proposes new types of landscapes (karsts and coral islands)

- \*\* Maintaining the notion of sparseness (implicit volumes)

- Proposes a particle-based erosion simulation method

- \*\* Terrain representation agnostic

- \*\* Lightweight, fast, easy to implement
- Aims to keep maximum control for the user
- \*\* In the generation process, but also to correct details upstream

### 1.2.1 Semantics

- Work oriented towards underwater generation
- Collaboration with a marine biologist
- ...

### 1.2.2 Modeling

- Generation of some landscape elements still new (karsts referring to Axel Paris, but coral islands new)
- Karst networks represented in a highly user-friendly manner
- \*\* Viewing karsts as a directed acyclic graph => close to tree structure
- \*\* Enhanced method for fractal generation with cycles (generation in multiple iterations)
- Coral islands using an interpretation of Darwin's theory
- \*\* Based on observations
- \*\* Based on travel journals
- ...

### 1.2.3 Amplification

- Increasing realism by adding details
- Particle-based erosion method
- \*\* Generalization for flexibility
- \*\* Speed, parallelization
- Towards a continuous erosion method.
- ...



# CHAPTER 2

---

## State of the art

---

### Contents

2.1	Procedural generation . . . . .	6
2.1.1	Definition . . . . .	6
2.1.2	History . . . . .	7
2.1.3	Models represented . . . . .	8
2.1.4	User interaction . . . . .	9
2.2	Terrain representation . . . . .	12
2.2.1	2.5D terrains . . . . .	12
2.2.2	3D terrains . . . . .	13
2.2.3	Other models . . . . .	13
2.2.4	Underwater landscapes . . . . .	13
2.2.5	Fluid simulations . . . . .	15
2.3	Coral reefs (biological aspects) . . . . .	16
2.3.1	Historical Discovery of Coral Reefs . . . . .	16
2.3.2	Coral Reef Structure and Formation . . . . .	17
2.3.3	Importance in Biodiversity . . . . .	17
2.3.4	Threats to coral reefs . . . . .	18
2.3.5	Conservation efforts . . . . .	18
2.3.6	Future Research and Monitoring . . . . .	19
2.4	Implicit terrains with materials . . . . .	19
2.4.1	Material density . . . . .	19
2.4.2	Scalar functions . . . . .	19
2.4.3	Blending functions . . . . .	20
2.4.4	Placement functions . . . . .	20
2.4.5	Material usage . . . . .	20

**Back to summary**

- ...

## 2.1 Procedural generation

- ...

### 2.1.1 Definition

- Algorithmic Content Creation: Procedural generation refers to the process of creating data algorithmically rather than manually. This technique is widely used in fields such as computer graphics, simulations, and game development.
- Generative Models: Utilizes predefined rules or algorithms to generate complex structures or systems. Examples include generating landscapes, textures, or entire worlds.
- Data Independence: The generated content is not explicitly stored but created in real-time or on-the-fly, allowing for more extensive and dynamic content creation.
- Applications: Commonly applied in video games for creating vast, varied, and detailed environments without requiring large amounts of storage space.
- Automated Data Creation: Procedural generation is a technique used to automatically create complex and diverse content through algorithmic processes. This involves defining a set of rules or procedures that can produce varied outputs.
- Dynamic and Flexible: Allows for the generation of content that can adapt and change in response to different inputs or conditions, making it highly suitable for applications requiring variability and adaptability.
- Integration of Algorithms and Data: Combines mathematical models, noise functions, and other algorithms to create realistic or abstract content. This can include generating landscapes, textures, or entire ecosystems.
- Real-World Relevance: Involves incorporating aspects of real-world phenomena or simulations (e.g., erosion patterns in terrain generation) to produce more believable and interactive environments.
- User-Driven Customization: Provides mechanisms for users to influence or guide the content generation process, allowing for customized or user-specific outcomes.
- Scalability and Efficiency: Offers scalability in content generation by producing large amounts of data with relatively low computational and storage costs compared to manually crafted content.
- Deterministic vs. Stochastic:
  - \*\* Deterministic: The output is predictable and repeatable given the same input parameters.
  - \*\* Stochastic: Incorporates randomness, leading to varied outputs even with the same initial conditions.
- Rule-Based Systems: Utilizes predefined rules or systems to generate content, allowing for controlled and structured outputs.
- Iteration and Refinement: Often involves iterative processes where initial results are refined or adjusted based on additional rules or parameters.
- Advantages
  - \*\* Efficiency: Reduces the need for extensive manual creation, saving time and resources.
  - \*\* Variability: Capable of generating a wide range of unique outputs from the same set of rules.
  - \*\* Adaptability: Can easily adapt to changes in requirements or user input, allowing for dynamic content creation.
  - \*\* Storage: Minimizes storage needs by generating content on-the-fly rather than storing large datasets.
- Challenges
  - \*\* Complexity: Developing and fine-tuning procedural generation algorithms can be complex

and require careful balancing of parameters.

\*\* Realism vs. Performance: Achieving a balance between realistic content and computational performance can be challenging.

\*\* User Expectations: Meeting user expectations for content quality and variety can be difficult, especially in interactive applications.

## 2.1.2 History

### - Early Developments

\*\* Mathematical Foundations:

\*\*\* Algorithmic Foundations: Early uses of procedural generation can be traced back to mathematical and algorithmic theories in the mid-20th century. Key concepts included randomness and noise functions.

\*\*\* Noise Functions: The introduction of noise functions, such as Perlin noise (1983), provided a method for generating smooth, natural-looking randomness in computer graphics.

\*\* Early Computer Graphics:

\*\*\* Simplex Noise: Developed by Ken Perlin in 1985, Simplex noise was a significant advancement, providing a more computationally efficient and visually pleasing alternative to Perlin noise.

\*\*\* Fractals: In the 1980s, fractal geometry was introduced as a method for generating self-similar structures, influencing terrain generation and procedural modeling.

### - Video Games and Interactive Media

\*\* Early Video Games:

\*\*\* Space Invaders (1978): The concept of procedural generation was used to create varied enemy formations and gameplay experiences.

\*\*\* Rogue (1980): The early example of procedural generation in game level design, with randomly generated dungeons and item placement.

\*\* Procedural Content Generation (PCG):

\*\*\* Dwarf Fortress (2006): A significant milestone in procedural generation for games, known for its deep and complex world generation that includes civilizations, histories, and intricate ecosystems.

\*\*\* Minecraft (2011): Revolutionized procedural generation in gaming by generating vast, open worlds with diverse biomes and features.

### - Applications in Simulation and Graphics

\*\* Scientific Simulations:

\*\*\* Terrain Generation: Used in geological simulations and virtual landscapes for scientific research and training.

\*\*\* Fluid Dynamics: Procedural methods were applied to simulate realistic fluid behavior in various scientific and engineering contexts.

\*\* Computer Graphics and Animation:

\*\*\* Film and Visual Effects: Procedural generation techniques have been used in films for creating complex visual effects, landscapes, and textures that would be time-consuming to model manually.

\*\*\* Real-Time Rendering: The advent of real-time graphics and game engines (e.g., Unreal Engine, Unity) leveraged procedural generation for dynamic content creation and environmental diversity.

### - Technological Advancements

\*\* Algorithmic Improvements:

\*\*\* Advanced Noise Functions: Developments in noise functions, such as Worley noise and new variations of Perlin noise, improved the quality and efficiency of procedural generation.

\*\*\* Machine Learning and AI: Recent advances in machine learning and artificial intelligence are being integrated with procedural generation to create more complex and adaptive content.

\*\* Computing Power:

\*\*\* Increased Processing Power: As computing power has increased, so has the capability to generate more complex and detailed procedural content in real time.

\*\*\* Parallel Computing: Use of parallel processing and GPUs to accelerate procedural generation processes, enabling real-time applications and high-resolution simulations.

- Current Trends and Future Directions

\*\* Hybrid Approaches: Combining procedural generation with manual design to achieve a balance between complexity and artistic control.

\*\* User-Driven Content: Integration of user input and customization options to allow players or users to influence procedural content generation.

\*\* Advanced Simulations: Use of procedural generation in advanced simulations for training, virtual reality, and scientific research, including climate modeling and urban planning.

### 2.1.3 Models represented

Noise: Techniques like Perlin noise and Simplex noise for creating natural variations.

Cellular Automata: Models like Conway's Game of Life for generating patterns and structures.

Neural Networks: Use of deep learning to generate and refine procedural content.

Physical Phenomena Modeling: Simulating natural processes like erosion and sedimentation for realistic terrain features.

- Noise

\*\* Perlin Noise:

\*\*\* Overview: Developed by Ken Perlin in 1983, Perlin noise is a gradient noise function used to generate smooth, coherent patterns that resemble natural phenomena.

\*\*\* Applications: Commonly used in texture generation, terrain modeling, and procedural landscapes to create realistic, natural-looking variations.

\*\*\* Characteristics: Provides continuous and smooth randomness, making it ideal for creating natural-looking terrains and textures.

\*\* Simplex Noise:

\*\*\* Overview: Introduced by Ken Perlin in 2001 as an improvement over Perlin noise. It is more computationally efficient and produces fewer directional artifacts.

\*\*\* Applications: Used in procedural texture generation, terrain creation, and simulations where higher performance and quality are needed.

\*\*\* Characteristics: Offers a higher degree of visual coherence and efficiency in high-dimensional space compared to Perlin noise.

\*\* Worley Noise:

\*\*\* Overview: Also known as Voronoi noise, Worley noise generates patterns based on the distance between points in a space, producing cellular structures.

\*\*\* Applications: Suitable for creating textures such as stone or marble, and for modeling natural phenomena like cloud patterns and cellular structures.

\*\*\* Characteristics: Produces a pattern of cells with distinct boundaries, useful for generating irregular, organic textures.

- Cellular Automata

\*\* Basic Concepts:

\*\*\* Definition: Cellular automata are discrete, grid-based models where each cell evolves based on a set of rules applied to its neighbors.

\*\*\* History: Originating in the 1940s with John von Neumann and Stanislaw Ulam, cellular

automata have been used to model complex systems and processes.

**\*\* Applications in Procedural Generation:**

\*\*\* Terrain Generation: Used to simulate natural processes like erosion, sediment deposition, and landform evolution. Examples include generating cave systems and cave-like features.

\*\*\* Pattern Formation: Employed to create various patterns and textures, such as forests, vegetation, and city layouts.

**\*\* Notable Models:**

\*\*\* Game of Life: A famous example of cellular automata, used to demonstrate how simple rules can lead to complex, self-organizing patterns.

\*\*\* Langton's Ant: A simpler automaton that produces interesting and complex behavior from basic rules, demonstrating the potential of cellular automata for generating diverse patterns.

- Neural Networks

**\*\* Overview:**

\*\*\* Artificial Neural Networks (ANNs): Computational models inspired by the human brain, used to learn patterns and generate data.

\*\*\* Generative Models: Types of neural networks, such as Generative Adversarial Networks (GANs) and Variational Autoencoders (VAEs), are specifically designed for content generation.

**\*\* Applications:**

\*\*\* Texture and Terrain Generation: Neural networks can be trained to generate realistic textures and terrains based on training data, producing highly detailed and varied results.

\*\*\* Image Synthesis: Used to generate photorealistic images, including landscapes, environments, and even character models in video games and simulations.

**\*\* Key Techniques:**

\*\*\* GANs (Generative Adversarial Networks): Consist of two neural networks, a generator and a discriminator, that work against each other to create realistic outputs.

\*\*\* VAEs (Variational Autoencoders): Learn to encode and decode data in a way that allows for the generation of new, similar data instances.

- Physical Phenomena Modeling

**\*\* Overview:**

\*\*\* Definition: Models that simulate real-world physical processes to generate natural features and behaviors in procedural content.

\*\*\* Types: Includes models for fluid dynamics, erosion, sediment transport, and other geological and environmental processes.

**\*\* Applications:**

\*\*\* Terrain Generation: Simulating erosion, sediment deposition, and other geological processes to create realistic terrain features such as mountains, valleys, and riverbeds.

\*\*\* Environmental Simulations: Used in simulations for weather patterns, climate modeling, and natural disaster scenarios.

**\*\* Key Models:**

\*\*\* Erosion Models: Simulate the effects of weathering and erosion on terrain, often using algorithms that mimic natural processes like water flow and wind.

\*\*\* Sediment Transport: Models that simulate the movement and deposition of sediment, contributing to realistic terrain formation and changes.

## 2.1.4 User interaction

### Realism-Speed-Control Balance

Realism: Achieving accurate representation of real-world features, useful in simulations

and visualizations.

**Speed:** Real-time generation needs, classified by J. Gain's metrics (real-time, interactive, near-interactive, long-term).

**Control:** Meeting user demands and customization, addressing the challenge of "impossible" requests.

- Realism:

\*\* Definition: The degree to which generated content mimics real-world characteristics, including visual accuracy, physical processes, and natural patterns.

\*\* Applications: Critical in scenarios where realistic simulations are required, such as natural disaster simulations, scientific visualizations, and training environments.

\*\* Techniques:

\*\*\* Physical Simulations: Implementing realistic physical processes (e.g., erosion, sediment transport) to enhance authenticity.

\*\*\* Expert Knowledge: Integrating domain-specific expertise (e.g., geology, ecology) to ensure accuracy in generated content.

\*\* Challenges:

\*\*\* Complexity: Balancing detail and realism can lead to complex simulations requiring substantial computational resources.

\*\*\* Expertise: Ensuring realism may necessitate expert input, which can be resource-intensive.

- Speed:

\*\* Definition: The efficiency of generating content within acceptable time constraints, categorized into different levels based on response time.

\*\* Categories:

\*\*\* Real-Time: Generation occurring in less than 30 milliseconds, essential for interactive applications and gaming (e.g., procedural environments in VR).

\*\*\* Interactive: Generation in less than 3 seconds, suitable for user-driven customization in games and simulations.

\*\*\* Near-Interactive: Generation in less than 5 minutes, applicable for applications where some delay is acceptable (e.g., large-scale simulations).

\*\*\* Long-Term: Generation that takes longer, often used for precomputed content or less time-sensitive applications (e.g., offline rendering).

\*\* Techniques:

\*\*\* Optimization: Using efficient algorithms and parallel processing to speed up generation processes.

\*\*\* Level of Detail (LOD): Adjusting detail based on the user's distance or focus to balance performance and visual quality.

- Control:

\*\* Definition: The extent to which users can influence or direct the procedural generation process to meet their specific needs or preferences.

\*\* Applications:

\*\*\* Customization: Allowing users to modify parameters or settings to tailor generated content to their preferences (e.g., terrain features, game worlds).

\*\*\* Artistic Control: Providing tools for artists and designers to guide the procedural generation process and integrate artistic elements.

\*\* Challenges:

\*\*\* User Demands: Addressing the challenge of fulfilling diverse and sometimes contradictory user expectations.

\*\*\* Complexity: Balancing user control with the complexity of procedural systems to avoid overwhelming users or producing unrealistic results.

## Interaction Mechanisms

### - Parameter Adjustment:

\*\* Sliders and Controls: User interfaces that allow adjustment of parameters such as terrain height, texture type, or weather conditions.

\*\* Real-Time Feedback: Immediate visual or functional feedback based on user input, enhancing the interactive experience.

### - Guided Creation:

\*\* Templates and Presets: Offering predefined templates or presets that users can modify to fit their needs while ensuring a coherent base for the generated content.

\*\* Assistive Tools: Providing tools or wizards that guide users through the generation process, helping them understand and control the outcome.

### - Direct Manipulation:

\*\* Interactive Tools: Tools that allow users to directly manipulate the generated content, such as sculpting terrain or painting textures.

\*\* Live Updates: Changes made by the user are reflected in real-time, enabling immediate validation and adjustment.

## Challenges and Considerations

- Balancing Complexity and Usability: Ensuring that complex procedural generation systems remain user-friendly and accessible, even when offering deep customization options.

- Performance Impact: Managing the performance implications of user interactions, especially in real-time applications where frequent updates are needed.

- Feedback and Iteration: Providing adequate feedback to users to help them understand the impact of their interactions and iterate on their designs effectively.

## Regeneration

### - Manual Actions: How users can influence or direct the regeneration process.

### - Issues with Regeneration:

\*\* What to regenerate: Criteria for selecting parts of the terrain to refresh.

\*\* How to regenerate: Techniques and algorithms used for regeneration.

- Problems with User Interactions: Handling user inputs and maintaining consistency.

- Action Storage: Possible use of formats like JSON to store and manage regeneration actions.

### - Manual Actions

\*\* User-Initiated Regeneration:

\*\*\* Triggering Regeneration: Users can manually trigger regeneration processes, such as refreshing a terrain or updating a landscape to reflect new parameters or conditions.

\*\*\* Interface Controls: Tools and options within user interfaces that allow users to initiate regeneration, such as buttons or commands for reloading or updating generated content.

\*\* Customizable Parameters:

\*\*\* Adjustment of Variables: Users can adjust parameters or settings before triggering regeneration to influence the outcome. This includes changing terrain features, texture types, or simulation conditions.

\*\*\* Preview and Validation: Offering preview modes or validation checks to help users understand potential outcomes before finalizing regeneration.

### - Issues with Regeneration

\*\* What to Regenerate:

\*\*\* Selective Regeneration: Deciding whether to regenerate the entire model or specific parts. For example, only regenerating terrain features while keeping other elements intact.

\*\*\* Scope and Scale: Determining the extent of regeneration, whether it involves minor updates or complete overhauls of generated content.

\*\* How to Regenerate:

\*\*\* Algorithmic Approaches: Different methods for regenerating content, such as reapplying algorithms or using new procedural rules to alter or update the existing content.

\*\*\* Incremental vs. Complete Regeneration:

\*\*\* Incremental: Applying changes gradually or updating only parts of the generated content to minimize disruption.

\*\*\* Complete: Full regeneration from scratch, which may be necessary for substantial changes or when previous results are no longer valid.

- Problems with User Interactions:

\*\* Consistency: Ensuring that regeneration maintains or improves the consistency and quality of generated content, avoiding artifacts or inconsistencies.

\*\* Feedback Handling: Managing user feedback and requests for regeneration, which can vary in scope and detail.

\*\* Performance: Addressing the impact on performance and resource usage when regenerating content, especially in real-time or interactive applications.

- Action Storage

\*\* Storage Formats:

\*\*\* JSON: Using JSON (JavaScript Object Notation) files to store regeneration actions and parameters. JSON provides a flexible, readable format for saving and retrieving procedural settings.

\*\*\* Other Formats: Potential use of alternative formats such as XML, binary files, or custom formats tailored to specific needs or systems.

\*\* Tracking Changes:

\*\*\* Action History: Maintaining a history of user actions and regeneration events, allowing users to revert to previous states or track changes over time.

\*\*\* Versioning: Implementing version control for procedural generation settings, ensuring that different versions of generated content can be managed and compared.

\*\* Restoration and Undo:

\*\*\* Undo Mechanisms: Providing options for users to undo recent regeneration actions or revert to previous states, enhancing flexibility and user control.

\*\*\* Restoration of Defaults: Allowing users to restore default settings or regeneration conditions if custom changes lead to unsatisfactory results.

- Implementation Considerations

\*\* Efficiency: Designing algorithms and systems to handle regeneration efficiently, minimizing computational overhead and ensuring responsive updates.

\*\* User Experience: Creating intuitive interfaces and feedback mechanisms to facilitate smooth user interactions with regeneration processes.

\*\* Error Handling: Implementing robust error handling and recovery mechanisms to address issues that may arise during regeneration, such as unexpected results or system failures.

## 2.2 Terrain representation

- ...

### 2.2.1 2.5D terrains

- ...

## Height maps

- ...

## Height functions

- ...

### 2.2.2 3D terrains

- Need for 3D concepts

\*\* Geological information

\*\* Volumetric data

- ...

## Main issues

- Memory

- Visualization

- Modifications

- Conversion between representations

\*\* Information loss

\*\*\* Error propagation on geometry (approximations on normals, Z resolution, surface, etc.)

\*\*\* Loss of subsurface information

- ...

## Types, definitions, advantages, disadvantages

- Voxel grids

- Material stacks

- Meshes

- Implicit surfaces

- Implicit materials

- ...

### 2.2.3 Other models

- Concept of semantics

- ...

### 2.2.4 Underwater landscapes

- 3D Data:

\*\* Coral Landscapes: Addressing challenges in modeling coral reefs and underwater features.

\*\* Cavities: Representing underwater caves and karst formations.

- Interdisciplinary Data:

\*\* Geological Validation: Integrating expert knowledge for accurate modeling.

\*\* Challenges: Fewer experts and more uncertainties in underwater environments.

\*\* Data Scarcity: Limited data availability for detailed underwater landscapes.

- Need for Multi-Scale:

\*\* Integration of large and small elements.

\*\* Level of Detail (LOD): Techniques for managing detail across different scales.

## 3D Data

- Coral Landscapes:

\*\* Complex Structures: Coral reefs feature complex 3D structures with intricate patterns including branching corals, coral mounds, and encrusting forms. These structures often have a high degree of variability and detail.

\*\* Void Spaces: Coral reefs contain many voids and cavities such as caves, grottos, and karst networks, adding to the complexity of modeling these environments.

\*\* Challenges: Modeling coral reefs requires accurately representing the porous and irregular nature of coral formations, which can be challenging due to the high level of detail and variability.

#### - Geological Features:

\*\* Sedimentary Layers: Representing sedimentary layers and underwater geological formations such as seamounts and underwater ridges.

\*\* Volcanic Activity: Incorporating features such as underwater volcanoes and hydrothermal vents, which affect the landscape and ecosystem.

#### - Measurement and Data Collection:

\*\* Sonar and LIDAR: Using sonar (e.g., multi-beam echo sounders) and LIDAR (Light Detection and Ranging) to collect detailed 3D data of underwater terrain.

\*\* Remote Sensing: Utilizing remote sensing technologies to map and model underwater landscapes, especially in areas that are difficult to access.

### Interdisciplinary Data

#### - Geological Validation:

\*\* Expert Consultation: Collaborating with geologists and marine scientists to validate and refine models based on real-world observations and data.

\*\* Data Accuracy: Ensuring that the generated models accurately reflect real underwater geological and biological features.

#### - Biological Data:

\*\* Coral and Marine Life: Integrating data on coral species, marine biodiversity, and ecosystem dynamics to create realistic and biologically accurate representations.

\*\* Ecological Impact: Considering the impact of various biological factors on the terrain, such as coral growth patterns and marine erosion.

#### - Challenges:

\*\* Data Scarcity: Limited availability of high-resolution data for some underwater environments, especially in less studied or remote areas.

\*\* Integration: Combining geological, biological, and hydrological data effectively to create comprehensive and accurate models.

### Multi-Scale Modeling

#### - Large vs. Small Scale Elements:

\*\* Macro Features: Incorporating large-scale features such as underwater mountains, ridges, and large coral formations.

\*\* Micro Features: Modeling small-scale elements such as individual coral polyps, marine vegetation, and detailed sedimentary textures.

#### - Level of Detail (LOD):

\*\* Adaptive LOD: Using techniques to adjust the level of detail based on user interaction or view distance to balance performance and visual fidelity.

\*\* Detail Preservation: Ensuring that both macro and micro-scale features are accurately represented without losing important details during scaling or zooming.

#### - Visualization Techniques:

\*\* Hydrographic Mapping: Employing specialized visualization techniques to represent underwater features clearly and accurately.

\*\* Texture and Lighting: Using textures and lighting models that simulate underwater conditions, such as light absorption and scattering in water.

### 2.2.5 Fluid simulations

- ...

#### Introduction to Fluid Simulations

- Definition and Purpose:

\*\* Overview: Explanation of fluid simulations and their role in representing natural phenomena in terrains, including water flow, erosion, and sediment transport.

\*\* Importance: Impact of accurate fluid simulations on creating realistic terrain and environmental models.

#### Types of Fluid Simulations

- 2D Fluid Simulations:

\*\* Particle-In-Cell (PIC):

\*\*\* Concept: Combines particles with a grid to simulate fluid dynamics.

\*\*\* Applications: Used for simpler simulations and visualizations.

\*\* Fluid-Implicit Particle (FLIP):

\*\*\* Concept: A hybrid method that combines particle and grid approaches for better accuracy and efficiency.

\*\*\* Applications: Suitable for capturing complex fluid behaviors in 2D environments.

\*\* Stable Fluids:

\*\*\* Concept: A grid-based method for simulating stable, incompressible fluids with less computational complexity.

\*\*\* Applications: Often used in interactive applications where real-time performance is crucial.

- 3D Fluid Simulations:

\*\* Smoothed Particle Hydrodynamics (SPH):

\*\*\* Concept: A particle-based method where fluid properties are represented by particles that interact based on smoothing kernels.

\*\*\* Applications: Useful for highly detailed simulations of fluids, including interactions with terrain.

\*\* Grid-Based Methods:

\*\*\* Concept: Methods like Marker-And-Cell (MAC) and Navier-Stokes equations applied on a grid to simulate fluid behavior.

\*\*\* Applications: Used for detailed and accurate 3D simulations, including large-scale environments.

\*\* Hybrid Methods:

\*\*\* Concept: Combining grid and particle approaches to leverage the strengths of both methods.

\*\*\* Applications: Balancing detail and performance in complex simulations.

#### Applications in Terrain Representation

- Erosion and Sediment Transport:

\*\* Simulation of Erosion: How fluid simulations model erosion processes affecting terrain features such as riverbeds and coastlines.

\*\* Sediment Movement: Modeling the transport and deposition of sediment, contributing to realistic terrain evolution.

- Water Flow and Hydrology:

\*\* Surface Water Dynamics: Representing the flow of water across terrain surfaces, including rivers, lakes, and wetlands.

\*\* Subsurface Flow: Simulating groundwater movement and interactions with terrain features.

- Interactive Environments:

\*\* Real-Time Simulations: Implementing fluid simulations in interactive applications, such as video games and virtual environments, where dynamic water interactions are crucial.

### Challenges and Considerations

- Computational Resources:

\*\* Performance Trade-Offs: Balancing simulation accuracy with computational efficiency, especially for real-time applications.

\*\* Hardware Requirements: The need for powerful processors and memory to handle complex 3D fluid simulations.

- Accuracy vs. Realism:

\*\* Detail vs. Performance: Finding the right balance between detailed fluid dynamics and the practical limitations of simulation resources.

\*\* Simulation Artifacts: Addressing potential artifacts or inaccuracies in simulations that can impact realism.

- Integration with Terrain Models:

\*\* Interaction with Terrain: Ensuring fluid simulations integrate seamlessly with terrain models, including handling interactions such as fluid erosion or deposition.

\*\* Data Consistency: Maintaining consistency between simulated fluid behaviors and terrain features for accurate representations.

### Recent Developments and Future Trends

- Advancements in Algorithms:

\*\* New Techniques: Emerging algorithms and methods that enhance the accuracy and efficiency of fluid simulations.

\*\* Real-Time Improvements: Innovations aimed at improving real-time performance and interactivity in fluid simulations.

- Integration with AI and Machine Learning:

\*\* AI-Enhanced Simulations: Using machine learning to improve fluid simulation accuracy and adaptivity.

\*\* Predictive Models: Leveraging AI to predict and simulate complex fluid behaviors based on historical data.

## 2.3 Coral reefs (biological aspects)

- Historical Discovery: Evolution of knowledge about coral reefs.

- Types of Coral Reefs:

\*\* Islands, Barriers, Atolls: Different forms and structures of coral reefs.

- Atoll Theories: Historical and scientific theories explaining the formation of atolls.

- Importance in Biodiversity: Coral reefs as critical ecosystems with high marine biodiversity.

- Threats and Protection: Current threats to coral reefs and conservation efforts.

### 2.3.1 Historical Discovery of Coral Reefs

- ...

#### Early Observations

- Ancient Knowledge: Initial observations by ancient civilizations (e.g., Greeks, Romans) and their interpretations of coral structures.

- Exploration Era: The role of early explorers and naturalists (e.g., Captain James Cook, Alexander von Humboldt) in documenting coral reefs and their biodiversity.

## Scientific Discovery

- 19th Century Advances: Key contributions from scientists such as Charles Darwin, who developed theories on coral reef formation.
- 20th Century Developments: Advances in marine biology and oceanography that improved understanding of coral reef ecosystems.

### 2.3.2 Coral Reef Structure and Formation

- ...

#### Coral Anatomy

- Coral Polyps: Basic building blocks of coral reefs, their structure, and function. Each polyp is a tiny, soft-bodied organism that secretes calcium carbonate to form the reef structure.
- Coral Colonies: How individual polyps form colonies and contribute to the growth of the reef structure.

#### Types of Coral Reefs

- Fringing Reefs:

\*\* Definition: Reefs that are directly attached to a coastline, extending out from the shore.

\*\* Characteristics: Shallow waters, often with a narrow reef crest and slope.

- Barrier Reefs:

\*\* Definition: Reefs that run parallel to the coastline but are separated by a lagoon or deep channel.

\*\* Characteristics: Typically found farther from the shore, with a more pronounced lagoon and deeper water.

- Atolls:

\*\* Definition: Circular or oval reefs that encircle a lagoon, often formed around a submerged volcanic island.

\*\* Characteristics: Reefs form a ring around a central lagoon, with no land in the center.

#### Reef Building Processes

- Calcium Carbonate Deposition: The process by which corals and other organisms secrete calcium carbonate to build the reef structure.

- Bioerosion: The natural process by which reef structures are eroded by marine organisms such as parrotfish and sea urchins.

### 2.3.3 Importance in Biodiversity

- ...

#### Species Diversity

- Marine Life: Coral reefs are among the most diverse ecosystems in the world, supporting thousands of marine species including fish, invertebrates, and algae.

- Endemism: Many species are found exclusively in coral reef environments, contributing to global biodiversity.

#### Ecosystem Services

- Habitat Provision: Coral reefs provide essential habitats for a wide range of marine species, including commercially important fish and invertebrates.

- Nutrient Cycling: Reefs play a critical role in nutrient cycling, supporting the productivity of marine ecosystems.

## Economic and Cultural Value

- Fishing and Tourism: Coral reefs support important fisheries and generate significant revenue through tourism and recreational activities.
- Cultural Significance: Many coastal communities have cultural and spiritual connections to coral reefs, incorporating them into traditions and practices.

### 2.3.4 Threats to coral reefs

- ...

#### Climate Change

- Coral Bleaching: Caused by elevated sea temperatures, leading to the expulsion of symbiotic algae (zooxanthellae) and subsequent coral bleaching.
- Ocean Acidification: Reduced calcification rates due to increased CO<sub>2</sub> levels, impacting coral growth and reef structure.

#### Pollution

- Nutrient Runoff: Increased nutrient levels from agricultural and urban runoff can lead to algal blooms that smother corals and disrupt reef balance.
- Marine Debris: Pollution from plastics and other debris that can damage coral reefs and harm marine life.

#### Overfishing

- Depletion of Fish Stocks: Overfishing can lead to the loss of key reef species and disrupt ecological balance.
- Destructive Fishing Practices: Practices such as blast fishing and cyanide fishing cause direct physical damage to reefs and harm marine biodiversity.

#### Coastal Development

- Habitat Destruction: Development activities such as dredging, land reclamation, and construction can destroy or degrade coral reef habitats.
- Sedimentation: Increased sedimentation from coastal construction and deforestation can smother corals and reduce light availability.

### 2.3.5 Conservation efforts

- ...

#### Marine Protected Areas (MPAs)

- Designated Zones: Areas where human activities are regulated or restricted to protect coral reefs and promote recovery.
- Success Stories: Examples of successful MPA implementations and their positive impacts on reef health and biodiversity.

#### Restoration Projects

- Coral Gardening: Techniques for growing and replanting corals to restore damaged reef areas.
- Artificial Reefs: Creation of artificial structures to provide new habitats for marine life and promote reef recovery.

#### Community Involvement

- Local Engagement: Involving local communities in reef conservation through education, stewardship, and sustainable practices.

- Citizen Science: Encouraging public participation in monitoring and research efforts to support reef conservation.

### Policy and Legislation

- International Agreements: Global and regional agreements aimed at protecting coral reefs and addressing climate change impacts (e.g., the Convention on Biological Diversity).
- National Policies: Policies and regulations at the national level to safeguard coral reefs and manage marine resources sustainably.

## 2.3.6 Future Research and Monitoring

- ...

### Innovative Technologies

- Remote Sensing: Use of satellite imagery and drones to monitor reef health and track changes over time.
- Genomics: Applying genetic research to understand coral resilience and adaptation to environmental stressors.

### Adaptive Management

- Dynamic Strategies: Developing flexible management approaches that can adapt to changing conditions and emerging threats.
- Collaboration: Promoting collaboration among scientists, policymakers, and local communities to address complex challenges facing coral reefs.

### Education and Awareness

- Public Outreach: Raising awareness about the importance of coral reefs and the actions individuals can take to support conservation efforts.
- Training Programs: Providing training for scientists, managers, and local stakeholders to enhance reef management and restoration practices.

## 2.4 Implicit terrains with materials

- Volumetric modeling is important for representing 3D structures
- Allows for the representation of cavities, arches, overlays, etc.
- The concept of materials allows for including much more information for the following parts: amplification and rendering
  - \*\* Amplification (e.g., erosion) needs to know the type of soil at the surface and subsurface to be realistic
  - \*\* Rendering needs to know the material at the surface to correctly display textures

- ...

### 2.4.1 Material density

- ...

### Material granularity

- ...

### Soil triangle

- ...

### 2.4.2 Scalar functions

- ...

### **2.4.3 Blending functions**

- ...

### **2.4.4 Placement functions**

- ...

### **2.4.5 Material usage**

- ...

#### **Defining the final material**

- ...

#### **Post-processing: material transformation**

- ...

# **Part I**

# **Semantic Representation**



---

## Abstract

---

- Terrain generation usually focus on geometry processing
  - Some works include soil materials in their process
  - But no semantic information is preserved
  - Many fields use topologic maps to describe the environment
- \*\* see Travel books
- Our method to abstract the geometry and focus on the symbolic
  - ...



# CHAPTER 3

---

## Generation de terrain sémantique

---

### Contents

3.1	Introduction . . . . .	26
3.2	Related works . . . . .	27
3.3	Overview . . . . .	28
3.3.1	Environmental attributes . . . . .	29
3.3.2	Semantic Terrain Entity . . . . .	30
3.3.3	Environmental modifiers . . . . .	30
3.4	Placing Semantic Terrain Entities in an environment . . . . .	30
3.4.1	Fitness function . . . . .	31
3.4.2	Skeleton fitting function . . . . .	32
3.5	Life cycle of Semantic Terrain Entity . . . . .	32
3.5.1	Hard constraints vs. soft constraints . . . . .	33
3.6	Communication between Semantic Terrain Entity . . . . .	33
3.6.1	Problem of direct communication . . . . .	33
3.6.2	Natural process (or cellular automata) . . . . .	33
3.7	Environment stability . . . . .	33
3.7.1	Dynamic system vs. stable system . . . . .	33
3.7.2	Dying . . . . .	33
3.8	Environmental attributes and environmental modifiers . . . . .	33
3.8.1	Influence on water currents . . . . .	34
3.9	Physics simulation . . . . .	35
3.9.1	Heights of Semantic Terrain Entity . . . . .	35
3.9.2	Combining heights . . . . .	35
3.10	User interaction . . . . .	35
3.10.1	Direct interactions on the Semantic Terrain Entities . . . . .	35
3.10.2	Indirect interaction of Semantic Terrain Entities . . . . .	36
3.11	Results . . . . .	38
3.12	Conclusion . . . . .	40

[Back to summary](#)



Figure 3.1: Our method can produce different scenes including coral islands and canyons at multi-scale using Semantic Terrain Entities to represent terrain features.

### 3.1 Introduction

Topographic maps are very useful tools for biologists, geologists or even oceanologists (which would call them "bathymetric charts"). These maps are displayed in 2D but provide 3D information about the altitude (or depth), but can also use symbology to represent the important elements that need to be visible. Map symbols are important in order to extract as much information as possible from a 2D object. In cartography, map symbols are defined as geometric primitives such as points, polylines, polygons, and (rarely) polyhedrons. These symbols are a simplification of the content of an environment, or an abstraction of the 3D shape of the terrain features. This is useful to understand the relationship between the different features, which enables to deduce rules in the evolution of a terrain.

In such way, geologists can study the distribution of peaks in a mountain range, the location of soil types in an area, which in turn allow to deduce possible locations of karst networks, for example. Using the same tools, a biologist may interpret the effect of natural or artificial reefs on coastal erosion, or understand better the interactions inside an ecosystem. Oceanologists may deduce the formation of canyons and fans from old river systems.

The abstraction of the details on the surface allows to focus on the undepth understanding of a process, which may be generalized to different terrain configurations.

Parallelly, terrain artists most of the time sketch the global shape of the terrain they will model beforehand, such that they can check before the modeling part that the consistency and plausibility of the terrain will be valid. Looking at a simplified map before starting the modeling step allows the designer to modify the overall shape of the terrain, at a large scale, before the 3D geometry comes in play, generating too much control points or vertices to be able to deal with.

Starting from an initial configuration or providing conditions on the desired output terrain, the algorithm we propose will let the different terrain features evolve as a multi-agent system, allowing for a simulation of evolution on multiple years, while, at any time, the user can apply modifications or new constraints on the state of the environment. The resulting configuration is an environment conform to the constraints shared by the user, which can be about the number of years of simulation and/or the distribution of features present in the scene.

As described in the previous chapter, most terrain generation algorithm use the geometry of an initial terrain surface to iteratively apply changes such as erosion simulation. While information about some environment variables or properties of the ground may influence the result of an algorithm, the control of the global shape of the terrain is lost as it treat locally the surface, without knowing which feature a certain point on the surface lies on.

The question which led to our solution is the multi-scale user interaction: "Is it possible to provide an interaction mean for terrain generation allowing the user to interact with a small structure like a rock in the same manner as with a large structure like a mountain?". In

this work, we want the user to be able to have a large scale representation of the terrain in order to generate a landscape that satisfies his needs while keeping the possibility to apply large modifications. In discussion with robotician users, we realise that we want to create a large landscape that can contain interesting , select a smaller region that have features in a disposition that. In the optic of generating a large scale terrain in which we could focus the generation effort in a certain region, we wished to be able to see a coarse representation that can be computed quickly.

We want this method to be adapted for terrains above and under the water level.

Because many geographical terms would become ambiguous in computer science terms, in which this thesis lie in, we will translate some vocabulary in a way that may be disapproved by geologists, but we are doing our best to keep it as acceptable for each field as possible.

## 3.2 Related works

Procedural terrain generation has been heavily studied for the last 40 years ( E. Galin et al., 2019). Researches in this topic try to find new solutions to compromise between realism, user control and efficiency ( Gain et al., 2009). Using fractal noise parametrized to resemble real landscape has been an important first step ( Musgrave et al., 1989) as it's a fast and light solution to generate procedurally the appearance of mountains. The lack of user control pushed newer works toward the use of controlled noise by including real DEM in the process through learning ( Brosz et al., 2007; Kapp et al., 2020), while the rise of deep learning technologies gave higher control to the user through sketches ( É. Guérin et al., 2017; Talgorn and Belhadj, 2018).

By including expert knowledge of tectonic process and subsurface geology, some algorithms tend to get more realistic ( Cortial et al., 2019; Michel et al., 2015; Patel et al., 2021).

While these algorithms are able to generate large-scale landscapes, the finer details of the terrain is often computed by the use of erosion simulation ( Cordonnier et al., 2023; Paris et al., 2019b; Schott et al., 2023). This process can be expensive in time but results in more plausible surfaces.

All the algorithms aim to reproduce plausible relief in terrestrial landscapes, mostly limited to alpine landscapes, but a lack of research can be found in almost all other biomes. Underwater landscapes generation, for example, has been almost completely absent from literature for many reasons: the difficulty of accessing the area, the lack of visibility under water and the complex physics of underwater geology and biology make the algorithms adapted for this environment scarce.

The majority of the ocean floor can be represented as a fractal terrain ( Mareschal, 1989). While stochastic noise can be sufficient to model the ocean floor, this process won't cover areas with the biggest biomass, near shallower waters such as near coasts and islands.

Due to the impossibility to observe the large-scale and the small-scale of underwater environments, some works related to geology model large structures like the profile shape of the coral reef ( BOSSCHER and SCHLAGER, 1992), simulate its surface growth ( Li, 2021), or use procedural algorithms for single polyp ( Abela et al., 2015). We however don't have a mix of the different scales, and neither methods take into account the environment such as the topography or the interaction of different terrain features. This is mainly due to the fact that the evolution time for each scale varies from a span of weeks to thousands of years.

In an ecosystem, any element of the system has an impact on their surrounding. Simulating each physical properties such as shading, heat, humidity may require enormous computation power. By considering these properties as scalar fields surrounding the whole scene, and that features of the terrain affect locally the scalar fields, we can simplify the

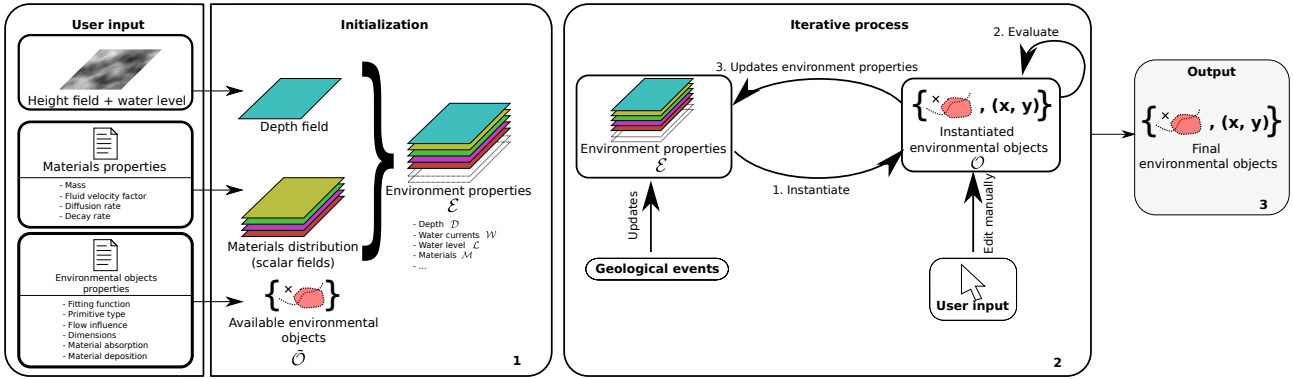


Figure 3.2: Overview of the pipeline of the method. The user provides as input an initial height field and sets the water level, as well as a definition of the environmental modifiers properties and Semantic Terrain Entities properties that will be used in the iterative process. These inputs are initialized as an initial set of Semantic Terrain Entities and scalar fields that represents the environmental attributes. In the iterative loop, new Semantic Terrain Entities are instantiated using the current state of the environment at their optimal position. The existing Semantic Terrain Entities in the terrain reevaluate their fitness function to grow or die and update the environmental attributes locally. At each iteration, geomorphic events can update the environmental attributes, while the user can interact directly with the Semantic Terrain Entities. The result of the whole process is a set of Semantic Terrain Entities which is a sparse representation of the features of the scene.

computation of the physical properties of the environment (Grosbellet et al., 2016; É. Guérin et al., 2016). This process provides a scalable system from which scene details are rendered in a plausible way. In a similar way, other works represent the wind flow as a composition of local vector fields (Wejchert and Haumann, 1991), avoiding complex fluid simulation while providing user control in a lightweight model. We extend these works by incorporating a time-evolution system such that the scene can be dynamic.

### 3.3 Overview

The generation of the terrain is initialized using an initial height field  $\mathcal{H}$  and a water level  $\mathcal{L}$ . The height field provides variation on the depth  $D$ , which can influence the generation process of the scene. We set  $D = \mathcal{H} - \mathcal{L}$ .

The list of available Semantic Terrain Entities  $\tilde{\mathcal{O}}$ , representing the different features that can be present in the scene, are provided with their properties: type, size, generation rules, growing conditions and effects on the environmental attributes (Section 3).

Finally, different environmental modifiers can be defined with their properties such as diffusion speed, mass, damping factor and influence from the water currents. Environmental modifiers distributions are represented as a scalar field  $\mathcal{M} : \mathbb{R}^2 \mapsto \mathbb{R}$  and water currents as a vector field  $\mathcal{W} : \mathbb{R}^2 \mapsto \mathbb{R}^2$  that can be evaluated by the Semantic Terrain Entities of the scene to simulate their growth and spawn at the most probable position. The environmental properties  $\mathcal{E} = (D, W, L, M)$  is composed of depth, water currents, water level and environmental modifiers distribution information at any point of the terrain (Section 3).

The definition of Semantic Terrain Entities' properties and environment properties is done with field experts, providing the pertinent parameters required to model the evolution of the terrain features using expert knowledge (Section ??). Additional properties can easily be added to the environment properties  $\mathcal{E}$  in order to fit to the experts needs, such as atmospheric

pressure, humidity, temperature, ...

The generation phase can optionally be started with an initial set of Semantic Terrain Entities present in the scene.

Once the initialization phase is done, the generation begins. The generation process is incremental and its main loop is composed of two different steps: the instantiation of new Semantic Terrain Entities then the update of the environment.

At each iteration, new Semantic Terrain Entities can be created at their most fitting locations if possible. The generation rules provided in the initialization phase are used to find the optimal position from stochastic sampling (Section 3). All Semantic Terrain Entities are evaluating their state analytically using the fitness function provided as input (Section ??).

Once the instantiation step is done, the environment's values are updated by each Semantic Terrain Entity by depositing and absorbing some of the available environmental modifiers (Section 3) while modifying the water currents (Section 3) around them. Finally, water currents and height field's gradient displace environmental modifiers of the terrain at each iteration. During the generation process, the user can alter directly the distribution and shapes of the Semantic Terrain Entities (Section 3) and perturb the generation process by planning geomorphic events that have impacts on the environmental attributes (Section 3).

The output of our system is a set of Semantic Terrain Entities disposed in the plane. We do not provide the 3D representation of the Semantic Terrain Entities, letting the user define the rendering method. The figures used in the paper use a mix of implicit surfaces and triangular meshes.

### 3.3.1 Environmental attributes

In geography, a "field" refers to a continuous spatial phenomenon across a region where each point has a specific value of a variable, unlike discrete objects with distinct boundaries. Fields can be scalar, representing a single value at every point (like temperature or elevation), or vector, representing quantities with magnitude and direction (like wind velocity). Examples include topographic fields for elevation, climatic fields for temperature or precipitation, and magnetic fields for magnetic forces. Fields are mathematically modeled using functions and represented in Geographic Information Systems (GIS) as raster data, where a grid of cells captures continuous variations. This representation is essential for studying spatial patterns and processes such as climate change and resource distribution. Because of the ambiguous nature of the term "field" in mathematics and computer science, we will define the geographic fields as environmental attribute.

In an ecosystem simulation, each actor of the ecosystem has an impact on all other actors, which results in an exponentially growing computation effort as the number of elements of the terrain increase. We avoid this problem by considering the environmental attributes as a proxy to allow any Semantic Terrain Entity to interact with any other one. Each of the Semantic Terrain Entity have a local impact on the environmental attributes without knowledge of neighboring Semantic Terrain Entities. This modification of the environmental attributes are presented as the effect of environmental modifiers defined for each Semantic Terrain Entity.

In this work, we integrated vector environmental attributes (water currents  $\mathcal{W}$ ) and scalar environmental attributes (depth  $\mathcal{D}$ , water level  $\mathcal{L}$ , environmental modifiers  $\mathcal{M}$ ) into the umbrella "environment"  $\mathcal{E} = (\mathcal{D}, \mathcal{W}, \mathcal{L}, \mathcal{M})$ . Environmental modifiers describe a change of environmental attribute at one point like an abundance of sand, salt, wetness, rocks, etc... As we do not consider the surface geometry in this work, the reader must restrict himself from seeing it as stacks of materials.

### 3.3.2 Semantic Terrain Entity

A geographical feature, also called object or entity, is a discrete phenomenon located at or near the Earth's surface, relevant in geography and geographic information science (GIScience). It represents geographic information that can be depicted in maps, geographic information systems (GIS), and other forms of geographic discourse. This term includes both natural and human-made objects, ranging from tangible items like buildings or trees to intangible concepts like neighborhoods or savana. Features are distinct entities with defined boundaries, differentiating them from continuous geographic masses or processes occurring over time. They can be categorized as natural features, such as ecosystems, biomes, water bodies, and landforms, or artificial features, such as settlements, administrative regions, and engineered constructs. Geographic features are described by characteristics including identity, existence, classification, relationships with other features, location, attributes, and temporal aspects. Information about these features is stored in geographic databases using models like GIS datasets, which organize and represent these features in structured formats. As the term "feature" is overused in computer science, we will use the term Semantic Terrain Entity in this work.

Each Semantic Terrain Entity has a simple geometric shape called a "skeleton" that defines where it is located and how it fits into the environment. These Semantic Terrain Entities interact with the environment  $\mathcal{E}$  by changing local conditions using the environmental modifier. For example, a river might increase the moisture in the surrounding area, while a mountain might add rockiness. They can also absorb changes from the environment, such as a forest taking in humidity from the air. The placement of Semantic Terrain Entity is determined by a fitness function, which evaluates how suitable a location is based on the environmental attributes. Once a suitable location is found, the skeleton fitting function optimizes the shape and position of the entity to fit as best as possible into the environment.

### 3.3.3 Environmental modifiers

The environment determine if a Semantic Terrain Entity does belong in a position. When a Semantic Terrain Entity is placed, its surrounding environmental attributes can be affected though environmental modifiers. Each Semantic Terrain Entity has intrinsic environmental modifiers that can be seen as "spreading" and "absorbed" around its skeleton over time. A coral reef may produce coral polyps and at the same time reduce the water currents. It grows thanks to the deposition of [RESIDUS CALCAIRES] from coral colonies. In our model, the colonies affect the environmental attributes through the deposition of environmental modifier  $\mathcal{M}_{\text{limestone}}$ , which in turn, is absorbed by the coral reef, without a direct exchange between the two Semantic Terrain Entities.

The alteration of a scalar environmental attribute is done by adding or removing some amount on the skeleton of the Semantic Terrain Entity and diffusing it in the space, influenced by the water currents. We consider the system to be steady-state, garantied by the introduction of a decay rate in the computation of the diffusion.

Altering the vector field of the water currents  $\mathcal{W}$  is done by the addition of the effect of each object at a position  $\mathbf{p}$  as introduced in Wejchert and Haumann, 1991, while we use the formulation of Kelvinlets (Goes and James, 2017) in the computation of effect of each Semantic Terrain Entity.

## 3.4 Placing Semantic Terrain Entities in an environment

At each iteration of our algorithm, we want our objects to be at plausible positions. We do not guaranty a temporal continuity between iterations as in Ecormier-Nocca et al., 2021, so

the objective is to add new Semantic Terrain Entity in order to satisfy the users wishes, while conserving the plausibility of the scene. For this task, we place a new element required at the most plausible position using the analysis of the fitness function of each Semantic Terrain Entity. We know that each Semantic Terrain Entity will modify the environment surrounding, which may make previously instantiated Semantic Terrain Entities unfitted. Knowing this, the goal is to add the new element at the position that will change the least the stability of the system.

Genetic algorithms or Depth First Search algorithms could be used to try many possibilities until a local or global minimum could be found, but this would require a large processing power. Basic genetic algorithms would place a Semantic Terrain Entity at a certain position at each iteration and evaluate the stability of the environment, repreating this operation while varying slightly the position of the Semantic Terrain Entities or the type of Semantic Terrain Entity instantiated at each iteration, resulting in way too much computation to be interactive. The Depth First Seach algorithms requires to compute all the possible combinations of objects and positions which, given the fact that we want a continuous position in order to work multi-scale, would require to compute an incredibly high amount of possible configurations in order to find a plausible situation, on average. We will work with an evolutionary algorithm to find a compromise between fast computation and a satisfying result.

Our placing algorithm is done in two steps: first we estimate at which global location the Semantic Terrain Entity fits the most given an environment using its fitness function, secondly we estimate the shape of the skeleton of this Semantic Terrain Entity should take given a skeleton fitting function.

Generation rules provides, for each Semantic Terrain Entity, a fitness function  $\Gamma_{obj}$  defining the most probable location for an Semantic Terrain Entity to spawn. Fitness functions' parameters contains, for every point  $p$ , the environmental attributes  $\mathcal{E}_p$  (the amount of each material available  $M(p)$  and the velocity and direction of the water currents  $W(p)$ ) and information about surrounding Semantic Terrain Entities  $\mathcal{O}$  (signed distance from the closest punctual Semantic Terrain Entity or curve defining curve- and region-based Semantic Terrain Entities, curvature of the curve, and start and end points of the curve-based Semantic Terrain Entities).

### 3.4.1 Fitness function

Whenever a new Semantic Terrain Entity is added to the scene, we desire to position it at the position that would be the most logical to find it. Following the idea of [INSERT FIELD HERE, GEOLOGY? BIOLOGY?], we observe the environment and estimate that a certain element have a probability to be present at this position. For example in hydraulics, if we find a river coming nowhere, we can expect that a kastic river is present uphill. Or in urbanism, if many roads cross at a certain point, expectations are that a city is located here.

We will follow the same intuition using a fitness function for each of the Semantic Terrain Entity that may be spawn in the terrain. The fitness function defined  $\Gamma : \mathcal{E} \mapsto \mathbb{R}$  provides a score (sometimes called "energy") providing information on how well the Semantic Terrain Entity may fit in this position. Evaluating this function at multiple position results in an approximation of the fitting map of the object. Once the most probable position is found, we can find the most plausible shape of the Semantic Terrain Entity.

Environment objects are evaluated at every iteration in order to determine the current state of the life cycle of the Semantic Terrain Entity. For punctual Semantic Terrain Entities, this evaluation is applied at its position  $\Gamma_{obj} = f(\mathcal{E}_p)$ . Curve Semantic Terrain Entities are evaluated along the parametric curve  $C$  such that  $\Gamma_{obj} = \int_C f(\mathcal{E}_{C(t)}) dt$ . In practice, we compute the evaluation as the average of all control points of the curve  $\frac{1}{n} \sum_i^n f(\mathcal{E}_{C_i})$ . Region

Semantic Terrain Entities are evaluated inside their region  $\Omega$  as such  $\Gamma_{obj} = \int_{\Omega} f(\mathcal{E}_p) dp$ . In practice, we compute the average of random points in the region  $\frac{1}{n} \sum_i^n f(\mathcal{E}_{p_i})$ . When deformations on the Semantic Terrain Entity's shape is applied, we apply cage deformation using Green's coordinates in order to keep consistent evaluation points during the whole life cycle of an Semantic Terrain Entity.

### 3.4.2 Skeleton fitting function

The seed point of a spawning Semantic Terrain Entity is defined by a stochastic sampling of the plane. We propose different optimization means to find the optimal fitting position, depending on the Semantic Terrain Entity shape.

The spawning position of a punctual Semantic Terrain Entity is found at the local maxima of the fitness function from a seed point. The optimisation process simply follows the field's gradient  $\nabla \Gamma_{obj}$  until the local maxima is reached.

A region is defined as an isocontour of the field for which the target area  $A$  is found. From the seed point, we follow the isolevel of the fitness function  $\nabla \Gamma_{obj}^{\perp}$  until a loop is created to define the initial condition of the shape. Using the Active Contours algorithm, we can optimize the region's energy defined as  $E = E_{internal} + E_{shape}$  with

$$E_{internal} = \frac{1}{2} \left( \alpha(t) \left\| \frac{dv}{dt}(t) \right\|^2 + \beta(t) \left\| \frac{d^2v}{dt^2}(t) \right\|^2 \right). \quad (3.1)$$

The internal energy  $E_{internal}$  force the shape compact while the shape energy  $E_{shape}$  force the shape into a specific target. For the Semantic Terrain Entities generated in the following examples, we used a constraint on a target area.

$$E_{shape} = (A - a)^2 \quad (3.2)$$

with  $a$  the current area of the shape and  $A$  the target area, provided by the user for each shape, with some randomness.

A curve have different generation rules. It can either follow the gradient of the fitness function  $\nabla \Gamma_{obj}$ , follow the isocontour  $\nabla \Gamma_{obj}^{\perp}$ , or follow the heat points. While the first two possibilities are trivial, the later can also be optimized using the Active Contours algorithm by optimizing the energy  $E = E_{internal} + E_{shape}$  with Equation (3.1). We applied a length constraint on the curves :

$$E_{shape} = (L - l)^2$$

with  $l$  the curve's length and  $L$  the target length. This algorithm is sensible to the initial shape of the curve, so we start with a straight line following the isolevel at the seed point.

## 3.5 Life cycle of Semantic Terrain Entity

We consider that all Semantic Terrain Entities follow a life cycle of spawning, growing and dying. While many Semantic Terrain Entities of a terrain is not a living being, we assume that evolution of relief, for example, starts at one point in time, grow as the geological factors force it to and is eroded until a point where this Semantic Terrain Entity can not be distinguished from the rest of the environment.

Semantic Terrain Entities are spawn stochastically in the terrain at the optimal fitting position. This position is determined from a generation rule given by the user for each of the Semantic Terrain Entities, which is dependant on the environment state. Once the Semantic

Terrain Entity is present in the scene, it will continuously evaluate its fitness function to determine its state in the life cycle. If the evaluation results as less than zero, the Semantic Terrain Entity dies and it is removed from the list of Semantic Terrain Entities present in the scene. While the Semantic Terrain Entity remains, it will continue influencing its environment, by absorbing and depositing material around it and by influencing the water currents.

### 3.5.1 Hard constraints vs. soft constraints

- ...

## 3.6 Communication between Semantic Terrain Entity

- ...

### 3.6.1 Problem of direct communication

- ...

### 3.6.2 Natural process (or cellular automata)

- ...

## 3.7 Environment stability

- ...

### 3.7.1 Dynamic system vs. stable system

- ...

### 3.7.2 Dying

An object spawn has a chance of disappearing if living conditions are unmet. At death, the Semantic Terrain Entity will deposits its remains in the environment properties.

We consider an object as dead when the fitting score drops to zero. At this point, the object is removed from the scene and environmental modifiers can be deposited in the environment following the same rule as the normal step rule.

## 3.8 Environmental attributes and environmental modifiers

The environment is composed of a scalar field for each of the possible material that can be found in the terrain. The scalar fields represents the availability of the material at any point, but not a height field. Each material is defined with a mass  $m$ , a fluid velocity factor  $v$ , a diffusion rate  $D$  and finally a decay rate  $k$ .

Each Semantic Terrain Entity in the terrain is a source and a sink of environmental modifiers. It is the main mean of communication between Semantic Terrain Entities as it allows them to interact with their surrounding environment. We define the amount of deposited material with  $D_M$  and  $A_M$  the amount of material deposited and absorbed by the Semantic Terrain Entity and  $\gamma(t) \in [0, 1]$  a factor related with the current state of the Semantic Terrain Entity, which state that more material will be displaced when the Semantic Terrain Entity is fully formed than when it was just spawn:

$$\int_0^t \gamma(t) (D_M - A_M) dt$$

The deposition and absorption around an Semantic Terrain Entity is defined using the Gaussian kernel distance computation from the skeleton.

The scalar field for the material  $\mathcal{M}$  is displaced by using a warp operator  $\omega$ , taking into account the water flow  $\mathcal{W}$  and the terrain slope  $\nabla\mathcal{H}$ . We unified the warp with  $m$  the mass of the material and  $\nu$  a influence factor of the fluid on the material:

$$\omega(\mathbf{p}, t) = m\nabla\mathcal{H}(\mathbf{p}, t) + \nu\mathcal{W}(\mathbf{p}, t)$$

The environmental modifiers are also dispersed at a diffusion rate  $D$ , for which we can use the advection-diffusion-reaction equation to evaluate the distribution after a time  $t$

$$\frac{\partial \mathcal{M}}{\partial t}\omega\nabla\mathcal{M} = D\nabla^2\mathcal{M} - k\mathcal{M} \quad (3.3)$$

We solve (3.3) numerically using Euler integration

$$\begin{aligned} \mathcal{M}(\mathbf{p}, t + dt) &= \mathcal{M}(\mathbf{p}, t) + dt(D\nabla^2\mathcal{M}(\mathbf{p}, t) - k\mathcal{M}(\mathbf{p}, t) \\ &\quad - \omega(\mathbf{p}, t)\nabla\mathcal{M}(\mathbf{p}, t)) \end{aligned} \quad (3.4)$$

The introduction of the decay rate  $k$  in the equation allows for the reach of a steady-state, where we can consider the simulation stable. As the user updates the state of the simulation manually, we observe the reach of this steady state before continuing the iterative steps.

### 3.8.1 Influence on water currents

We define our water currents as a vector field defined as

$$\mathcal{W}(\mathbf{p}) = \mathcal{W}_{\text{user}}(\mathbf{p}) + \mathcal{W}_{\text{simulation}}(\mathbf{p}) + \mathcal{W}_{\text{objects}}(\mathbf{p})$$

With  $\mathcal{W}_{\text{user}}$  a user-defined vector field,  $\mathcal{W}_{\text{simulation}}$  an analytical solution inspired by a wind flow simulation ( Paris et al., 2019a), and  $\mathcal{W}_{\text{objects}}$  the water flow alteration computed from the Semantic Terrain Entities. The component  $\mathcal{W}_{\text{simulation}}$  is terrain-induced. Given an input flow direction  $a$ , we modify the vector field by warping it with the terrain gradient smoothed at multiple scales :

$$\mathcal{W}_{\text{simulation}}(\mathbf{p}) = \sum_{i=0}^{i=n} c_i \omega_i \cdot v$$

with  $v = (a(1 + k_w \mathcal{D}(\mathbf{p})))$  and  $\mathcal{D}(\mathbf{p})$  the depth at point  $\mathbf{p}$  and  $k_w$  a scaling factor, used to simulate the Venturi effects.  $\omega_i \cdot v$  is the warping operator at scale  $i$  with a coefficient  $c_i$  defined as

$$\omega_i \cdot v = (1 - \alpha)v + \alpha k_i \nabla \tilde{h}_i^\perp(\mathbf{p}) \quad \alpha = \|\nabla \tilde{h}_i(\mathbf{p})\|$$

with  $k_i$  a deviation coefficient,  $\alpha$  the slope of the smoothed terrain and  $\nabla \tilde{h}_i^\perp(\mathbf{p})$  the orthogonal vector of the smoothed terrain. As proposed by the authors, we used two scaling levels  $n = 2$  with gaussian kernels of radii 200m and 50m with weights 0.8 and 0.2 and deviation coefficients  $k_0$  and  $k_1$  of 30 and 5.

$\mathcal{W}_{\text{objects}}$  is a deformation field defined as the accumulation of flow primitives ( Wejchert and Haumann, 1991). Kelvinlets are applied on each Semantic Terrain Entities to deflect the water flow. We use the scale and grab formulations of the regularized Kelvinlets brushes ( Goes and James, 2017), denoted as  $s_\varepsilon(r)$  and  $g_\varepsilon(r)$  respectively to simulate obstruction and diversion, are defined as

$$\begin{aligned} s_\varepsilon(r) &= (2b - a) \left( \frac{1}{r_\varepsilon^3} + \frac{1}{2r_\varepsilon^5} \right) (sr) \\ g_\varepsilon(r) &= \left[ \frac{a - b}{r_\varepsilon} I + \frac{b}{r_\varepsilon^3} rr^t + \frac{ae^2}{2r_\varepsilon^3} \mathbf{I} \right] \mathbf{F} \end{aligned}$$

with  $a = \frac{1}{4\pi\mu}$  and  $b = \frac{a}{4(1-v)}$  provided  $\mu$  a shear modulus and  $v$  a Poisson ratio provided for each Kelvinlet,  $r = \mathbf{p} - \mathbf{q}$  for  $\mathbf{p}$  the evaluation position and  $\mathbf{q}$  the center point of the Kelvinlet,  $r_\varepsilon = \sqrt{\|r\|^2 + \varepsilon^2}$  the regularized distance,  $\varepsilon$  a radial scale for the deformation field,  $s$  a scaling factor and  $\mathbf{F}$  the force vector of the grab operation. Deformations defined on curves use  $\mathbf{q} = C(\mathbf{p})$  with  $C(\mathbf{p})$  the closest point on the curve from the point  $\mathbf{p}$  and  $f = C'(\mathbf{p})$ . We can then define  $u_o(\mathbf{p}) = s_\varepsilon(\mathbf{q} - \mathbf{p}) + g_\varepsilon(\mathbf{p} - \mathbf{q})$ . Finally, we can retrieve the velocity field from the objects:

$$\mathcal{W}_{\text{objects}}(\mathbf{p}) = \sum_{o \in \mathcal{O}} \lambda_o u_o(\mathbf{p})$$

## 3.9 Physics simulation

### 3.9.1 Heights of Semantic Terrain Entity

### 3.9.2 Combining heights

## 3.10 User interaction

The user can guide the generation process. The use of simple shapes as Semantic Terrain Entities facilitate the edition of the simulation, as we can interactively add, remove or modify Semantic Terrain Entities, or focus the generation process in a restricted area. Interaction with the environmental attributes is also provided as geomorphic events, that the user can invoke during the simulation. While the direct interactions on the Semantic Terrain Entities are instantaneous, as the geomorphic events are active on a given duration.

### 3.10.1 Direct interactions on the Semantic Terrain Entities

The interactive nature of our simulation enables the user to modify the state of the terrain by manipulating directly the Semantic Terrain Entities of the scene. We assume the modifications applied between two iterations of the simulation.

Translating an Semantic Terrain Entity is trivial, we simply requires to evaluate the state of the Semantic Terrain Entities at a translated position. The deformation of Semantic Terrain Entities can be applied on curve and region Semantic Terrain Entities by updating the control points of the skeleton and recomputing the resulting implicit surfaces. The evaluation positions used for region Semantic Terrain Entities are displaced by applying a cage deformation of the 2D shape using the Green coordinates of points in the shape. After the alteration of the region, evaluation points should be keeping a similar distribution than before, avoiding unexpected results during the interaction. By modifying an Semantic Terrain Entity, the environmental attributes may change, which can result in the destruction of the now incompatible environment objects in the scene (Figure 3.3).

As long as a non-zero fitness function is defined in the terrain, new Semantic Terrain Entities can be forced by the user at any point of the simulation.

Control over the region of the terrain that should be updated can be given by adjusting all fitness functions through a scalar field  $\lambda : \mathbb{R}^2 \mapsto \mathbb{R}$  such that the fitness function  $\Gamma_{obj}(\mathbf{p})$  of any new Semantic Terrain Entity is evaluated as  $\Gamma_{obj}^*(\mathbf{p}) = \lambda \mathbf{p} \Gamma_{obj}(\mathbf{p})$ . This is especially useful in the planning of robotic simulations as we can first generate the overall shape of our



Figure 3.3: Starting from a coral colony developed around a canyon (*left*), the user edits the shape of the canyon, resulting in a different configuration of the scene, killing the corals that ends too deep in the water (*center*) and the development and growth of new corals at the previous location of the canyon (*right*).

terrain and secondly focus the generation process around the areas that may be visited by the robot, avoiding useless simulations and computer power. Figure 3.7 shows an example of colonization of the coral polyps that we limited manually into an annulus.

Our water current simulation is modeled as a simple vector field. As such, the user is able to interact with it at any moment of the simulation, allowing for the death of sensible Semantic Terrain Entities while it will guide the simulation into a new landscape. By modifying the water currents, the user also modifies the transport rate of environmental modifiers at this position. The modification of currents is given as a stroke, a parametric curve  $C$  for which we evaluate  $\Delta\mathcal{W}_{\text{user}}(\mathbf{p})$  just as for curved environment objects (Section 3).

### 3.10.2 Indirect interaction of Semantic Terrain Entities

A configuration file can define in advance the different geomorphic events that should be triggered during the simulation. This can be useful to generate landscapes that are close to some existing locations. Multiple geomorphic events can be triggered either as sudden or continuous environmental changes. These changes play a huge role in the morphology of landscapes. We define geomorphic events with a starting point and an ending point, such that at any time of the simulation we can compute the progress of the geomorphic event as  $t_e \in [0, 1]$ .

Water level changes are important geomorphic events that shape the underwater landscapes. As previously submerged Semantic Terrain Entities get elevated above water level, flora and fauna terrain features dry and die. Deprived from the living part of the features, everything is more affected by terrestrial erosion. By updating the value of the depth  $\mathcal{D}$  evaluated in the fitness functions, any Semantic Terrain Entity that is sensible to the depth will be impacted automatically, that may be causing death (Figure 3.4). The modification of the water level is defined as

$$\mathcal{D}(\mathbf{p}) = \mathcal{D}_0(\mathbf{p}) + \sum_{e \in \text{events}} \Delta\mathcal{D}_e t_e$$

with  $\Delta\mathcal{D}_e$  the amount of water rising or lowering during an geomorphic event. We assumed a linear evolution of the water level during an geomorphic event. This allows to evaluate the depth at any point in space and in time.

Subsidence and uplift are the main geomorphic events that create or destroy islands in the long term. These geomorphic events are simulated as a simple factor on the height field of the generated terrain (Figure 3.5). Subsidence is not always uniform in the terrain. As such, the user can provide a position  $\mathbf{q}$  at which the subsidence is the strongest, the amount



Figure 3.4: Lowering the water level by a few meters caused most of the coral objects to satisfy  $\Gamma_{obj} \leq 0$ , causing their death. Since the water level (blue) decrease slowly, new coral objects spawn progressively at a lower altitude.



Figure 3.5: Simulating subsidence on a part of the terrain (brown area) cause the depth value to change locally, resulting in the death of coral objects that find themselves too deep to survive. Here two subsidence geomorphic events are triggered in parallel.

of subsidence applied  $\Delta\mathcal{H}_e$  and a standard deviation  $\sigma$  for which we can then compute at any point in space and time of the simulation the height of the terrain

$$\mathcal{H}(\mathbf{p}) = \mathcal{H}_0(\mathbf{p}) \cdot \sum_{e \in \text{events}} \frac{G(\|\mathbf{p} - \mathbf{q}\|)}{G(0)} \Delta\mathcal{H}_e t_e$$

with  $G(x)$  the Gaussian function

$$G(x) = \frac{1}{\sigma\sqrt{2\pi}} \exp\left(-\frac{x^2}{2\sigma^2}\right)$$

Storms are factors of the geomorphology of coral reefs (Oron et al., 2023; Vila-Concejo and Kench, 2016) and coasts (Cowart et al., 2010; Domínguez et al., 2005). Due to the extreme wind and wave velocities coasts are highly eroded in a short time period and the more fragile corals near the water surface are broken, possibly causing breaches in the reefs and spreading polyps in the currents direction. While there are many factors at play to understand the apparition of storms and the hydrodynamics affecting it, we simplified the model of storms to the user as a single epicenter  $\mathbf{q}$  with a wind velocity  $v_{wind}$  and a standard deviation  $\sigma$

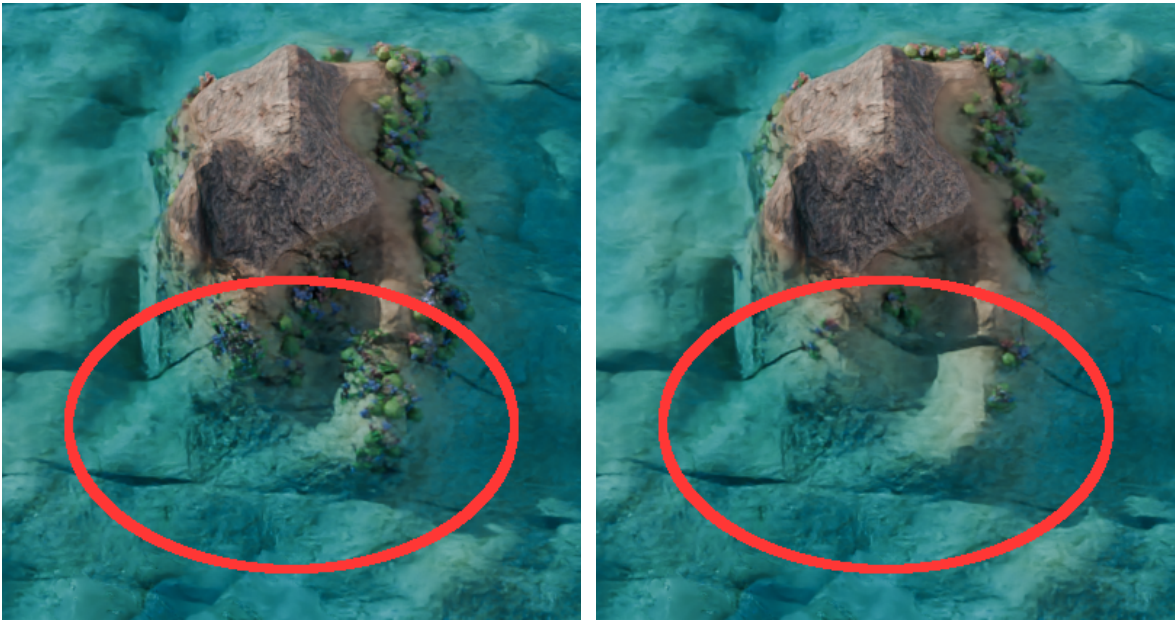


Figure 3.6: The result of a storm localized on one side of the island (red area) modifies the result of the evaluation of Semantic Terrain Entities around its epicenter for a short period of time. Most of the coral objects died from the geomorphic event, except few Semantic Terrain Entities less sensible to water currents strength.

representing the spread around the epicenter (Figure 3.6). The computation of water currents are then computed as

$$\mathcal{W}_{\text{user}}(\mathbf{p}) = \mathcal{W}_{\text{user}}^*(\mathbf{p}) + \sum_{e \in \text{events} | t_e \in [0,1]} v_{\text{wind}} \frac{G(\|\mathbf{p} - \mathbf{q}\|)}{G(0)}$$

In this case, we did not include the linear factor  $t_e$  as storms are usually conserving a constant force for the time of the few weeks or months of their occurrence.

with  $\Delta T_e$  the change of heat during an geomorphic event,  $T_0$  the temperature at the water surface, and  $c$  a very small factor.

The framework can easily be extended as the geomorphic event system stays similar for all geomorphic events. Including higher level simulations in the geomorphic event system can be added, such as the simulation of tectonic activity, the use of fluid dynamics for tsunami geomorphic events, the integration of human activity, ...

### 3.11 Results

Our method provides a way to generate scenes at different scales. We demonstrate this capacity with the generation of a large scene of an island (Figure 3.1) after what we focused the generation process in a canyon (Figure 3.8), then a small-scale visualization of coral colonies (Figure 3.7). In the examples, we rendered the Semantic Terrain Entities as a implicit tree or as individual meshes. The island, lagoons, reefs, canyons and sand ripples as implicit surfaces

A canyon scene can be generated using our method. The water flow is affected by the curve of the canyon such that the currents are oriented in the direction of the curve's tangent. In this example, we force the position of arches to be inside the canyon. The arches deposits a material "rock deposit", which is the main element of the fitness function of the Rock object. The "rock deposit" is slightly affected by water currents, but its mass make it highly affected

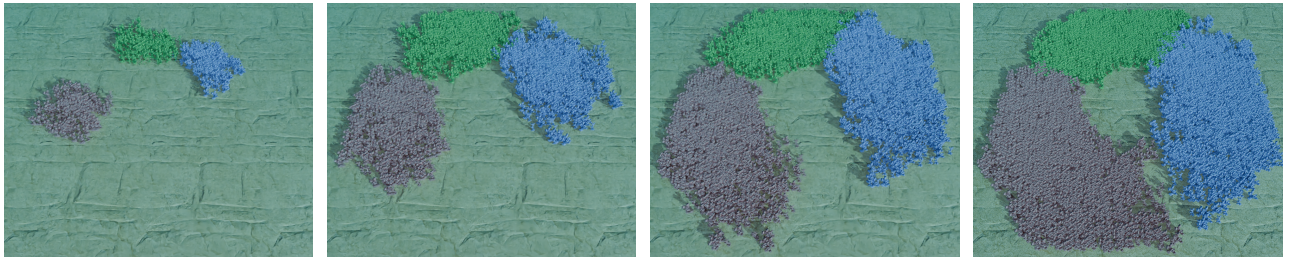


Figure 3.7: Three colonies of coral (red, blue, green) restricted to an annulus the middle section of the terrain fighting for the space.

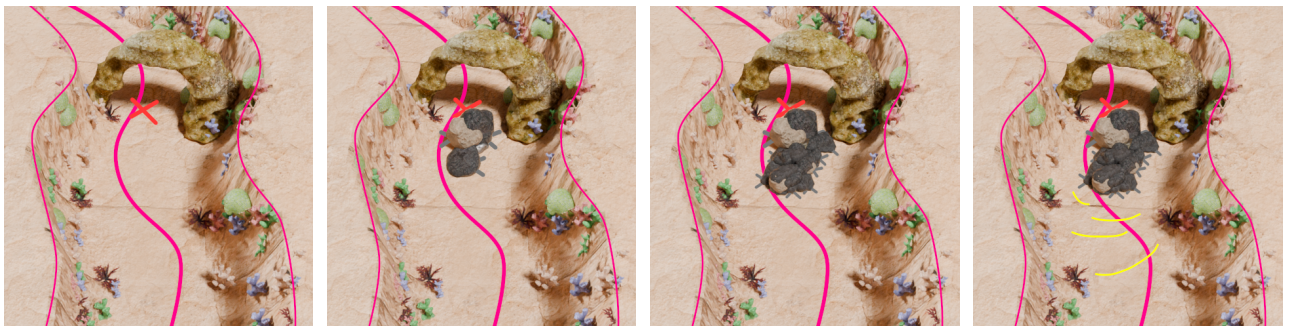


Figure 3.8: Evolution of a canyon scene at different iterations of the simulation. The apparition of an arch causes the spawning of rocks, pebbles, and finally some deposition of sand at the bottom of the canyon, spawning ripples.

by gravity. As such, rocks will spawn underneath arches. In reality, an arch is often created as part of a large coral boulder that sees the calcareous bottom part detached by the water currents, often resulting in an arch surrounded by big rocks and smaller rocks from the erosion of the first rocks. As such, we define an Semantic Terrain Entity "Arch" with a fitness function  $\Gamma_{arch}(\mathbf{p}) = 5 - d(canyon - \mathbf{p}) * \|\mathcal{W}(\mathbf{p})\|$ , an Semantic Terrain Entity "Rock" using  $\Gamma_{rock}(\mathbf{p}) = \mathcal{M}_{rock\_deposit}(\mathbf{p})$  and Pebble using  $\Gamma_{pebble}(\mathbf{p}) = \mathcal{M}_{smaller\_rock\_deposit}(\mathbf{p})$ . Finally, sand ripples are simply described as curves appearing where there is a lot of sand available:  $\Gamma_{ripple}(\mathbf{p}) = \mathcal{M}_{sand}(\mathbf{p})$ . Following these simple rules, Figure 3.8 shows the emergence of details in the scene.

In this example we defined three different types of corals, coralA, coralB and coralC, to illustrate the possibility to model behaviours from the choice of fitness functions. Each of the coral types deposits a material "coral polyp" and "coral polyp A" ("coral polyp B" and "coral polyp C" respectively). By considering a fitness function that minimize the ratio  $\frac{\text{coral polyp}}{\text{coral polyp A}}$ , we can see an emergent behavior of the three types of coral fighting for the space colonization. Figure 3.7 shows the result of this simulation at three different interations. At the border between two colonies, none of the colonies make progression due to the amount of coral polyp specific from the other colony.

The proposed method aims to generate plausible landscapes using simplified versions of the evolution of an ecosystem and of the 3D representation. The biological realism of the result is highly correlated to the amount of simplification and assumptions, while the visual realism is completely dependent to the geometric functions used for the 3D modeling of the Semantic Terrain Entities. While proposing a flexible method that propose a generic approach for terrain generation, a close collaboration with fields experts and with graphists is needed to achieve optimal results.

Most simulation algorithm's quality depends on the size of the time step used, but with the

introduction of a decay rate in the environmental modifiers properties, we limit the influence of time steps by considering that steady-state are reachable. The material deposition and absorption on punctual Semantic Terrain Entities can be seen as a Dirac function  $\delta$  centered at their position resulting in the advantage that material displacement function can use the definition of the diffusion equation instead of the advection-diffusion-reaction equation. This equation allowing us to evaluate the state of the material  $\mathcal{M}$  without intermediate steps, but this is not applicable with curve- and region-based Semantic Terrain Entities.

## 3.12 Conclusion

We have proposed a method to generate terrains procedurally using sparse representations. This representation, the Semantic Terrain Entities, enables to introduce expert knowledge by the mean of the fitness functions that rule the Semantic Terrain Entities life cycle, but also to integrate the user in the loop during the generation process. We reduced the terrain resolution limitations by defining the environment objects as parametric features. Thanks to the sparse representation based on single points, curves and regions, we allow for direct manipulation of the Semantic Terrain Entities of the scene by the user which, thanks to the environment steady state consideration, also enables to include these interactions in the automatic simulation process. Integrating environmental properties in the fitness function of Semantic Terrain Entities allows the user to guide the generation through geomorphic events. Our method enables each Semantic Terrain Entity of the scene to influence the environment locally, reducing the need of computations while also retrieving environmental attributes locally, which result in a parallelizable life-like simulation process. The genericity of the environment properties definitions should be sufficient for plausible generation of other landscape types as long as expert knowledge can be translated to Semantic Terrain Entity's formalism.

We limited our work to the use of 2D scalar fields as they are more easily differentiable, interpretable and lighter than volumetric representations. However, future works include using 3D representations of the terrain and the environment to generate 3D terrains, including cavities, sub-terrestrial areas and the interior of coral structures.



Figure 3.9: A simple coral island is generated using an island, a lagoon, reefs coral polyps, beaches, trees and algae Semantic Terrain Entities. Trees appear on beaches and algae grow in the lagoon's sand.



# **Part II**

# **Modelisation**



---

## Abstract

---

- Methods completely different
  - \*\* Physical phenomena are different
  - \*\* => Simulation/generation methods must be specific for one landscape
- Methods are developed at different instants of the thesis work,
  - \*\* We will see different procedural generation domains:
    - \*\*\* Analytical solutions (coral islands #1)
    - \*\*\* Deep Neural Networks (coral islands #2)
    - \*\*\* 3D user interaction (karst networks)
  - Deep Learning tends to replace procedural methods in 2D domain,
  - \*\* But still too complex for 3D models
    - \*\*\* (lack of data, lack of research interest for now)
  - \*\* Still requires a lot of data, which, is (while not easy) possible using aerial images, but is way too sparse with underwater landscapes or underground biomes.
  - We want to control the area in which an element is modeled in the terrain
    - \*\* Because that's how we define them in the previous chapter.
    - \*\* Thus we cannot use simple random noise methods => no bounds
      - \*\*\* Only solution is to use falloff maps, but meh...
    - As such, we want to keep the skeleton of our elements using primitives (points, curves, regions)
      - \*\* => Much easier to add constraints / manipulate primitives in a "procedural generation" way.
      - Warning: usage of Deep Learning is at the limit of "procedural generation" and is not considered as part of it by the whole community.  
(Complete with the Reddit poll).
      - ...



# CHAPTER 4

---

## Graphical representation of environmental objects

---

- Implicit surfaces
- Meshes
- ...



# CHAPTER 5

---

## Automatic Generation of Coral Islands

---

### Contents

5.1	Introduction . . . . .	49
5.1.1	Multiple theories . . . . .	50
5.1.2	Darwinian theory . . . . .	52
5.1.3	Overview . . . . .	52
5.2	Related works . . . . .	52
5.3	Example generation . . . . .	53
5.3.1	Closed form of coral growth . . . . .	54
5.3.2	Labeling of the map . . . . .	54
5.3.3	Automation . . . . .	54
5.4	cGAN . . . . .	54
5.4.1	Definition of cGAN . . . . .	54
5.4.2	Why cGAN? . . . . .	55
5.4.3	Training . . . . .	55
5.4.4	Model usage . . . . .	55

[Back to summary](#)

### 5.1 Introduction

- Definition of coral islands
- \*\* Different types of coral islands
- \*\*\* Here, volcanic islands
- Presentation of corals
- Difference from regular landscapes
- \*\* Concept of corals
- \*\*\* Long-term evolution (island) and short-term evolution (corals)
- \*\*\*\* Geological process of island subsidence
- ...

### 5.1.1 Multiple theories

- Complexity of Coral Reef Ecosystems
- \*\* Biological Diversity
  - \*\*\* Varied species of corals and their differing growth patterns
  - \*\*\* Interaction with marine flora and fauna
- \*\* Environmental Factors
  - \*\*\* Influence of water temperature, salinity, and light availability
  - \*\*\* Impact of ocean currents and wave action
- Geological Processes
  - \*\* Dynamic Nature of Earth's Crust
    - \*\*\* Plate tectonics and volcanic activity
    - \*\*\* Subsidence and uplift processes
  - \*\* Variations in Sea Levels
    - \*\*\* Historical fluctuations due to glacial and interglacial periods
    - \*\*\* Current sea level rise and its impact on coral reefs
- Historical and Technological Context
  - \*\* Historical Developments in Marine Science
    - \*\*\* Early exploration and observations by naturalists like Darwin and Wallace
    - \*\*\* Advances in geological and oceanographic methods
  - \*\* Technological Advancements
    - \*\*\* Development of deep-sea exploration tools
    - \*\*\* Use of sonar mapping, core sampling, and seismic surveys
- Limitations of Early Theories
  - \*\* Inadequate Data and Observation
    - \*\*\* Limited access to deep-sea environments in the 19th and early 20th centuries
    - \*\*\* Reliance on surface observations and anecdotal evidence
  - \*\* Evolving Scientific Understanding
    - \*\*\* Changes in scientific paradigms and theories over time
    - \*\*\* Integration of new findings and methodologies
- Different Perspectives and Disciplines
  - \*\* Geological vs. Biological Perspectives
    - \*\*\* Focus on geological processes like subsidence and sea level change
    - \*\*\* Emphasis on biological factors such as coral growth and reproduction
  - \*\* Interdisciplinary Approaches
    - \*\*\* Collaboration between geologists, marine biologists, and oceanographers
    - \*\*\* Diverse methodologies leading to different interpretations
- Regional and Case-Specific Variations
  - \*\* Geographical Differences
    - \*\*\* Variations in reef types and formations across different regions
    - \*\*\* Influence of local environmental conditions and geological settings
  - \*\* Case Studies of Specific Islands
    - \*\*\* Unique formation histories of individual atolls and coral islands
    - \*\*\* Examples from the Pacific, Indian, and Atlantic Oceans
- Ongoing Research and Discoveries
  - \*\* New Findings and Theories
    - \*\*\* Continuous exploration leading to new hypotheses and models
    - \*\*\* Advances in climate science impacting understanding of historical sea levels
  - \*\* Reevaluation of Existing Theories

\*\*\* Critical assessment of long-standing theories with new data

\*\*\* Adaptation and refinement of theories over time

### Theory 1: Subsidence Theory

- Origin and proponents

\*\* Charles Darwin (The Structure and Distribution of Coral Reefs, 1842)

\*\* Alfred Russel Wallace

- Mechanism

\*\* Initial formation around a volcanic island (fringing reef)

\*\* Gradual sinking of the volcanic island (subsidence)

\*\* Transition to a barrier reef with a lagoon

\*\* Complete submersion of the volcanic island leading to atoll formation

- Supporting evidence

\*\* Observations from the HMS Beagle voyage

\*\* Modern geological surveys and core samples

### Theory 2: Growth on Submarine Mountains Theory

- Origin and proponents

\*\* John Murray

\*\* Alexander Agassiz

- Mechanism

\*\* Coral colonization on underwater mountains (guyots)

\*\* Vertical growth of corals towards the sea surface

\*\* Formation of atolls without the need for subsidence

- Supporting evidence

\*\* Studies on deep-sea coral formations

\*\* Distribution of guyots and seamounts in tropical regions

### Theory 3: Sea Level Change Theory

- Origin and proponents

\*\* Reginald Daly (The Coral Reef Problem, 1915)

- Mechanism

\*\* Impact of glacial and interglacial periods on sea levels

\*\* Lowered sea levels exposing coral reefs, allowing vertical growth

\*\* Rising sea levels creating conditions for atoll formation

- Supporting evidence

\*\* Geological records of sea level changes

\*\* Correlation with coral reef growth periods

### Theory 4: Erosion and Sedimentation Theory

- Origin and proponents

\*\* Maurice Ewing

\*\* William Donn

- Mechanism

\*\* Erosion of coral reefs by waves and currents

\*\* Accumulation of coral debris forming islands

\*\* Continuous process of erosion and sediment deposition

- Supporting evidence

\*\* Sediment analysis around coral reefs

\*\* Observations of island formation from coral rubble

## Theory 5: Platform Reef Theory

- Origin and proponents
  - \*\* William Morris Davis
- Mechanism
  - \*\* Coral growth on stable continental or insular platforms
  - \*\* Formation of reef structures (platform reefs)
  - \*\* Development into coral islands when conditions are favorable
- Supporting evidence
  - \*\* Studies on platform reefs and their distribution
  - \*\* Geological stability analysis of coral platforms

### Comparative Analysis

- Similarities and Differences
  - \*\* Common themes: coral growth, geological activity, sea level changes
  - \*\* Differences in primary mechanisms (subsidence vs. growth on seamounts)
- Complementary Aspects
  - \*\* Integration of multiple theories for a comprehensive understanding
  - \*\* Case studies showing multiple processes at work

### Modern Advances and Technologies

- Geological Surveys
  - \*\* Core sampling techniques
  - \*\* Seismic and sonar mapping
- Environmental Studies
  - \*\* Impact of climate change on coral growth and sea levels
  - \*\* Conservation efforts and their implications for island formation

### 5.1.2 Darwinian theory

- Several theories
- Difficulty in studying environments
  - \*\* Use of observations
- Theory refuted by ( Droxler and Jorry, 2021)
  - \*\* But it's too early to judge
  - \*\* Practical for our case.
- ...

### 5.1.3 Overview

- Proposed tool
  - \*\* Sketching the island
  - \*\* Sketching the profile
  - \*\* Wind simulation
- Automation of examples
  - \*\* Data augmentation
- ...

## 5.2 Related works

- Perlin + falloff
  - \*\* But lacks control
- Uplift [SCHOTT UPLIFT] ( Cordonnier et al., 2016; 2017a)

- \*\* But we propose a method that limits the required interaction
- Sketching [PEYAVIE SKETCHING, EMILIEN FIRST PERSON] ( Gain et al., 2009)
- \*\* Added radial constraint to simplify interaction
- Geological modeling ( Patel et al., 2021)
- \*\* For us, it's hard to know what's happening underground (?)
- Unlike the literature, integration of the underwater part
- \*\* Integration of observation data into our process
- \*\*\* -> Typical shape and profile of an island
- \*\* Difficult to integrate physical simulations due to uncertainty
- Layer-based generation could improve the realism of examples by considering layer/environment interactions.
- ...

## 5.3 Example generation

- We use Darwin's theory in our case because generation is relatively simple.
- 2 steps:
  - \*\* Generation of the island
  - \*\* Generation of the reef
  - Numerous assumptions:
    - \*\* Island has a relatively round shape
    - \*\* Coral grows to a constant height around the island
    - \*\* All "features" are radial
    - \*\* Deformations of islands caused by winds and waves
    - \*\* Islands are independent of each other
    - \*\* The profile is relatively identical all around the island
  - ...

### Input

- Sketching of the island from above + profile view
- Wind strength
- Water level
- Subsidence rate
- ...

### "Simulation"

- Subsidence calculated by simple scaling
- \*\* Note: No geological consistency
- \*\*\* Here, using a zero level to scale in Z
- \*\*\* No consideration of different soil materials
- Reef growth
  - \*\* Does not consider any weather events
  - \*\* Considers the "keep up" strategy (as opposed to "give up" and "catch up") [large simplification]
- Wind deformation
  - \*\* using directly  $f(\mathbf{p}) = f(\omega(\mathbf{p}))$ .
- ...

### Output

- Height map of the island's surface
- Island zones and coral zones

- Possibility to recalculate ground height and coral height
- ...

### 5.3.1 Closed form of coral growth

- Proposes a closed-form solution for surface calculation
- Calculation of ground height:
  - \*\* Calculation of height by revolution around the origin point
  - \*\* Deformation of the revolution profile using the top-down sketch
  - \*\* Deformation of the height field by the wind map.
- Calculation of growth:
  - \*\* On the initial heightmap,
  - \*\*\* Any surface  $z_{min} < h(p) < z_{max}$  becomes coral
  - \*\*\* Calculation of the "low" contour  $h(p) = z_{min}$  and "high" contour  $h(p) = z_{max}$
  - \*\*\* ...
- Deformation of the map using the wind map:
  - \*\* ...
  - ...

### 5.3.2 Labeling of the map

- Using top-down sketch:
  - \*\* Features "Mountain", "Island borders", "Beach" are radial  $(\theta, r)$ , so we can label each point of the map as the "next" feature
- Using coral simulation information:
  - \*\* Provides the labels "Lagoon" and "Reef {begin, peak, end}".
  - The height map is directly associated to the feature map
- This is perfect to feed a cGAN.
- ...

### 5.3.3 Automation

- Take advantage of the radial nature of the features
- Some features can be optional (mountains)
- Deformation of the feature lines
  - \*\* Influence on the radius:  $\tilde{r}(\theta) = r(\theta) + \eta(\theta)$  with  $\eta$  continuous noise function  $2\pi$ -periodic.
  - ...

## 5.4 cGAN

- Conditional GAN: A type of Generative Adversarial Network (GAN) where the generation process is conditioned on additional information.
- ...

### 5.4.1 Definition of cGAN

- Two Networks: Consists of two neural networks, a Generator and a Discriminator, which compete against each other.
- \*\* Generator: Takes both random noise and additional information (like class labels or data) to produce synthetic data.
- \*\* Discriminator: Evaluates whether a given data instance is real (from the actual dataset) or fake (produced by the Generator), while also considering the additional information.
- \*\* Additional Information: This can be labels, data from other modalities, or any other contextual information that guides the generation process.

- Training Process: The Generator tries to create realistic data to fool the Discriminator, while the Discriminator tries to correctly classify data as real or fake based on both the data and additional information.
- Objective: The goal is to improve the Generator's ability to produce realistic data that matches the given conditions and to enhance the Discriminator's ability to distinguish between real and fake data.
- Applications: Used in various domains including image-to-image translation, text-to-image synthesis, and other tasks where generating data based on specific conditions is required.
- ...

## 5.4.2 Why cGAN?

- Flexibility of input
- Moving beyond the "radial" input condition
- Output even for "inconsistent" data (e.g., ocean in an island)
- No math, geometry, geology, or complicated things to master (hehe)
- ...

## 5.4.3 Training

- ...

### Use of synthetic data

- + Problem with synthetic data

- ...

### Data augmentation

- ...

## 5.4.4 Model usage

- ...

### Generation from sketch

- ...

### Interactive times

- ...

### Realism

- ...



# CHAPTER 6

---

## Generation of karst networks

---

### Contents

6.1	Introduction	57
6.2	Related works	59
6.3	Space colonization	59
6.4	Our method	59
6.5	Modeling	60
6.6	User Control	60
6.7	Results	60
6.8	Conclusion	60

[Back to summary](#)

- ...

### 6.1 Introduction

- Definition: Complex subterranean systems formed primarily in soluble rocks like limestone, dolomite, and gypsum.
- Importance: Significant for water resources, unique ecosystems, and land use management.
- Formation and Development
  - \*\* Chemical Weathering
    - \*\*\* Study the role of rainwater acidity (carbonic acid) in dissolving carbonate minerals.
  - \*\* Underground Drainage
    - \*\*\* Analyze the development of subterranean drainage systems, including caves, tunnels, and sinkholes.
  - \*\* Speleogenesis
    - \*\*\* Examine the process of cave formation, especially at or below the water table.
- Key Features of Karst Networks
  - \*\* Caves and Caverns
    - \*\*\* Document major cave systems and their formation processes.
  - \*\* Sinkholes (Dolines)
    - \*\*\* Identify areas prone to sinkhole formation and study their causes.

**\*\* Disappearing Streams and Springs**

\*\*\* Trace the path of streams that vanish into the ground and re-emerge.

**\*\* Karst Valleys**

\*\*\* Investigate valleys formed by the collapse of underground voids.

**\*\* Stalactites and Stalagmites**

\*\*\* Study the formation of these features within caves.

**- Hydrology of Karst Networks****\*\* Aquifers**

\*\*\* Assess the productivity and structure of karst aquifers.

**\*\* Groundwater Flow**

\*\*\* Model the rapid and turbulent flow of water through karst systems.

**\*\* Vulnerability to Contamination**

\*\*\* Evaluate the risks and sources of contamination in karst aquifers.

**- Ecology of Karst Environments****\*\* Unique Habitats**

\*\*\* Research cave-dwelling species (troglobites) and their adaptations.

**\*\* Biodiversity Hotspots**

\*\*\* Identify and document biodiversity hotspots in karst regions.

**- Human Interaction with Karst Networks****\*\* Water Resources**

\*\*\* Study the dependence of regions on karst aquifers for freshwater.

**\*\* Tourism**

\*\*\* Assess the impact of tourism on karst landscapes and caves.

**\*\* Land Use Challenges**

\*\*\* Develop guidelines for construction and land use planning in karst regions.

**\*\* Environmental Concerns**

\*\*\* Identify and mitigate pollution and land degradation impacts.

**- Examples of Significant Karst Regions**

\*\* The Mammoth Cave System (USA): Explore and document the world's longest cave system.

\*\* The Guilin Karst (China): Study the unique limestone peaks and river systems.

\*\* The Dinaric Karst (Balkans): Investigate extensive cave systems and karst phenomena.

**- Research and Study in Karst Science****\*\* Speleology**

\*\*\* Promote the scientific study of caves and karst features.

**\*\* Geohydrology**

\*\*\* Conduct studies on water flow in karst systems for resource management.

**\*\* Geomorphology**

\*\*\* Research the development of karst landforms over geological timescales.

**- Action Steps****\*\* Field Surveys and Mapping**

\*\*\* Conduct detailed field surveys and create maps of karst features.

**\*\* Hydrological Studies**

\*\*\* Implement hydrological modeling and water quality testing.

**\*\* Ecological Research**

\*\*\* Carry out biodiversity assessments and ecological studies in karst habitats.

**\*\* Human Impact Analysis**

\*\*\* Study the impact of human activities on karst systems and develop mitigation strategies.

**\*\* Education and Outreach**

\*\*\* Educate local communities and stakeholders about the importance of karst networks and

sustainable practices.

- Goals

- \*\* Conservation

- \*\*\* Preserve unique karst ecosystems and landscapes.

- \*\* Sustainable Development

- \*\*\* Ensure that human activities in karst regions are sustainable and minimize environmental impacts.

- \*\* Scientific Advancement

- \*\*\* Promote research and understanding of karst processes and features.

## 6.2 Related works

- State of the art:

- \*\* ( Paris et al., 2021)

- \*\*\* In our case, we do not rely on a graph and path finder, which allows us to compute sections of the karst on the fly (no need to know the whole network to find paths)

- \*\* ( Pytel and Mann, 2015)

- \*\*\* Based on voxels, looks plausible, with a low number of parameters, but take way too long (10 to 20 minutes per generation)

- \*\*\* Which makes it unfit for user interaction

- \*\* ( Collon et al., 2015; 2017)

- With some imagination, we can see the shape of trees:

- \*\* [Prusinkiewicz : ANY]

- \*\* ( Runions, 2008)

- Or miscellaneous networks:

- \*\* ( Fernandes and Fernandes, 2018; É. Galin et al., 2010)

- Maybe even look for Lichen or ant colonies

- ...

## 6.3 Space colonization

- Not really a tree, but...

- \*\* Some networks are branching

- \*\* Some have low number of cycles

- SC is easy to manipulate for an user

- For these reasons, we will consider the use of SC.

- Description of the algorithm:

- \*\* Definition of a root and sinks

- \*\* Evolution from the root toward closest sinks

- \*\* Branching [WHEN NEEDED]

- ...

## 6.4 Our method

- Based on classic SC

- \*\* Merging branches

- \*\* Closing paths based on angle and distances to create cycles

- Adding width to the branches

- \*\* Destroying paths when width too small

- Leaves as chambers/cavities

- ...

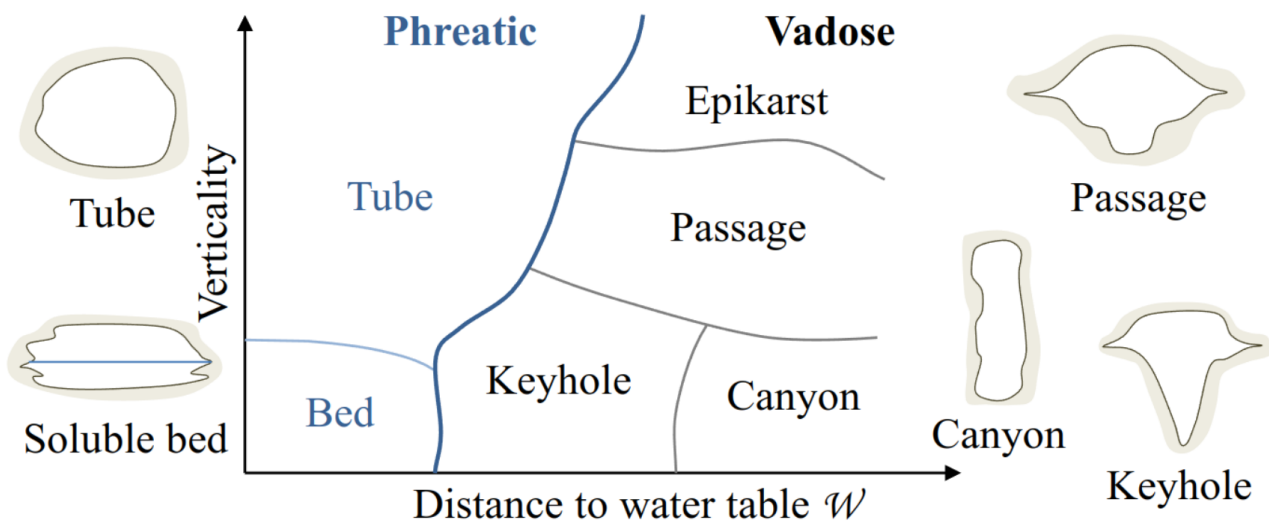


Figure 6.1: Classification of tunnel shapes

## 6.5 Modeling

- Tunnels:
- \*\* The output of SC is a set of paths
- \*\* (Paris et al., 2021) provides a classification of tunnel shapes (6.1).
- ...

## 6.6 User Control

- Importance of keeping user control
- \*\* Shape of a karst is close to randomness
- \*\* Want to be predictable
- Manipulation of control points
- \*\* Source
- \*\* Sink
- Paths tortuosity
- Inclusion of soil properties in the formation of paths, using the gradient of:
  - \*\* Humidity,
  - \*\* Porosity
- Real-time editing
  - \*\* Allows for precise manipulation
- ...

## 6.7 Results

- ...

## 6.8 Conclusion

- ...

# **Part III**

## **Erosion Simulation**



---

## Abstract

---

- Work carried out at the beginning of the thesis
  - Representation choice still uncertain
  - Search for abstraction of the representation
- \*\* Drives the generalization of the erosion system



# CHAPTER 7

## Érosion par particules

### Contents

7.1	Introduction . . . . .	66
7.2	State of the art . . . . .	67
7.2.1	Terrain Representations . . . . .	67
7.2.2	Erosion Processes . . . . .	68
7.3	Particle erosion . . . . .	68
7.3.1	Overview . . . . .	69
7.3.2	Erosion process . . . . .	69
7.3.3	Transport . . . . .	70
7.4	Our erosion method . . . . .	72
7.4.1	Application on height fields . . . . .	73
7.4.2	Application on layered terrains . . . . .	73
7.4.3	Application on implicit terrains . . . . .	74
7.4.4	Application on voxel grids . . . . .	75
7.5	Results . . . . .	76
7.6	Comparisons . . . . .	79
7.7	Discussion . . . . .	81
7.8	Conclusion . . . . .	82

[Back to summary](#)



Figure 7.1: Applying shading and textures on the generated geometry can produce a plausible aspect of a coast eroded by waves on a long timespan, or a desertic landscape eroded by wind, or a mountainous area flatten by thermal erosion.

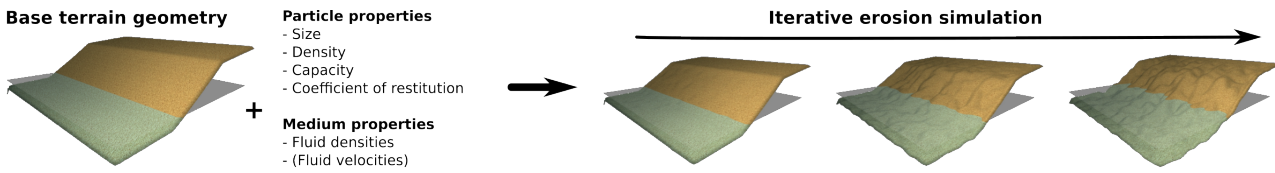


Figure 7.2: Our method require a base geometry, a small number of parameters for the particles and the medium used for the erosion simulation. It can be easily adapted to be compatible with different mediums and terrain representations.

## 7.1 Introduction

Automated terrain generation is a key component of natural scene digital modeling for animated movies and video games. A standard approach is to first generate a base terrain geometry using noise to define the height on the input domain ( Musgrave et al., 1989; Olsen, 2004; Roudier, 1993), the result will most likely lack realism and feel synthetic. Erosion simulation algorithms are applied, to simulate thousands of years of ageing by reproducing physical phenomena - i.e. effects of the elements (rain, wind, running water...) - affecting the terrain making it more believable ( E. Galin et al., 2019; Smelik et al., 2009; Stachniak and Stuerzlinger, 2005).

The process of terrain alteration caused by the effect of water, air, or any other element - natural or not - over time is usually performed in three steps ( Neidhold et al., 2005): **detachment** - pieces of the ground of variable dimensions, ranging from complete ledges to grains of sand, are removed from the terrain depending on the simulated meteorological phenomenon - **transport** - pieces of ground fallen from their initial position are moved to a different one (e.g. a cornice falls down a slope or a grain of sand is thrown into the air) - and **deposition** - transported pieces of land are accumulated at a new part of the landscape. Various phenomena can cause these alterations: **thermal erosion** (bursting of rocks caused by expansion of water under frost, then falling of debris to the bottom of a slope), **hydraulic erosion** (detachment caused by the impact of water particles on surfaces and the transport of sediments by the flow of runoff), **wind erosion** (fine particles carried away in the wind and hit surfaces on their way, creating new fine particles which then also fly away), **chemical erosion** (chemical decomposition of rocks caused by rainwater or other fluids), other exceptional phenomena such as avalanches, animals, lightning, etc... modify the terrain ( Argudo et al., 2020; Cordonnier et al., 2017b; 2017a; 2018; 2023).

In practice, the core idea to simulate erosion is to add or remove material from the terrain at given positions on the interface between the terrain and fluid eroding it (e.g. air or water). Hence, the two major problems to tackle are: how to locally alter the terrain geometry for material detachment and deposition and where to perform these alteration given the properties of the environment (terrain slope, fluid density and velocity). A terrain is more than often represented in 2.5D using a 2D image called a heightmap which grey scale values define terrain elevation. While being the major terrain representation, only a limited number of environments can be modeled. Indeed, natural landscapes are intrinsically 3D (overhangs, cavities or geological structures such as arches or gobelins), this is particularly true for underwater environments generation. Alternate representation such as voxel grids, material layers or implicit surfaces can be used. A wide variety of methods have been proposed to simulate natural erosion phenomena on heightmaps as the partial differential equations to model erosion can be discretized and solved in 2D and the material detachment and deposition at a given point of the terrain surface can be easily performed by elevating or lowering the ground

level i.e. changing locally pixel intensities. For volumetric representations, the alteration of the terrain is not as trivial. To define where to perform the erosion process the local slope variations are more often used combined with eroding medium information. This fluid can be simulated using particle systems, Smoothed Particle Hydrodynamics (SPH) ( Krištof et al., 2009) or approximated using a simple vector field. Proposed methods offer a specific erosion effect tailored to a single terrain representation and fluid simulation.

In this work we propose an approach to simulate a large part of the geomorphological and meteorological phenomena present in the literature of terrain generation (including 3D and volumetric effects). We introduce a generalized algorithm performing the three stages of erosion on surface and volume representations alike, and expose very few intuitive parameters to be adjusted by the user (Figure 7.2). We propose to tackle separately the material variation and the fluid simulation. Our method relies on a particle system to simulate eroding agents, each thrown particle will collide with the terrain, perform terrain alteration at the collision point and transport material along its path. Their motion is computed using simple particle physics accounting for the medium density and particle properties (buoyancy and gravity forces). We consider each particle as independent, hence, they do not interact with each other, no collision detection or response. This simplification allows for efficient parallel computation. When more accuracy or control is needed, we propose to provide a vector field used to modify the particle speed at each time step. The nature of this vector field is flexible, it can be computed using a more or less accurate fluid simulation (SPH, FLIP,...) or be manually defined by the user. We propose a particle-based strategy for material alteration that can be applied on surface and volumetric representation.

The main contributions of this paper are:

- a generalized particle-based algorithm performing the three stages of erosion on surface and volume representations,
- decoupling the erosion system from the fluid simulation, making the process more flexible in its usage and implementation and opening the door for richer effects that can easily be produced.

## 7.2 State of the art

In this section, we first present the major terrain representations (height fields, layered representations, voxel grids, and scalar functions) and a subset of the major simulated phenomena used to erode terrains. We highlight the fact that, in the literature, a specific erosion method tailored to a given terrain representation is proposed for given phenomena which might lead to limitation in term of terrain modeling. Indeed, changing representation costs information and precision loss.

### 7.2.1 Terrain Representations

A terrain can be represented in various ways, each of them suited for a given application of which we give a brief overview, more details can be found in ( E. Galin et al., 2019).

**Height Fields** represents the surface of the terrain by defining the elevation at each point in a 2D grid. This representation is simple, regular, and fast to process allowing for easy manipulation, such as raising or lowering the terrain ( Emilien et al., 2015; Gain et al., 2009).

**Layered Representations** are an extension of height fields using a 2D grid where each cell represents a stack of different materials instead of a simple height ( Beneš and Forsbach, 2001; Peytavie et al., 2009) allowing for memory efficient representation of volumetric terrains. To create complex structures, arches or caves, solid materials can be transformed into more

granular ones, that can be stabilized ( Peytavie et al., 2009).

**Voxel Grids** are regular, uniform volumetric grids that encode information on the presence or absence of material for each 3D point in the domain. Voxel grids are advantageous due to their regularity ( Dey et al., 2018) and ability to represent volumetric models at the cost of high memory footprint, which has limited their use in terrain generation ( Ito et al., 2003; Kaufman et al., 1993; Lengyel, 2010). We consider two voxel grid representations : *density-voxel* grids for which each voxel contains a scalar value, for instance the occupation percentage ( Eisemann and Decoret, 2008) and *binary voxel* grids that can be seen as a mask containing the presence of material information.

**Implicit terrains** represent landscapes as an implicit surface defined by a scalar function. This allows for high definition large terrain modeling. The application of combinable scalar function overlays ( É. Guérin et al., 2016) or the definition of user-defined gradients ( E. Guérin et al., 2022) can be used to create complex terrain features. Altering a implicitly defined surface is a challenging task hence limited option exist for erosion simulation ( Paris et al., 2019b).

## 7.2.2 Erosion Processes

Erosion processes play a crucial role in shaping landscapes over time. We present different kind of erosion and how they apply to given terrain representations. Note that using existing methods all erosion methods can not be used on all representation.

**Thermal Erosion** is driven by large temperature shifts, transferring material based on slope thresholds. The process is iterative, redistributing material until slopes stabilize. It can be computed efficiently on height fields and layered terrains due to their manipulable height nature ( Beneš and Forsbach, 2001; Musgrave et al., 1989; Peytavie et al., 2009). However, its application on voxel grids is challenging due to limited Z-axis resolution.

**Hydraulic Erosion** stems from water movement, eroding and depositing sediment based on water flow intensity. 2.5D terrains are widely studied for this simulation, using either water slope velocities ( Neidhold et al., 2005) or water simulations for erosion effects ( Mei et al., 2007). For smaller scales, 3D fluid simulations on voxel grids have been proposed ( Beneš et al., 2006). Kristof et al ( Krištof et al., 2009) used SPH (Smoothed Particle Hydrodynamics) for meshless erosion simulations on various terrains. Their method involves numerous particle interactions, demanding significant computational power. Our approach draws inspiration from this but enhances efficiency by removing certain particle interactions.

**Wind Erosion** shifts material through wind force, notably impacting areas with fine surface particles like deserts. It has been modeled on discrete height fields ( Paris et al., 2019a; Roa and Benes, 2004) by mimicking sand's wind-driven trajectory and using thermal erosion for corrections. This process is simulated by iteratively displacing small amounts of matter, which make it less suitable for representations with discrete height resolution.

**Erosion by Other Forces** includes influences like glaciers, snow, tectonic movements, and fauna, each introducing distinctive terrain patterns, enriching its intricacy ( Argudo et al., 2020; Cordonnier et al., 2016; 2017b; 2017a; 2018). However, most methods are tailored by a given terrain representation, often the height fields, and might not be applicable to other representations due to their intrinsic properties.

## 7.3 Particle erosion

Erosion occurs in three stages: material detachment, transport and deposition (respectively in red, black and green in Figure 7.3). In our approach, particles move through the medium following its flow (i.e. wind in air or currents in water) and then absorb or deposit a small amount of material upon contact with the land surface, effectively fulfilling the three stages

of erosion.

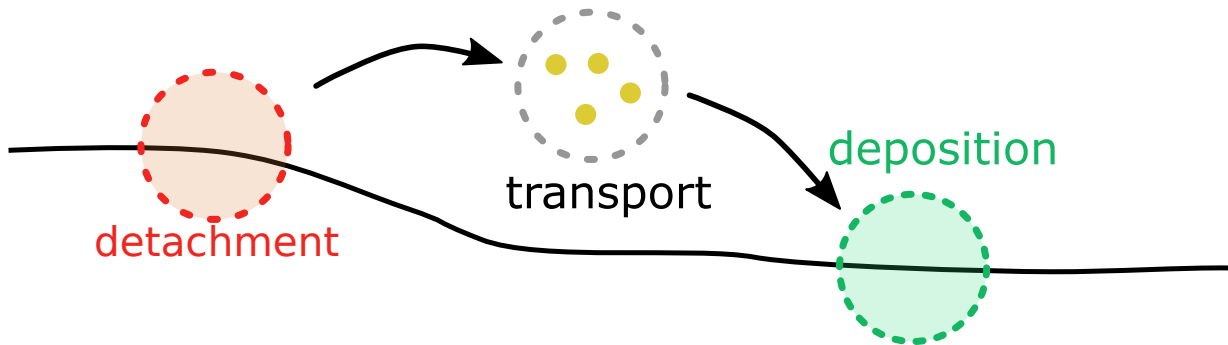


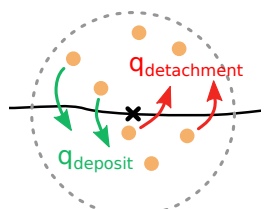
Figure 7.3: Three steps of the erosion process from the sediment point of view: detachment from its original location - dotted red circle -, transport in a fluid - dotted black circle -, deposition at a new location - dotted green circle.

### 7.3.1 Overview

Particles are transported through the medium and can pass through several different media. Each medium is defined by a density and a flow. Consider, for example, water density to be  $1000 \text{ kg m}^{-3}$  and that of air to be  $1 \text{ kg m}^{-3}$ . The gravity applied to the particles is then very different between open and submerged environments due to the difference in buoyancy, while the process remains similar. Using a pre-calculated flow field to guide particle movement simplifies the simulation by treating particles as independent entities, eliminating the need for inter-particle calculations. This not only reduces significantly the overall execution time but also offers users high flexibility over the quality of the simulation and simplify the implementation.

### 7.3.2 Erosion process

Every time the particle hits the ground, a given amount  $q_{\text{detachment}}$  of sediment is detached from the ground (red arrows) while another amount  $q_{\text{deposit}}$  of sediments is deposited at this location (green arrows). Our erosion model is based on the work of Wojtan et al where regular 3D grids are used to estimate the fluid velocity and sediment transport (Wojtan et al., 2007). In the spirit of (Krištof et al., 2009), we transposed their method into a particle-based erosion simulation, but, in our proposition, we decouple the particle system from the fluid simulation, making the process more flexible and opening the door for richer effects that can easily be produced.



**Detachment.** As a particle approaches the surface of the terrain, its motion applies friction at the interface between fluid and ground, causing bedrock to dislocate microscopic parts, that we call abrasion. We use pseudoplastics model to approximate the amount of matter removed due to the shear forces while considering the physical properties of the fluid and the ground (Wojtan et al., 2007).

The shear rate  $\theta$  is approximated by the relative velocity of the fluid to the solid boundary  $v_{\text{rel}}$  over a short distance  $l$ . We approximate the shear stress  $\tau$  at the solid boundary by a power-law:

$$\tau = K\theta^n \quad (7.1)$$

where  $\theta = v_{rel}/l$ ,  $K$  is the shear stress constant (often set to 1) and  $n \in [0, 1]$  is the flow behaviour index. Shear-thinning models typically assume  $n$  close to  $\frac{1}{2}$ , which is why we used this value as a constant.

We can then compute the erosion rate  $\varepsilon$  at any contact point between a fluid and a solid boundary using (7.1) by

$$\varepsilon = K_\varepsilon (\tau - \tau_{\text{critical}})^a \quad (7.2)$$

with  $K_\varepsilon \in [0, 1]$  a user-defined erosion constant,  $\tau_{\text{critical}}$  the critical shear stress value for which the matter starts to behave like a fluid and  $a$  a power-law constant, typically considered as  $a = 1$ .

In our method, the eroded quantity is approximated as the material contained in the half sphere, of radius  $R$ , in the normal opposite direction at the particle impact point (Figure 7.6). We then use (7.2):

$$q_{\text{detachment}} = \varepsilon \frac{2\pi R^3}{3} \quad (7.3)$$

to get the final eroded amount  $q_{\text{detachment}}$ . The particle is also defined by a maximal amount of sediments that can be contained in its volume before being saturated noted  $C_{\max}$ . Note that this constant will be used for the settling velocity computation (7.7).

**Deposition.** The eroded sediments are considered in suspension in a fluid and are affected by its velocity. A fluid particle then transports the sediments in its flow until gravity settles it onto the ground again. The effect of gravity is modeled by a settling velocity  $w_s$  defined in Eq (7.7). We consider that the amount of sediment settled is proportional to the norm of the settling velocity as proposed in (Wojtan et al., 2007) with  $\omega \in [0, 1]$ :

$$q_{\text{deposit}} = \omega \|w_s\|. \quad (7.4)$$

### 7.3.3 Transport

Our simulation is computed by integrating the full trajectory of multiple particles at each iteration unlike most other erosion methods. This allows to constantly have a terrain in a plausible state, while giving the possibility to increase the aging effect by running more iterations. Note that, reducing progressively the overall erosion strength can be used as a strategy to adapt the computation time to a chosen level-of-details.

We first present how to compute the particle speed using particle's physics then how to add optional medium velocity field to add a fluid simulation or user control.

**Particle's physics.** From its independence with other particles: we consider each particle following Newton's laws of motion.

First, we define the external forces  $\vec{F}_{\text{ext}}$  applied on each particle, we consider gravity and buoyancy. We calculate the buoyancy force  $\vec{F}_{\text{buoyancy}} = -\rho_{\text{fluid}} V \vec{g}$  with  $\rho_{\text{fluid}}$  the density of the fluid,  $V$  the volume of the particle and  $\vec{g}$  the gravitational acceleration, but we can also calculate the force of gravity  $\vec{F}_{\text{gravity}} = m_{\text{particle}} \vec{g}$  with  $m_{\text{particle}}$  the mass of the particle. We then have the final external force  $\vec{F}_{\text{ext}} = \vec{F}_{\text{gravity}} + \vec{F}_{\text{buoyancy}} = m_{\text{particle}} \vec{g} - \rho_{\text{fluid}} V \vec{g}$  knowing the density of an object  $\rho_{\text{particle}} = \frac{m_{\text{particle}}}{V}$ , we have:

$$\vec{F}_{\text{ext}} = V \vec{g} (\rho_{\text{particle}} - \rho_{\text{fluid}}). \quad (7.5)$$

The particle velocity  $v$  can be integrated from (7.5) by:

$$v = \int \vec{F}_{\text{ext}} dt + w_s + v_0, \quad (7.6)$$



Figure 7.4: The coefficient of restitution affects the amount of energy absorbed from the particle when hitting the ground. Here, rain is applied on an initial slope (yellow). Only two particles are displayed, with a high (blue) and low (red) coefficient of restitution. The resulting slope after erosion is displayed in blue and red (right).

with  $w_s$  the settling speed of sediments in a fluid with a viscosity  $\mu$  given by Stoke's Law ( Stokes, 2009):

$$w_s = \frac{2}{9} \vec{g} R^2 \frac{(\rho_{\text{particle}} - \rho_{\text{fluid}})}{\mu} f(C). \quad (7.7)$$

We use the Richardson-Zaki relation as the hindered settling coefficient:

$$f(C) = 1 - \left( \frac{C}{C_{\max}} \right)^n$$

with  $C$  and  $C_{\max}$  respectively the fraction of volume of sediments contained and the maximal fraction of sediments the particle can contain, and  $n$  an exponent typically 4–5.5, which we set to 5 ( Richardson and Zaki, 1954; Wojtan et al., 2007).

Finally, the particle position can be integrated as:

$$\mathbf{p} = \int v dt + \mathbf{p}_0.$$

When the particle hits the ground, a coefficient of restitution affects its behaviour by reducing its velocity post-collision. This value depends on ground material as it is influenced mainly by the material's particle shape, coefficient of friction and density ( Yan et al., 2020). Less bouncy particles lose speed quickly and settle down sooner, forming a steeper pile (Figure 7.4 blue), or a higher talus angle like chalk. On the other hand, more bouncy particles disperse more widely upon hitting a surface, resulting in a gentler accumulation like clay (Figure 7.4 red).

**Velocity field.** In our model, we allow the user to add a velocity field to the environment that influences particles motion. This velocity field can be the result of a complex fluid simulation, a uniform vector field, or an artistic motion field. We modify Equation (7.6) such that the particle's speed will be influenced by the velocity field as follows:

$$v = \int \vec{F}_{\text{ext}} dt + w_s + \alpha v_{\text{fluid}} + v_0, \quad (7.8)$$

with  $v_{\text{fluid}}$  medium velocity field modulated by  $\alpha \in [0, 1]$ .

Our particle system can model intricate scenarios, like the erosion caused by water currents on the seabed or aeolian erosion. The velocity field remains static during the erosion, which may cause inconsistencies in the fluid velocity field. However, minor changes can be overlooked to maintain a balance between realism and computational efficiency ( Tychonievich and Jones, 2010). We offer several velocity improvement methods:

-**Fluid simulation refinement:** Many erosion systems incorporate fluid simulation, requiring

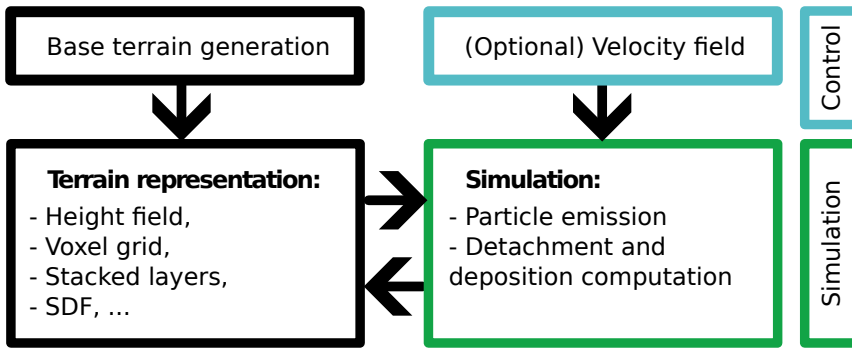


Figure 7.5: Our overall pipeline: our erosion process compute matter displacement of a terrain using an arbitrary representation as long as intersections between particles and the ground can be detected. An optional velocity field, provided by the user, guides the particles trajectories. We propose surface alteration methods to apply the erosion to the terrain in a coherent way between possible representations.

regular updates for erosion and velocity ( Krištof et al., 2009; Wojtan et al., 2007). Our method can use fluid simulations with multi-resolution refinement, with the possibility to focus the velocity field adjustments near the updated boundaries of the surface ( Roose et al., 2011).

**-Particle velocities in fluid simulation:** With a Lagrangian fluid simulation relying on particle systems ( Koschier et al., 2022), our particle velocities can be incorporated in its computation. This approach is only a provisional solution due to potential parameter mismatches with main fluid simulation.

**-Velocity field diffusion:** Given the minor changes to the surface level at each erosion iteration, which reflect the gradual alterations in terrain surface, we can estimate that the velocity at a fixed point transitioning between the inside and outside of the terrain closely mirrors the velocities observed in its surrounding area. In this context, we can simply interpolate the velocity field at any transitioning point. This simple method, as used in Figure 7.9, allows us to find a balance between achieving realistic flow simulations and maintaining computational efficiency.

## 7.4 Our erosion method

In this section, we describe how to apply detachment and deposition to different terrain representations with our method (Figure 7.5). We cover the most commonly used representations namely height fields, layered terrains, voxel grid and implicit surfaces, note that our work could be extended to additional representations. Two conditions need to be satisfied for a representation to be eligible for our erosion method: being able to evaluate the intersection of a particle with the ground and compute the normal of the terrain at this point. To the best of our knowledge, all representation do.

We use Verlet integration for the particle's physics ( Verlet, 1967), with low error rate and stability even for high  $dt$ , reducing computation time for negligible imprecision ( Baraff and Witkin, 1998; Swope et al., 1982).

For all the representations, the amount of material absorbed by the particle, i.e. the erosion value  $q_{\text{detachment}}$  from (7.3), is taken around the particle at a radius  $R$ , meaning that the modification of the terrain by a particle at position  $c$  will only occur for the positions  $\mathbf{p}$  satisfying  $\|\mathbf{p} - c\| < R$ . At the same time, the amount  $q_{\text{deposit}}$  from (7.4) is deposited, resulting in a change  $Q = q_{\text{deposit}} - q_{\text{detachment}}$

In our simulation, while the dynamics are informed by physical principles, the particle size is conceptualized within a dimensionless framework. This provides the flexibility to adapt our

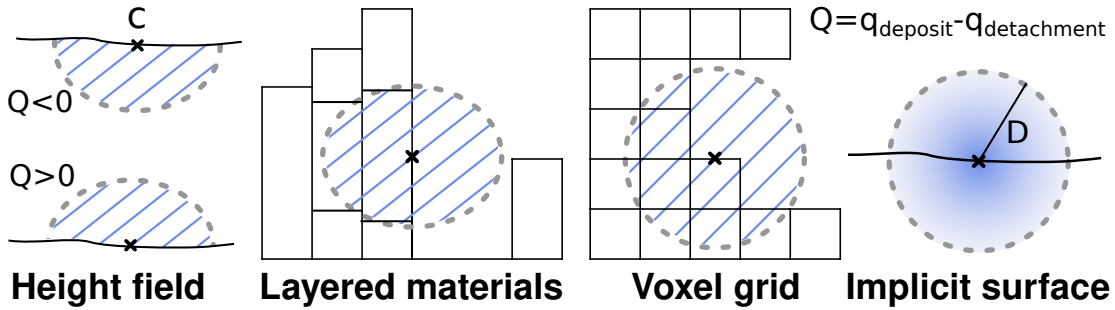


Figure 7.6: Illustration of the material detachment in the (half-)sphere at contact point C (cross) on different representations. (height field) When  $Q < 0$  material detachment happen in the bottom scaled half sphere of the particle's contact with the ground, while the deposition is applied on the upper half sphere of volume when  $Q > 0$ . Unlike the height field, for 3D terrains detachment and deposit are applied in the full sphere around the contact point.

results to various real-world scales, ensuring the applicability of our model across diverse scenarios. Note that, for a 2.5D terrain, we can consider that half of the sphere surrounding the particle is affected which has a volume of  $V_{2.5D} = \frac{2\pi R^3}{3}$  while a 3D terrain is affected by the full sphere  $V_{3D} = \frac{4\pi R^3}{3}$  (as illustrated Figure 7.6). In the following sections, we will describe the strategies used to modify the amount of matter for different representations.

#### 7.4.1 Application on height fields

On a height field defined by  $h(\mathbf{p}) = z$ , the intersection point with the surface is verified at  $\mathbf{p}_z = h(\mathbf{p})$ , and the normal can be computed at the intersection point.

For this representation, the half sphere is scaled in the  $z$  direction to fit  $\alpha V = Q$  using  $\alpha = \frac{Q}{V}$ . We then can decrease the height  $h'(\mathbf{p})$  at all points  $\mathbf{p}$  by the height of the scaled half sphere at position  $\mathbf{p}$ . Given the height of the scaled half sphere of center  $c$  and the distance of the particle to the center  $d = \|\mathbf{p} - c\|$  by  $h_{\text{half sphere}}(\mathbf{p}) = \alpha \sqrt{R^2 - d^2}$  for all  $\mathbf{p}$  such that  $d \leq R$  the radius around a particle.

This change of height can be sampled at all points of the 2D grid by reducing the height by

$$\Delta h(\mathbf{p}) = \frac{\sqrt{R^2 - d^2}}{\alpha} = \frac{Q}{\frac{2}{3}\pi R^3} \sqrt{R^2 - d^2} \quad (7.9)$$

The height at each point after an erosion is then computed as  $\tilde{h}(\mathbf{p}) = h(\mathbf{p}) + \Delta h(\mathbf{p})$ .

#### 7.4.2 Application on layered terrains

Layered terrains are defined as  $\mu : \mathbb{R}^3 \mapsto \mathbb{N}$  assigning a discrete material index  $\mu$  for any point in space ( Beneš and Forsbach, 2001; Peytavie et al., 2009). In the original work, outer borders stack elements of the terrain are transformed into density-voxels to enable global erosion through height changes. We enable the erosion/deposition process directly on the layers hence removing the need for representation changes.

When intersecting the terrain, the amount eroded for each material stack should be the integration of the volume of the intersection between the sphere surrounding the particle and the cubicle represented by the stack. Since there is no easy solution ( Jones and Williams, 2017), we approximate the volume of the stack we need to alter using the previously defined

height field equation (7.9). At a distance  $d$  from the particle, the height is defined as:

$$H(d) = \frac{|Q|}{\frac{2}{3}\pi R^3} \sqrt{R^2 - d^2}. \quad (7.10)$$

If  $Q > 0$  (more deposition is applied than detachment) then we transform the materials in the stack contained in the sphere to become ground material. For  $Q < 0$  the materials are transformed in background material.

### 7.4.3 Application on implicit terrains

Implicit terrain are defined using a function  $f(\mathbf{p})$  and its variation resulting from the erosion process using  $\Delta f(\mathbf{p})$ . We propose a strategy to compute  $\Delta f(\mathbf{p})$  at any point of the sphere surrounding the erosion point based on metaball primitives. At each contact point a metaball is added to create a hole or a bump in the terrain. A metaball is defined as:

$$\Delta f(\mathbf{p}) = \frac{3Q}{\pi} \frac{(1-d)}{R} \quad (7.11)$$

with  $d$  the distance of the point  $\mathbf{p}$  to the sphere center. For all point  $\mathbf{p}$  for which  $d \geq R$ ,  $\Delta f(\mathbf{p}) = 0$  (see IV).

As they are the most commonly used representations, we propose a formulation to erode implicit terrains defined by Signed Distance Functions (SDF) and by gradient or vector fields.

**Signed Distance Functions** Considering SDF, the terrain is defined as the 0-set of the signed distance function  $f : \mathbb{R}^3 \mapsto \mathbb{R}$ , hence, for  $f(\mathbf{p}) = 0$ , the inside as  $f(\mathbf{p}) < 0$  and outer-part (i.e. air or water) as  $f(\mathbf{p}) > 0$ .

The particle erosion applies at impact points at discrete positions, so we propose to add or subtract metaballs defined using equation (7.11) to respectively deposit or erode material using a composition tree:

$$\text{metaball}(\mathbf{p}) = -\Delta f(\mathbf{p}).$$

Now the eroded terrain function  $\tilde{f}(\mathbf{p})$  will be evaluated at each point  $\mathbf{p}$  from the initial terrain value  $f(\mathbf{p})$ , the erosion function  $\text{metaball}(\mathbf{p})$  and the composition function  $g(f_1, f_2)$ :

$$\tilde{f}(\mathbf{p}) = g(f(\mathbf{p}), \text{metaball}(\mathbf{p})).$$

As a metaball is added for each particle bounce on the terrain space partitioning optimization algorithms such as k-d trees, BSP trees or BVH can easily be used to improve performances.

**Other implicit terrains** are present in the literature, notably a 2.5D representation based on the surface gradient ( E. Guérin et al., 2022) and a 3D representation based on curves ( Becher et al., 2017) for which the trajectory of each particle projected to the closest surface could be used to define the alteration of the terrain.

In the case of gradient-based representation, we propose to use the partial derivative from the equation of the 2D scalar fields (7.9) that gives:

$$\nabla h' = -\frac{Q}{\frac{2}{3}R^3} \frac{1}{\sqrt{R^2 - d^2}} \vec{CP} \quad (7.12)$$

with  $\vec{CP}$  the vector from the position  $\mathbf{p}$  to evaluate to the center of the erosion point  $c$ . Now the new gradient field can be computed as:

$$\nabla \tilde{h}(\mathbf{p}) = \nabla h(\mathbf{p}) + \nabla h'(\mathbf{p}).$$

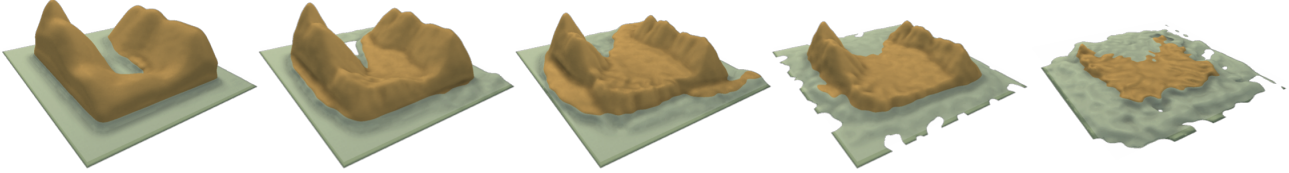


Figure 7.7: Our erosion method is applied iteratively on a completely synthetic island, the terrain is altered to obtain a plausible shape by forming rills. The use of particles with hydraulic densities dropped from the sky results in a strong erosion on the sides of the mountains, and the particles that slide to the sea are mainly drifting offshore resulting in the formation of small beaches and a weaker erosion on the bottom of the water body. Repeating the process causes the island height to decrease progressively up to the point where only the submerged part of the terrain is sheltered from erosion.

#### 7.4.4 Application on voxel grids

We consider two of the voxel grids representations: density-voxel grids and binary voxel grids for which we present our material alternation strategy.

**Density voxels.** We consider "density-voxel" grids defined on  $f : \mathbb{Z}^3 \mapsto [-1, 1]$  for which a voxel is full for  $f(\mathbf{p}) = 1$ , partially full for  $-1 < f(\mathbf{p}) < 1$  or empty for  $f(\mathbf{p}) \leq -1$ . This definition allows us to erode them smoothly. Since this kind of grid is a discretization of a scalar function, We could directly use (7.11), as described previously, but we take advantage of the discrete nature of the representation to avoid expensive computation.

We apply the erosion from a particle at position  $c$  on all points  $\mathbf{p}$  in the volume proportionally to the distance from the center of the sphere  $d = \|\mathbf{p} - c\|$  to find an approximation to the real erosion value per voxel  $Q_{approx} = Q \frac{1-d}{R}$ . Using their discrete nature, we rectify this value to sum up the total erosion value to  $Q$  by dividing each value by the sum of the distances. We now consider eroding the "empty" voxels since their density can drop until  $-1$ . We then have for all surrounding voxels:

$$\Delta f(\mathbf{p}) = Q \frac{(1 - \frac{d}{R})}{\sum (1 - \frac{d}{R})}. \quad (7.13)$$

Resulting voxel value is computed as  $\tilde{f}(\mathbf{p}) = f(\mathbf{p}) + \Delta f(\mathbf{p})$ . In our implementation, when  $f(\mathbf{p}) > 1$ , we simply transport the density excess to the above voxel, giving it a very close analogy to height fields as long as  $|\Delta f| < 1$ .

**Binary voxels** The terrain can be represented using an occupancy function as  $f : \mathbb{Z}^3 \mapsto \{0, 1\}$  where a voxel  $f = 1$  defines the ground and  $f = 0$  the background.

We propose to apply particle erosion by assigning voxels a number of hits, and transform them as air or as ground when this number reaches a critical value  $C$  that is proportional to the particle's strength parameter  $K_\epsilon$  ( Beardall et al., 2010).

On a hit, all voxels in a radius  $R$  receive a hit number:

$$\Delta hits = \lfloor \alpha \Delta f \rfloor \quad (7.14)$$

with  $\Delta f$  the erosion per voxel computed using (7.13) and  $\alpha$  a coefficient high enough to obtain values above 1.

All voxels with  $\#hits > C$  are transformed to background and voxels with  $\#hits < -C$  are transformed to ground.

Name	Rep.	Dimensions	Res	#P	#N	R	COR	$\rho_{\text{particle}}$	$C_{\text{factor}}$	$\varepsilon$	$\omega$	Vel f
Rain	H	100x100	20	100	10	1.0	1.0	1000	10.0	2.5	0.3	None
Coastal	DV	100x100x30	10	80	3	5	0.1	500	10.0	5.0	0.5	Uniform
Meanders	I	N/A	N/A	10	20	5.0	1.0	1000	1.0	1.0	1.0	( <sup>1</sup> )
River	H	100x100	5	100	50	1.5-5	0.5	900	0.1	1.0	1.0	None
Landslide	H	100x100	20	200	10	2.5	0.2	500	0.1	1.0	1.0	None
Volcano	DV	100x100x40	50	150	30	1.0	5.0	2000	1.0	1.0	5.0	None
Karst	BV	100x100x50	2	1000	40	5	0.5	500	10.0	5.0	0.5	Uniform
Tunnel	DV	100x100x50	1	100	100	2.5	0.1	500	1.0	1.0	1.0	None
Wind	DV	100x100x50	0.2	100	10	1.5	0.9	1.5	1.0	1.0	1.0	( Paris e)
Underwater	H	100x100	10	100	50	2.5	0.9	1000	1.0	1.0	1.0	( Stam, 2

Table 7.1: Parameters used for the generation of the terrains presented in Figure 7.14, with "Rep" the representation (H: Heightmap, DV: Density-voxels, BV: Binary voxels, I: Implicit) "Res" the resolution in meter per voxel or cell, #P the number of particles per iteration, #N the number of iterations, R the particles radius (in voxel or cell unit), COR the coefficient of restitution,  $\rho_{\text{particle}}$  the particle density in  $\text{kg m}^{-3}$ ,  $C_{\text{factor}}$ ,  $\varepsilon$  and  $\omega$  respectively the capacity, erosion and deposition factors, "Vel field" the type of velocity field used and t the computation time of the simulation in seconds on CPU.

(<sup>1</sup>) The velocity field is a vector field defined as  $v_{\text{fluid}}(\mathbf{p}) = [0 \sin(\mathbf{p}_x) 0]^T$ .

Note that, a binary voxel grid can also be transformed into a density-voxel grid to be eroded smoothly.

Our formulation for height fields (7.9), can be used to erode 2D scalar field-based representations. Similarly, our proposition for SDF (7.11) enables erosion for continuous 3D scalar fields and voxels (7.13) for discrete 3D scalar fields respectively.

## 7.5 Results

Our erosion process enables the simulation of a wide range of erosion effects on the major terrain representations alike. In this section, we present applications that demonstrate the versatility of our method by changing the particle's effect size, quantity, density, maximum capacity, deposition factor and the velocity fields. The results of each process are presented in Figure 7.14, parameters used are available at Table 7.1. It is important to note that all erosion examples presented in this section are available for any 3D terrain representation. However, we cannot create volumetric structure, such as overhangs, using 2.5D representations (height fields).

Environment density  $\rho_{\text{fluid}}$  is set to  $1 \text{ kg m}^{-3}$  above water level (terrain blue part) and to  $1000 \text{ kg m}^{-3}$  below it. Velocity field's refinement is done by using the presented diffusion strategy.

**Rain.** Hydraulic erosion from rain is the most common process used in terrain generation. In this case, particles are seen as water droplets falling from the sky and rolling downhill due to the gravitational force of Earth. No velocity field is required from fluid simulation. These parameters result in a detailed geometry of the rills on the side of mountains that quickly emerge and deposit many sediments in the valley. We demonstrate the result of rain erosion in *Figure 7.14: Rain* with a computation time of 4 seconds.

Using this erosion parameters in combination with water bodies results in different outcomes (Figure 7.7). The terrain above water is directly affected by the erosion process while particles colliding with the underwater part of the terrain are slowed down and filled with sediments,

leading to mainly apply deposition. The result is a typical hydraulic erosion on mountains and the formation of slopes and beaches near water level.

**Coastal erosion.** Waves repeated motion creates coastal erosion, that can be seen as cliffs with holes at the water level.

We apply a uniform velocity field in the water pointing towards the coast to simulate waves and emit particles from the water area with a large size, a density between air and water densities, a high capacity factor and a low deposition factor  $\omega$ . Using these parameters, the erosion process is focused at the interface of air and water, and apply a coarse detachment while depositing a very small quantity of sediments, simulating the corrosive effect of water on limestone.

This effect can only be simulated on 3D terrain representations, but will create cliffs on a 2D representation. *Figure 7.14: Coastal* presents the result of coastal erosion on a density-voxel grid that creates overhangs around sea level using a small amount of particles. Note that, the same effect using an alternate implicit representation based on SDF is displayed in Figure 7.10. A shaded version of this effect is presented in Figure 7.1.

**Rivers.** Given a source point, we generate particles that run downhill, simulating the formation of a river. More complex erosion simulation using fluid simulations like SPH (Krištof et al., 2009) would create realistic results at the cost of high processing time. Our method offers the flexibility to be applied either with a velocity field (simple, used given or resulting from a fluid simulation) or without allowing for simplicity and efficiency.

When provided with a hand-made or procedural velocity field, our particle system can reproduce simple river meanders (*Figure 7.14: Meanders*).

*Figure 7.14: River* presents a river that has been modeled by emitting water particles with different sizes that ranges from 1.5 m to 5 m, a high coefficient of restitution and a low capacity factor. Random sizes are used to simulate a river for which the flow rate had fluctuated over formation time, while the low capacity ensure that the banks of the river stays smooth. A high coefficient of restitution is a strategy that let the particles flow with low friction, approaching a water behaviour. Our particles are affected only by gravity, without fluid simulation.

**Landslide** are mainly caused by large amount of water saturating the ground and flowing downhill, transporting matter in its path.

By using water particles with a medium size, a low coefficient of restitution and a low capacity factor but a high deposition factor  $\omega$ , they transport sediments on short distances as the velocity quickly drops to 0, and ground material is completely spread along its path since it is easier to deposit the same amount of sediment than the eroded amount at each collision point. Reducing the density of the particle simulates a rise of viscosity in the settling velocity formula, increasing again the quantity of matter to deposit at contact with the ground. By this means, we can simulate landslides as illustrated on *Figure 7.14: Landslide*. A smoother surface is resulting, compared to the rain erosion as the rills are filled with sediments as soon as they begin to form. By setting the initial capacity of the particle equal to 10% of its max capacity, the mass of the terrain increases, simulating a volcano eruption as illustrated on *Figure 7.14: Volcano*.

**Karsts** networks are created over hundreds of years from the corrosion of water on the limestone in the ground. A limited number of methods have been proposed for the procedural generation of karsts (Paris et al., 2021).

By reducing the deposition factor  $\omega$ , the particles simulate corrosion (without mass conservation). We can use the same particle parameters than the coastal erosion (big size, a density between air and water densities, a high capacity factor and a low  $\omega$ ) and optionally provide a 3D shear stress map. The karst will automatically follow the softest materials, which is geologically coherent as given in example in *Figure 7.14: Karst*, where we can observe a

"pillar" that is formed in the center, and thus the karst forms two corridors that finally merge partially. Underground results are only available for representations allowing 3D structures. Another underground terrain simulation is shown in *Figure 7.14: Tunnel* in which a water runoff is eroding a tunnel without the use of a fluid simulation. Here, when particles bounce often on the terrain surface, the coefficient of restitution may be seen as a viscosity parameter.

**Wind** erosion is a significant process in deserts shaping since there are no obstacles on the airflow path. Air particles can reach high velocities, transporting sand over long distances forming either dunes or are blasted into rocks, eroding into goblins.

By setting the density of our particles close to  $1 \text{ kg m}^{-3}$ , two erosion simulations can be applied at once. Air particles follow closely the flowfield given by the user in air. This flowfield can be given from a complex simulation, a user-defined wind rose ( Paris et al., 2019a) or a random flowfield with a general direction.

The generation of the different sand structures depends on the velocity field provided, and a simple field will easily generate linear dunes. On contact with a rock block, the simulation will automatically erode block borders, creating shapes looking like gobelins.

*Figure 7.14: Wind* gives an example of wind erosion on a flat surface with rock columns being eroded. Given a strong 2D velocity field computed by the high wind simulation proposed in ( Paris et al., 2019a) is used on light particles, the simulation is fast thanks to the low number of collisions each particle has with the ground.

**Multiple phenomena** A terrain eroded with multiple erosion phenomena applied on a  $500 \times 500 \times 50$  density-voxel grid is illustrated in Figure 7.8. Here, water-density particles are applying rain on the terrain while the coasts of the river are being eroded thanks to a velocity field defined at the water level. The velocity field defined in the air mainly affects particles with air-density, such that wind erosion can be applied at the same time. The computation of these effects took 7 seconds on CPU.

**Underwater currents** Procedural generation of underwater 3D terrains has received little attention. The difference between the underwater and the surface rely on the buoyancy force that is much stronger, meaning that the water flow has a much more impacting effect on erosion than wind. Taking into account the density of the environment and the velocity field of water in our formulas are the keys to be able to apply any erosion in this environment. Our method works in a water environment by giving at least water density to particles. Given a velocity field describing underwater currents from a complex simulation or from a sketch, the particle system erodes the terrain.

In the example presented in *Figure 7.14: Underwater*, the velocity field is given by a simple 3D fluid simulation ( Stam, 1999) applied on the terrain.

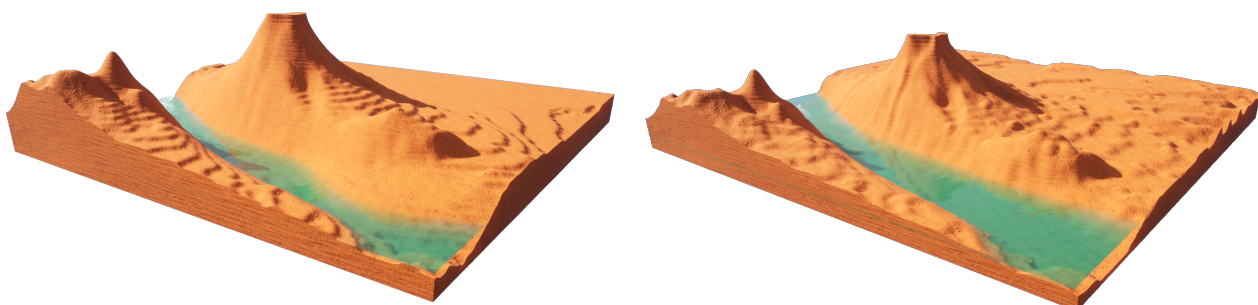


*Figure 7.8:* Multiple erosion types can be combined. On an initial synthetic  $500 \times 500 \times 50$  density voxel grid, the a wind erosion is applied on the surface of the terrain while hydraulic erosion shapes the rills and the base of the mountains. A water current digs its borders and spreads sediments at the bottom.

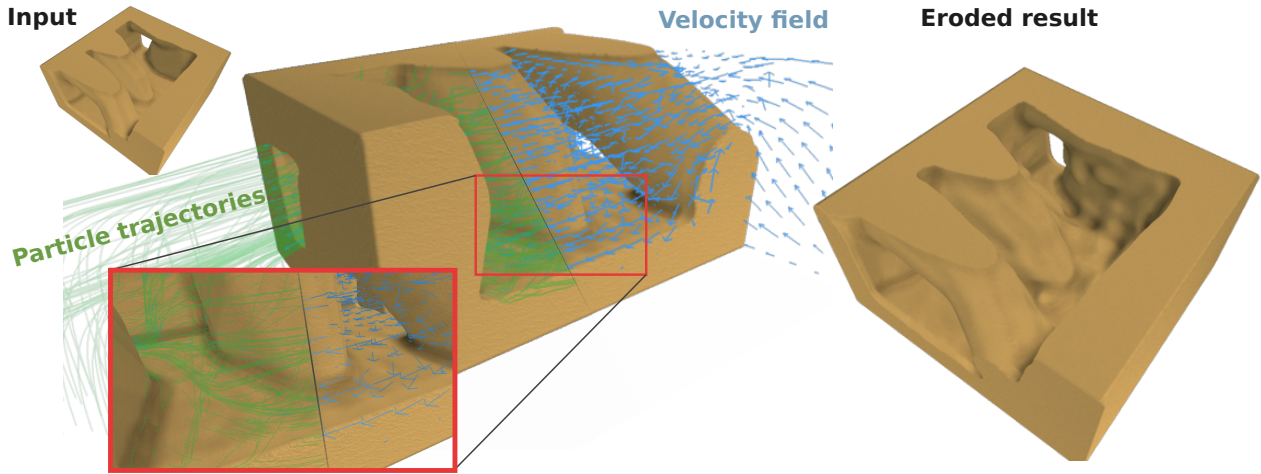


Figure 7.9: A complex water flow simulation is computed using OpenFOAM. Particle trajectories (green) are highly affected by the fluid velocity (blue). Most the terrain exposed surfaces is eroded (bottom).

A complex water flow simulation is computed using SIMPLE (Caretto et al., 1973) fluid simulation with OpenFOAM. The resulting erosion can then follow complex water movement and erode the terrain at the most affected parts of the 3D terrain as the trajectories of the particles (green) is highly affected by the fluid velocity (blue). The density of the particles and the environment being close, the buoyancy cancels most of the gravity force, leaving the velocity of the particles computed by the fluid velocity  $v_{\text{fluid}}$  and settling velocity  $w_s$  from (7.8) (Figure 7.9).

## 7.6 Comparisons

In the following section, we compare our method with existing ones to show that while we are versatile on the terrain representation, we are also able to reproduce various effects without applying specific algorithms. The other works are displayed in blue to distinguish them from ours.

**Coastal erosion on implicit terrain representation:** Paris et al present an erosion simulation method applied to implicit terrains able to create coastal erosion, karsts and caves by adding negative sphere primitive in the terrain's construction tree (Paris et al., 2019b). The positions of the spheres are determined using a Poisson disk sampling at the weakest terrain area defined by the Geology tree of their model. They are simulating the corrosion effect of water on the rocks. Our work is also able to approximate this phenomena by defining the position of these sphere primitives at the position where the water particles hit the surface. While the computation time of the positions of the sphere is higher due to the fact that we are evaluating the position of our particles at every time step in the implicit model (which could be improved by the triangulation of the implicit surface, or better, a dynamic triangulation), the distribution of our erosion primitives is based on a physical model instead of a mathematical model, meaning that we can integrate more easily the direction and strength of the waves for example. The management of their sphere primitives can be replicated with our method by considering that a particle exists until a collision occurs, at which point it disappears. Their method is not conserving the mass of the terrain, which is acceptable for the corrosion simulation, but limits its validity for other erosion simulations. In our method,



Figure 7.10: The algorithm proposed by Paris et al ( Paris et al., 2019b) allows for the simulation of coastal erosion (left) that we can reproduce almost identically by allowing our particles to collide only once with the ground and applying only erosion (center). If we apply our erosion with the full tracking of our particles and using deposition, we can achieve more diverse results (right).

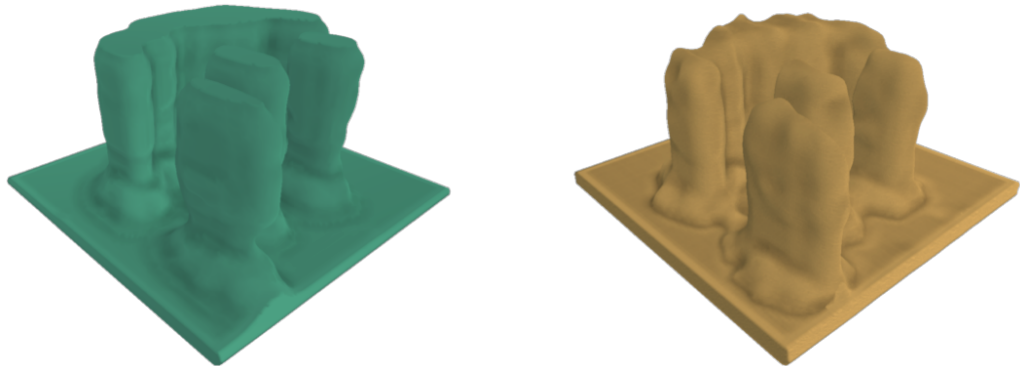


Figure 7.11: The algorithm proposed by Jones et al ( Beardall et al., 2010) allows for an efficient simulation of the spheroidal erosion, making the creation of gobelins on voxel grids in a plausible way (left). Our algorithm naturally erodes the most exposed areas of the terrain when particles are affected by the wind (right).

the particle can be tracked until it settles, ensuring mass conservation (Figure 7.10);

**Wind erosion on voxel grid representation:** Jones et al propose a weathering erosion on voxel grids by approximating and eroding continuously the most exposed voxels ( Beardall et al., 2010). When a solid voxel is decimated, it is considered deposit and is displaced down the slope until a minimal talus angle in the terrain is reached and if the deposition is eroded again, it disappears. Our work is able to reproduce their algorithm by sending our particles from a close distance to the terrain surface. By doing so, we reproduce the erosion process as much as the deposition process since the air particles, filled with sediments, is falling automatically towards the local minimum of the erosion point. Just like in their work, we can easily define the resistance value of the materials to add diversity in the results. By adding the possibility of a wind field, even a very simple uniform vector field, to the simulation, we naturally add the wind shadowing effect that protects a goblin surrounded by bigger gobelins, and also allows the deposit slope to fit more closely to the wind direction (Figure 7.11).

**Hydraulic erosion on height field representation:** Mei et al integrate and adapt to the GPU the pipe model proposed in ( O'Brien and Hodgins, 1995) for the fluid simulation ( Mei et al., 2007). This simulation is simple but efficient enough to approximate the Shallow-Water equations in real time and use the speed of columns of water to compute the erosion and

deposition rate on the 2D grid of the terrain at each time step. Using columns of water even allows the flow to overpass small bumps on the terrain over time. Our method initially rely on a stable fluid flow that is consistent during the whole life time of a particle, but by refining the simulation at each time step instead of at the end of the particles lifetime, our erosion model is able to reproduce this effect, allowing the terrain to have a single batch of fluid going through it. Our method can be seen as a generalization of Mei et al. that can then be used on more than discrete 2D grids (Figure 7.12).

**Wind erosion on stacked materials representation:** Paris et al ( Paris et al., 2019a) simulate the effect of wind over sand fields defined on stacked materials, creating dune structures, even taking into account obstacles like ( Roa and Benes, 2004) and different material layers like vegetation ( Cordonnier et al., 2017a) that are not affected by abrasion( Paris et al., 2019a). A wind field simulation is required to produce results, and while ( Roa and Benes, 2004) and ( Onoue and Nishita, 2000) consider a uniform vector field, this work consider a dynamic vector multi-scaled warped field from the terrain height. The sand grains then apply multiple moves: sand lift, bounces, reptation and avalanching. Once the sand is lifted by the wind, the trajectory of the grains can be seen as the displacement of particles, fitting completely with our model as illustrated Figure 7.13.

## 7.7 Discussion

This work is a generalization of erosion that is applicable to any terrain representation. In practice, while similar particle physics is used on different terrain representations, using similar parameters does not ensure resulting in the same eroded terrain. Surfaces and normals being approximated differently have rippling effect on particle trajectories. Note that, not all effects can be applied to all representations, for instance, karsts generation on 2.5D data structures.

*Realism* Realism of the erosion simulation is highly correlated to the size and quantity of particles used and their distribution. Using too few or distributing them too sparsely will result in a terrain that is unrealistic since the alteration will have localized effects, breaking process homogeneity.

The resolution is also limited by the number and size of the particles, which can be problematic on implicit terrains that can theoretically have a infinite resolution.

Our method allows to perform erosion on implicit terrains. However, in its current form, our algorithm is time expensive on implicit representations since a large number of primitives are added in the composition tree. Using skeletons-defined primitives ( Hong, 2013; Rigaudi  re et al., 2000)from particles trajectories and erosion/deposition values could be a solution to optimize the computation time.

*Usage of velocity fields* In our erosion algorithm, we simplify particle physics to enhance computational efficiency and facilitate parameterization. We use the velocity field from fluid simulations to approximate particle velocities. Sediment mass is harnessed to compensate for this approximation, allowing compatibility with various fluid simulation algorithms. Velocity fields can be recomputed at a frequency meeting the applications needs, ranging from "classic erosion simulation" (recomputed at each time step) to "simple simulation" (never recomputed). We addressed provisional adjustments to mitigate discrepancies when terrain changes due to erosion are not reflected in a static velocity field in section "3.3 Transport". However, it is important to note that these are expedient solutions and may not fully capture precise dynamics of an evolving terrain.

*Performances* To facilitate parallelization, we intentionally overlook particle interactions and sediment exchanges, albeit at the expense of achieving smoother results. Surface collisions are simplified to basic bounces with a damping parameter instead of relying on complex

particles and ground properties (Young's modulus, friction, material, ...)( Yan et al., 2020), further easing the parameterization process. However, these simplifications, combined with the inherent discrete nature of particles, as opposed to the continuous nature of erosion, result in a correlation between realism and particle count.

The performance of our method is influenced by the time required for collision detection. Consequently, we mainly observe better performances with explicit terrain models than with implicit models.

*Particle's atomicity* While we can replicate various effects, the "fan" shape commonly observed in natural erosion patterns is not perfectly represented. This limitation arises because we do not account for the splitting of a particle, a process that significantly influences the multidirectional dislocation and trajectory of individual particles ( Ranz et al., 1960). Additionally, we acknowledge an issue where particles may collide with the ceiling and the deposition is stuck. While a potential resolution involves splitting particles upon impact rather than simply depositing sediments, this introduces complexities to the parallelization layer of the method. Allowing particles to split introduces unpredictability in the total number of particles that will exist in the simulation. This unpredictability can complicate the use of multi-threading. Future works includes finding a data structure allowing this splitting efficiently, leading to more realistic erosion patterns.

*Simulation with multiple materials* One aspect we haven't addressed is a layered terrain with multiple materials. In the native way our method is done, we do not consider the transport of different materials (all sediments are considered as sand), but by storing a list of the different materials and the quantity transported by each particle, the same simulation process could be done at the cost of some memory and performance overhead.

Another possible adaptation of the erosion strategy for material voxels is to extend the erosion computation from binary voxels by define transformation rules from one material to another when a voxel is eroded a number  $\#hits < -C$  or  $\#hits > C$ . For example, the material "clay" may transform to "sand" when eroded or to "rock" when many depositions occurred.

## 7.8 Conclusion

We introduced a flexible particle-based erosion system that is easy to use and simple to implement. We have presented how to adapt the process for various terrain representations and generate a variety of erosion phenomenon due to rain, wind, water bodies... by adjusting intuitive parameters hence generate automatically realistic 2.5D and 3D terrains. The use of external velocity fields provides a high flexibility i.e. using the simulations that best fits the user's needs (precision, control, implementation efficiency...). Our method can also be applied to underwater environments with identical physics simulation since our erosion method can be applied on 3D representations. Erosion algorithms are often limited to the use of height fields, but by finding more generalized methods, we can go toward a global use of 3D terrains, which can offer richer and more diverse landscapes.

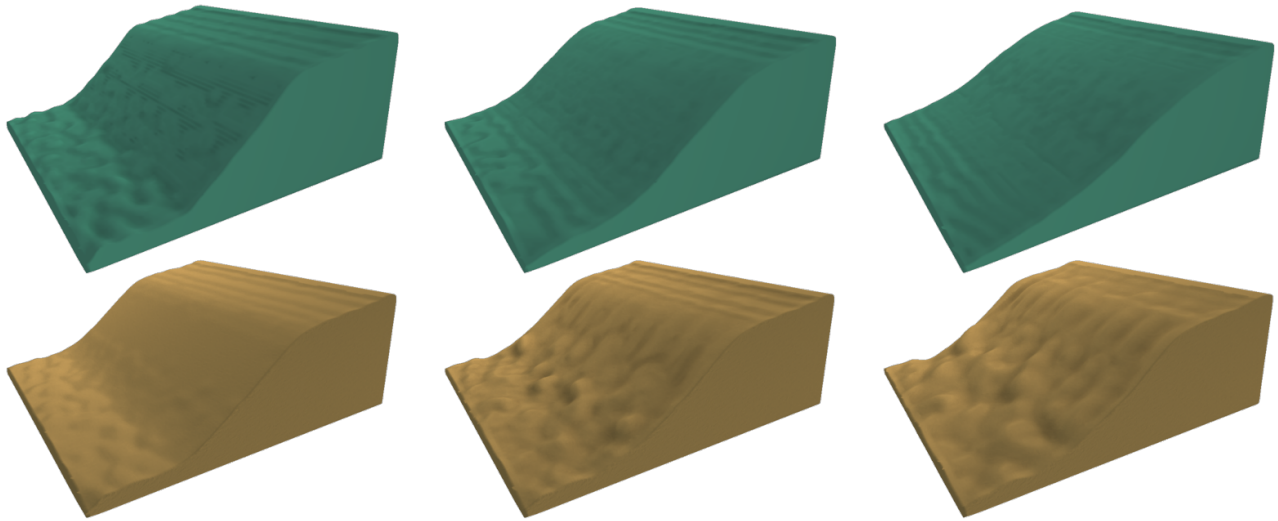


Figure 7.12: While our resulting geometry on the hydraulic erosion (bottom) is less smoothed than the one proposed by Mei et al. (Mei et al., 2007) (top), our method allows the application on more terrain representations than the height fields only.

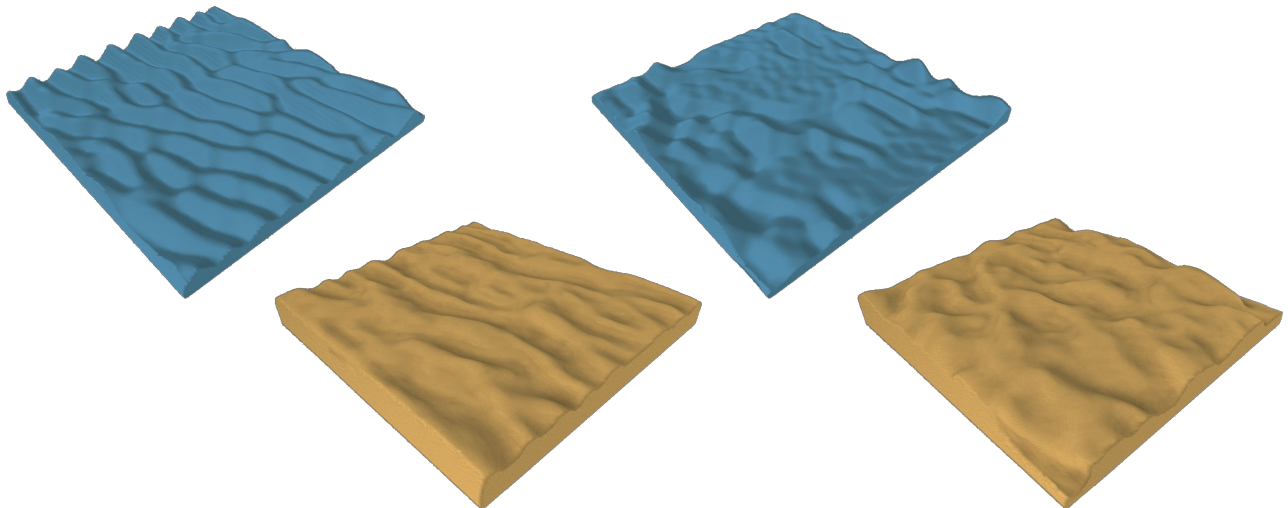


Figure 7.13: The algorithm from Paris 2020 allow the generation of desertscapes (top), which we can (at least partially) reproduce with our erosion simulation (bottom). The different effects are achieved by affecting the wind direction and strength.

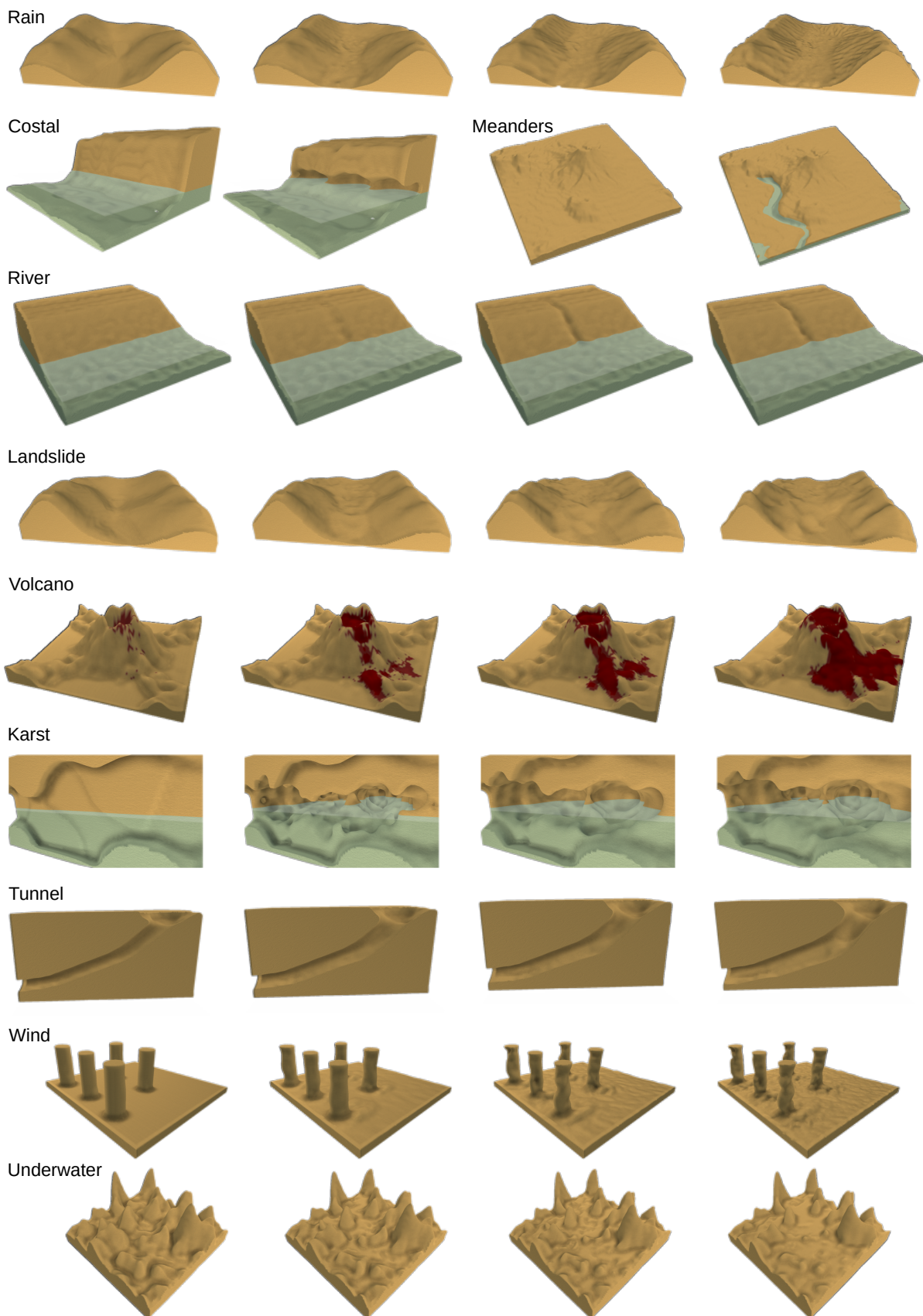


Figure 7.14: Erosion processes results on various representations presented in section 7. Used parameters used are detailed in Table 7.1.

## **Part IV**



---

## Conclusion

---

- ...



---

## References

---

- Abela, R., Liapis, A., & Yannakakis, G. N. (2015). A constructive approach for the generation of underwater environments. *Proceedings of the FDG workshop on Procedural Content Generation in Games* (cit. on p. 27).
- Argudo, O., Galin, E., Peytavie, A., Paris, A., & Guérin, E. (2020). Simulation, modeling and authoring of glaciers. *ACM Transactions on Graphics*, 39, 1–14. <https://doi.org/10.1145/3414685.3417855> (cit. on pp. 66, 68).
- Baraff, D., & Witkin, A. (1998). Large steps in cloth simulation. *Proceedings of the 25th Annual Conference on Computer Graphics and Interactive Techniques, SIGGRAPH 1998*, 43–54. <https://doi.org/10.1145/280814.280821> (cit. on p. 72).
- Beardall, M., Butler, J., Farley, M., & Jones, M. D. (2010). Directable weathering of concave rock using curvature estimation. *IEEE Transactions on Visualization and Computer Graphics*, 16, 81–94. <https://doi.org/10.1109/TVCG.2009.39> (cit. on pp. 75, 80).
- Becher, M., Krone, M., Reina, G., & Ertl, T. (2017). Feature-based volumetric terrain generation. *Proceedings - I3D 2017: 21st ACM SIGGRAPH Symposium on Interactive 3D Graphics and Games*. <https://doi.org/10.1145/3023368.3023383> (cit. on p. 74).
- Beneš, B., & Forsbach, R. (2001). Layered data representation for visual simulation of terrain erosion. *Proceedings - Spring Conference on Computer Graphics, SCCG 2001*, 80–86. <https://doi.org/10.1109/SCCG.2001.945341> (cit. on pp. 67, 68, 73).
- Beneš, B., Těšínský, V., Hornyš, J., & Bhatia, S. K. (2006). Hydraulic erosion. *Computer Animation and Virtual Worlds*, 17, 99–108. <https://doi.org/10.1002/cav.77> (cit. on p. 68).
- BOSSCHER, H., & SCHLAGER, W. (1992). Computer simulation of reef growth. *Sedimentology*, 39, 503–512. <https://doi.org/10.1111/j.1365-3091.1992.tb02130.x> (cit. on p. 27).
- Brosz, J., Samavati, F. F., & Sousa, M. C. (2007). Terrain synthesis by-example. *Communications in Computer and Information Science*, 4 CCIS, 58–77. [https://doi.org/10.1007/978-3-540-75274-5\\_4](https://doi.org/10.1007/978-3-540-75274-5_4) (cit. on p. 27).
- Caretto, L. S., Gosman, A. D., Patankar, S. V., & Spalding, D. B. (1973). Two calculation procedures for steady, three-dimensional flows with recirculation. *Proceedings of the Third International Conference on Numerical Methods in Fluid Mechanics*, 19, 60–68 (cit. on p. 79).
- Collon, P., Bernasconi, D., Vuilleumier, C., & Renard, P. (2017). Statistical metrics for the characterization of karst network geometry and topology. *Geomorphology*, 283, 122–142. <https://doi.org/10.1016/j.geomorph.2017.01.034> (cit. on p. 59).

- Collon, P., Steckiewicz-Laurent, W., Pellerin, J., Laurent, G., Caumon, G., Reichart, G., & Vaute, L. (2015). 3d geomodelling combining implicit surfaces and voronoi-based remeshing: A case study in the lorraine coal basin (france). *Computers and Geosciences*, 77, 29–43. <https://doi.org/10.1016/j.cageo.2015.01.009> (cit. on p. 59).
- Cordonnier, G., Braun, J., Cani, M.-P., Benes, B., Galin, É., Peytavie, A., & Guérin, É. (2016). Large scale terrain generation from tectonic uplift and fluvial erosion. *Computer Graphics Forum*, 35, 165–175. <https://doi.org/10.1111/cgf.12820> (cit. on pp. 52, 68).
- Cordonnier, G., Cani, M.-P., Beneš, B., Braun, J., & Galin, É. (2017a). Sculpting mountains: Interactive terrain modeling based on subsurface geology. *IEEE Transactions on Visualization and Computer Graphics*, 24. <https://doi.org/10.1109/TVCG.2017.2689022> (cit. on pp. 52, 66, 68, 81).
- Cordonnier, G., Ecormier-nocca, P., Galin, É., Gain, J., Beneš, B., & Cani, M.-P. (2018). Interactive generation of time-evolving, snow-covered landscapes with avalanches. *Computer Graphics Forum*, 37, 497–509. <https://doi.org/10.1111/cgf.13379> (cit. on pp. 66, 68).
- Cordonnier, G., Galin, É., Gain, J., Beneš, B., Guérin, É., Peytavie, A., & Cani, M.-P. (2017b). Authoring landscapes by combining ecosystem and terrain erosion simulation. *ACM Transactions on Graphics*, 36. <https://doi.org/10.1145/3072959.3073667> (cit. on pp. 66, 68).
- Cordonnier, G., Jouvet, G., Peytavie, A., Braun, J., Cani, M.-P., Benes, B., Galin, E., Guérin, E., & Gain, J. (2023). Forming terrains by glacial erosion. *ACM Transactions on Graphics*, 42, 14. [\\"{i}](https://doi.org/10.1145/3592422) (cit. on pp. 27, 66).
- Cortial, Y., Peytavie, A., Galin, É., & Guérin, É. (2019). Procedural tectonic planets. *Eurographics Computer Graphics Forum*, 38, 1–11. <https://doi.org/10.1111/cgf.13614> (cit. on p. 27).
- Cowart, L., Walsh, J. P., & Corbett, D. R. (2010). Analyzing estuarine shoreline change: A case study of cedar island, north carolina. *Journal of Coastal Research*, 265, 817–830. <https://doi.org/10.2112/jcoastres-d-09-00117.1> (cit. on p. 37).
- Dey, R., Doig, J. G., & Gatzidis, C. (2018). Procedural feature generation for volumetric terrains using voxel grammars. *Entertainment Computing*, 27, 128–136. <https://doi.org/10.1016/j.entcom.2018.04.003> (cit. on p. 68).
- Domínguez, L., Anfuso, G., & Gracia, F. J. (2005). Vulnerability assessment of a retreating coast in sw spain. *Environmental Geology*, 47, 1037–1044. <https://doi.org/10.1007/s00254-005-1235-0> (cit. on p. 37).
- Droxler, A. W., & Jorry, S. J. (2021). The origin of modern atolls : Challenging darwin's deeply ingrained theory. *Annual Review of Marine Science*. <https://doi.org/https://doi.org/10.1146/annurev-marine-122414-034137> (cit. on p. 52).
- Ecormier-Nocca, P., Cordonnier, G., Carrez, P., Moigne, A. M., Memari, P., Benes, B., & Cani, M. P. (2021). Authoring consistent landscapes with flora and fauna. *ACM Transactions on Graphics*, 40. <https://doi.org/10.1145/3450626.3459952> (cit. on p. 30).
- Eisemann, E., & Decoret, X. (2008). Single-pass gpu solid voxelization for real-time applications. *Proceedings - Graphics Interface*, 73–80 (cit. on p. 68).
- Emilien, A., Poulin, P., Cani, M.-P., & Vimont, U. (2015). Interactive procedural modelling of coherent waterfall scenes. *Computer Graphics Forum*, 34, 22–35. <https://doi.org/10.1111/cgf.12515> (cit. on p. 67).
- Fernandes, G. D., & Fernandes, A. R. (2018). Space colonisation for procedural road generation. *2018 International Conference on Graphics and Interaction (ICGI)*, 1–8. <https://doi.org/10.1109/ITCGI.2018.8602928> (cit. on p. 59).
- Gain, J., Marais, P., & Straßer, W. (2009). Terrain sketching. *Proceedings of I3D 2009: The 2009 ACM SIGGRAPH Symposium on Interactive 3D Graphics and Games*, 1, 31–38. <https://doi.org/10.1145/1507149.1507155> (cit. on pp. 27, 53, 67).

- Galin, E., Guérin, E., Peytavie, A., Cordonnier, G., Cani, M.-P., Benes, B., & Gain, J. (2019). A review of digital terrain modeling. *Computer Graphics Forum*, 38, 553–577. <https://doi.org/10.1111/cgf.13657> (cit. on pp. 27, 66, 67).
- Galin, É., Peytavie, A., Maréchal, N., & Guérin, É. (2010). Procedural generation of roads. *Computer Graphics Forum*, 29, 429–438. <https://doi.org/10.1111/j.1467-8659.2009.01612.x> (cit. on p. 59).
- Goes, F. D., & James, D. L. (2017). Regularized kelvinlets: Sculpting brushes based on fundamental solutions of elasticity. *ACM Transactions on Graphics*, 36, 401–411. <https://doi.org/10.1145/3072959.3073595> (cit. on pp. 30, 34).
- Grosbellet, F., Peytavie, A., Guérin, É., Galin, É., Mérillou, S., & Benes, B. (2016). Environmental objects for authoring procedural scenes. *Computer Graphics Forum*, 35, 296–308. <https://doi.org/10.1111/cgf.12726> (cit. on p. 28).
- Guérin, E., Peytavie, A., Masnou, S., Digne, J., Sauvage, B., Gain, J., & Galin, E. (2022). Gradient terrain authoring. *Computer Graphics Forum*, 41, 85–95. <https://doi.org/10.1111/cgf.14460> (cit. on pp. 68, 74).
- Guérin, É., Digne, J., Galin, É., & Peytavie, A. (2016). Sparse representation of terrains for procedural modeling. *Computer Graphics Forum*, 35, 177–187. <https://doi.org/10.1111/cgf.12821> (cit. on pp. 28, 68).
- Guérin, É., Digne, J., Galin, É., Peytavie, A., Wolf, C., Beneš, B., & Martinez, B. (2017). Interactive example-based terrain authoring with conditional generative adversarial networks. *ACM Transactions on Graphics*, 36. <https://doi.org/10.1145/3130800.3130804> (cit. on p. 27).
- Hong, Q. (2013). A skeleton-based technique for modelling implicit surfaces. *Proceedings of the 2013 6th International Congress on Image and Signal Processing, CISIP 2013*, 2, 686–691. <https://doi.org/10.1109/CISP.2013.6745253> (cit. on p. 81).
- Ito, T., Fujimoto, T., Muraoka, K., & Chiba, N. (2003). Modeling rocky scenery taking into account joints. *Proceedings of Computer Graphics International Conference, CGI, 2003-Janua*, 244–247. <https://doi.org/10.1109/CGI.2003.1214475> (cit. on p. 68).
- Jones, B. D., & Williams, J. R. (2017). Fast computation of accurate sphere-cube intersection volume. *Engineering Computations*, 34, 1204–1216. <https://doi.org/10.1108/EC-02-2016-0052> (cit. on p. 73).
- Kapp, K., Gain, J., Guérin, E., Galin, E., & Peytavie, A. (2020). Data-driven authoring of large-scale ecosystems. *ACM Transactions on Graphics*, 39. <https://doi.org/10.1145/3414685.3417848> (cit. on p. 27).
- Kaufman, A., Cohen, D., & Yagel, R. (1993). Volume graphics. *Computer*, 26, 51–64. <https://doi.org/10.1109/MC.1993.274942> (cit. on p. 68).
- Koschier, D., Bender, J., Solenthaler, B., & Teschner, M. (2022). A survey on sph methods in computer graphics. *Computer Graphics Forum*, 41, 737–760. <https://doi.org/10.1111/cgf.14508> (cit. on p. 72).
- Krištof, P., Beneš, B., Křivánek, J., & Šťava, O. (2009). Hydraulic erosion using smoothed particle hydrodynamics. *Computer Graphics Forum*, 28, 219–228. <https://doi.org/10.1111/j.1467-8659.2009.01361.x> (cit. on pp. 67–69, 72, 77).
- Lengyel, E. (2010). Voxel-based terrain for real-time virtual simulations, 148 (cit. on p. 68).
- Li, W. (2021). Procedural modeling of the great barrier reef. *Lecture Notes in Computer Science (including subseries Lecture Notes in Artificial Intelligence and Lecture Notes in Bioinformatics)*, 13017 LNCS, 381–391. [https://doi.org/10.1007/978-3-030-90439-5\\\_30](https://doi.org/10.1007/978-3-030-90439-5\_30) (cit. on p. 27).

- Mareschal, J. C. (1989). Fractal reconstruction of sea-floor topography. *Pure and Applied Geophysics PAGEOPH*, 131, 197–210. <https://doi.org/10.1007/BF00874487> (cit. on p. 27).
- Mei, X., Decaudin, P., & Hu, B. G. (2007). Fast hydraulic erosion simulation and visualization on gpu. *Proceedings - Pacific Conference on Computer Graphics and Applications*, 47–56. <https://doi.org/10.1109/PG.2007.27> (cit. on pp. 68, 80, 83).
- Michel, E., Emilien, A., & Cani, M.-P. (2015). Generation of folded terrains from simple vector maps. *Eurographics 2015 short paper proceedings*, 4–8. <https://doi.org/10.2312/egsh.20151019> (cit. on p. 27).
- Musgrave, F. K., Kolb, C. E., & Mace, R. S. (1989). The synthesis and rendering of eroded fractal terrains. *Proceedings of the 16th Annual Conference on Computer Graphics and Interactive Techniques, SIGGRAPH 1989*, 41–50. <https://doi.org/10.1145/74333.74337> (cit. on pp. 27, 66, 68).
- Neidhold, B., Wacker, M., & Deussen, O. (2005). Interactive physically based fluid and erosion simulation. *Natural Phenomena*, 25–32 (cit. on pp. 66, 68).
- O'Brien, J. F., & Hodgins, J. K. (1995). Dynamic simulation of splashing fluids. *Proceedings Computer Animation, CA 1995*, 198–205. <https://doi.org/10.1109/CA.1995.393532> (cit. on p. 80).
- Olsen, J. (2004). Realtime procedural terrain generation. *Department of Mathematics And Computer Science* (..., 20 (cit. on p. 66).
- Onoue, K., & Nishita, T. (2000). A method for modeling and rendering dunes with wind-ripples. *Proceedings - Pacific Conference on Computer Graphics and Applications, 2000-Janua*, 427–428. <https://doi.org/10.1109/PCCGA.2000.883978> (cit. on p. 81).
- Oron, S., Akkaynak, D., Tchernov, B. N. G., & Shaked, Y. (2023). How monster storms shape fringing reefs: Observations from the 2020 middle east cyclone. *Ecosphere*, 14. <https://doi.org/10.1002/ecs2.4602> (cit. on p. 37).
- Paris, A., Guérin, E., Peytavie, A., Collon, P., & Galin, E. (2021). Synthesizing geologically coherent cave networks. *Computer Graphics Forum*, 40, 277–287. <https://doi.org/10.1111/cgf.14420> (cit. on pp. 59, 60, 77).
- Paris, A., Peytavie, A., Guérin, E., Argudo, O., & Galin, E. (2019a). Desertscape simulation. *Computer Graphics Forum*, 38, 47–55. <https://doi.org/10.1111/cgf.13815> (cit. on pp. 34, 68, 78, 81).
- Paris, A., Galin, E., Peytavie, A., Guérin, E., & Gain, J. (2019b). Terrain amplification with implicit 3d features. *ACM Transactions on Graphics*, 38, 1–15. <https://doi.org/10.1145/3342765> (cit. on pp. 27, 68, 76, 79, 80).
- Patel, D., Natali, M., Lidal, E. M., Parulek, J., Brazil, E. V., & Viola, I. (2021). Modeling terrains and subsurface geology. *Interactive Data Processing and 3D Visualization of the Solid Earth*, 1–43. [https://doi.org/10.1007/978-3-030-90716-7\\_1](https://doi.org/10.1007/978-3-030-90716-7_1) (cit. on pp. 27, 53).
- Peytavie, A., Galin, E., Grosjean, J., & Merillou, S. (2009). Arches: A framework for modeling complex terrains. *Computer Graphics Forum*, 28, 457–467. <https://doi.org/10.1111/j.1467-8659.2009.01385.x> (cit. on pp. 67, 68, 73).
- Pytel, A., & Mann, S. (2015). Procedural modeling of cave-like channels. (Cit. on p. 59).
- Ranz, W. E., Talandis, G. R., & Guttermann, B. (1960). Mechanics of particle bounce. *AIChE Journal*, 6, 124–127. <https://doi.org/10.1002/aic.690060123> (cit. on p. 82).
- Richardson, J. F., & Zaki, W. N. (1954). The sedimentation of a suspension of uniform spheres under conditions of viscous flow. *Chemical Engineering Science*, 3 (cit. on p. 71).
- Rigaudière, D., Gesquière, G., & Faudot, D. (2000). Shape modelling with skeleton based implicit primitives. *Methods* (cit. on p. 81).

- Roa, T., & Benes, B. (2004). Simulating desert scenery. *Winter School of Computer Graphics SHORT communication Papers Proceedings*, 17–22 (cit. on pp. 68, 81).
- Roose, D., Leuven, K. U., & López, Y. R. (2011). Dynamic refinement for fluid flow simulations with sph particle refinement for fluid flow simulations with sph. (Cit. on p. 72).
- Roudier, P. (1993). Synthèse de paysages réalistes par simulation de processus d'érosion (cit. on p. 66).
- Runions, A. (2008). Modeling biological patterns using the space colonization algorithm. *A Thesis submitted to the faculty of graduate studies for degree of master of science*, 74 (cit. on p. 59).
- Schott, H., Paris, A., Fournier, L., Guérin, E., & Galin, E. (2023). Large-scale terrain authoring through interactive erosion simulation. *ACM Transactions on Graphics*, 42, 1–15. <https://doi.org/10.1145/3592787> (cit. on p. 27).
- Smelik, R. M., Kraker, K. J. D., Groenewegen, S. A., Tutenel, T., & Bidarra, R. (2009). A survey of procedural methods for terrain modelling. *Proceedings of the CASA workshop on 3D advanced media in gaming and simulation (3AMIGAS)* (cit. on p. 66).
- Stachniak, S., & Stuerzlinger, W. (2005). An algorithm for automated fractal terrain deformation. In *Proceedings of Computer Graphics and Artificial Intelligence*, 64–76 (cit. on p. 66).
- Stam, J. (1999). Stable fluids. *Proceedings of the 26th Annual Conference on Computer Graphics and Interactive Techniques, SIGGRAPH 1999*, 121–128. <https://doi.org/10.1145/311535.311548> (cit. on p. 78).
- Stam, J. (2003). Flows on surfaces of arbitrary topology. *ACM Transactions on Graphics*, 22, 724–731. <https://doi.org/10.1145/882262.882338> (cit. on p. 76).
- Stokes, G. G. (2009, July). On the effect of the internal friction of fluids on the motion of pendulums. Cambridge University Press. <https://doi.org/10.1017/CBO9780511702266.002> (cit. on p. 71).
- Swope, W. C., Andersen, H. C., Berens, P. H., & Wilson, K. R. (1982). A computer simulation method for the calculation of equilibrium constants for the formation of physical clusters of molecules: Application to small water clusters. *The Journal of Chemical Physics*, 76, 637–649. <https://doi.org/10.1063/1.442716> (cit. on p. 72).
- Talgorn, F. X., & Belhadj, F. (2018). Real-time sketch-based terrain generation. *ACM International Conference Proceeding Series*, 13–18. <https://doi.org/10.1145/3208159.3208184> (cit. on p. 27).
- Tychonievich, L. A., & Jones, M. D. (2010). Delaunay deformable mesh for the weathering and erosion of 3d terrain. *Visual Computer*, 26, 1485–1495. <https://doi.org/10.1007/s00371-010-0506-2> (cit. on p. 71).
- Verlet, L. (1967). Computer "experiments" on classical fluids. i. thermodynamical properties of lennard-jones molecules. *Physical Review*, 159, 98–103. <https://doi.org/10.1103/PhysRev.159.98> (cit. on p. 72).
- Vila-Concejo, A., & Kench, P. (2016, August). Storms in coral reefs. Wiley Blackwell. <https://doi.org/10.1002/9781118937099.ch7> (cit. on p. 37).
- Wejchert, J., & Haumann, D. (1991). Animation aerodynamics. *Proceedings of the 18th Annual Conference on Computer Graphics and Interactive Techniques, SIGGRAPH 1991*, 25, 19–22. <https://doi.org/10.1145/122718.122719> (cit. on pp. 28, 30, 34).
- Wojtan, C., Carlson, M., Mucha, P. J., & Turk, G. (2007). Animating corrosion and erosion. *Natural Phenomena*, 15–22 (cit. on pp. 69–72).
- Yan, P., Zhang, J., Kong, X., & Fang, Q. (2020). Numerical simulation of rockfall trajectory with consideration of arbitrary shapes of falling rocks and terrain. *Computers and Geotechnics*, 122. <https://doi.org/10.1016/j.compgeo.2020.103511> (cit. on pp. 71, 82).



---

## Glossary

---

**Environmental attribute** Meh.... iv, 25, 28–31, 33, 35, 40

**Environmental modifier** Meh.... iv, 25, 28–30, 33, 34, 36, 40

**Fitness function** Meh.... iv, 25, 28–33, 35, 36, 38–40

**Generation rule** Meh.... 28, 29, 31, 32

**Geomorphic event** Meh.... 28, 29, 35–38, 40

**Semantic Terrain Entity** Meh.... iv, 25, 28–36, 38–41, 97

**Skeleton fitting function** Meh.... iv, 25, 30–32



---

## Acronyms

---

**STE** Semantic Terrain Entity. *Glossary:* Semantic Terrain Entity



# Appendices



---

## Data structures

---

- ...

### .1 3D grids

- In this manuscript, all 3D grids are defined as signed float32.
- Not optimal, especially for representing binary voxels (uses 32x more memory and computation than necessary), but flexible...
- Voxel grids stored as lists of sub-grids ("local modifications") to navigate undo-redo. Cell evaluation by summing sub-grids.
- ...



- ...

## .2 Points

- Defined in 3D space as  $(x, y, z)^T$ .
- When projected in 2D,  $z = 0$  is implicit.
- Represented in the manuscript as:  $\mathbf{p} \in \mathbb{R}^3$
- ...

## .3 Curves

- Parametric function  $C : [0, 1] \mapsto \mathbb{R}^3$ .
- Unless otherwise specified, use of Centripetal Catmull–Rom spline [CITE CATMULL 1974]:
- \*\* Let  $\mathbf{p}_i$  denote a point. For a curve segment  $C$  defined by points  $\mathbf{p}_0, \mathbf{p}_1, \mathbf{p}_2, \mathbf{p}_3$  and knot sequence  $t_0, t_1, t_2, t_3$ , the centripetal Catmull-Rom spline can be produced by:

$$C(t) = \frac{t_2 - t}{t_2 - t_1} B_1 + \frac{t - t_1}{t_2 - t_1} B_2 \quad (15)$$

where

$$B_1(t) = \frac{t_2 - t}{t_2 - t_0} A_1(t) + \frac{t - t_0}{t_2 - t_0} A_2(t) \quad (16)$$

$$B_2(t) = \frac{t_3 - t}{t_3 - t_1} A_2(t) + \frac{t - t_1}{t_3 - t_1} A_3(t) \quad (17)$$

$$A_1(t) = \frac{t_1 - t}{t_1 - t_0} \mathbf{p}_0 + \frac{t - t_0}{t_1 - t_0} \mathbf{p}_1 \quad (18)$$

$$A_2(t) = \frac{t_2 - t}{t_2 - t_1} \mathbf{p}_1 + \frac{t - t_1}{t_2 - t_1} \mathbf{p}_2 \quad (19)$$

$$A_3(t) = \frac{t_3 - t}{t_3 - t_2} \mathbf{p}_2 + \frac{t - t_2}{t_3 - t_2} \mathbf{p}_3 \quad (20)$$

and

$$t_{i+1} = \sqrt{(x_{i+1} - x_i)^2 + (y_{i+1} - y_i)^2 + (z_{i+1} - z_i)^2}^\alpha + t_i \quad (21)$$

where  $\alpha$  ranges from 0 to 1 for knot parameterization, and  $i = 0, 1, 2, 3$  with  $t_0 = 0$ . For centripetal Catmull-Rom spline, the value of  $\alpha$  is 0.5. When  $\alpha = 0$ , the resulting curve is the standard uniform Catmull-Rom spline; when  $\alpha = 1$ , the result is a chordal Catmull-Rom spline.

\*\* We will keep  $\alpha = 0.5$  for all the work in this manuscript, as it felt like a good compromise between smoothness and control on the curve. The value of  $\alpha$  has not been studied deeply.

- Advantages: Centripetal Catmull-Rom spline has several desirable mathematical properties compared to the original and other types of Catmull-Rom formulations. First, it will not form loops or self-intersections within a curve segment. Second, cusps will never occur within a curve segment. Third, it follows the control points more tightly. [COPY PASTE WIKIPEDIA]

- Additionally, we do not use "handles" (invisible control points) like for Bézier curves. At the cost of a little user control, I feel the use is simplified.

- The calculation of first and second derivatives (tangent and normal) is quick.

- ...

---

## Snake - Modèle de contour actif

---

Nous souhaitons symboliser une zone de corail mort comme étant un objet environemental "récif". Pour cela, les objets corail déposent continuellement une quantité de materiau "corail mort". Ce materiau, stocké dans un champ scalaire discret, contient alors de fortes intensités là où un récif devrait, semblerait-il, exister. Il faut alors tracer une courbe pour représenter ce nouvel objet. Les contraintes de cette courbe est qu'elle doit traverser les points de plus haute intensité, tout en conservant une longueur donnée. L'algorithme de Snake, ou Active Contour Model (Modèle de Contour Actif en français) s'approche de cette application. L'algorithme propose de donner une énergie à la courbe, qui essaie alors de la minimiser par descente de gradients. L'énergie, dans le papier initial est défini par

$$E_{\text{snake}}^* = \int_0^1 E_{\text{snake}}(\mathbf{v}(s)) ds = \int_0^1 (\alpha + \beta) E_{\text{internal}}(\mathbf{v}(s)) + \gamma E_{\text{image}}(\mathbf{v}(s)) + E_{\text{cont}}(\mathbf{v}(s))) ds$$

L'énergie interne représente les propriétés de la courbe :

$$E_{\text{internal}} = \alpha E_{\text{cont}} + \beta E_{\text{curv}}$$

Le coût de continuité  $E_{\text{cont}}$ , originellement definit comme la minimisation de l'espacement entre les points  $\left\| \frac{d\bar{v}}{ds}(s) \right\|^2$ , n'a pas beaucoup de sens dans la forme discrète de l'algorithme. Dans sa forme discrète on cherche à conserver un interval régulier entre les points en appliquant  $E_{\text{cont}} = (\tilde{d} - \|p_i - p_{i-1}\|)^2$  avec  $\tilde{d}$  la distance moyenne entre chaque point.

Le coût de courbure  $E_{\text{curv}}$  cherche à minimiser les oscillations de la courbe et peut alors se définir comme la derivée seconde au carré  $\left\| \frac{d^2\bar{v}}{ds^2}(s) \right\|^2$ . La forme discrète  $E_{\text{curv}}^* = \|p_{i-1} - 2p_i + p_{i+1}\|^2$  n'est pas nécessaire avec des splines, dû à leur forme close.

Le coût d'image  $E_{\text{image}}$  essaie d'attirer les points de la courbe vers un maximum local du gradient de l'image. On le définit par  $E_{\text{image}} = -\|\nabla I\|$

Nous souhaitons voir notre courbe garder une longueur donnée  $L$ . On modifie alors la formulation du cout de continuité pour devenir  $E_{\text{cont}} = (\tilde{l} - \|p_i - p_{p-1}\|)^2$  avec  $\tilde{l} = \frac{L}{n-1}$  sachant  $n$  le nombre de sommets de la courbe. De plus, on souhaite une courbe qui suit les points de haute intensité plutôt que le gradient, ce qui revient à modifier le coût d'image  $E_{\text{image}} = -I$ .

Le calcul du gradient  $\nabla E_{\text{snake}}$  reste trivial par parties :

$$\begin{aligned}\frac{\partial E_{\text{image}}}{\partial p_i} &= -\nabla I(p_i) \\ \frac{\partial E_{\text{curv}}^*}{\partial p_i} &= -\frac{2(p_{i-1} - 2p_i + p_{i+1})}{\|p_{i-1} - 2p_i + p_{i+1}\|} \\ \frac{\partial E_{\text{cont}}^*}{\partial p_i} &= 2(l - \|p_i - p_{i-1}\|) \cdot \frac{p_i - p_{i-1}}{\|p_i - p_{i-1}\|}\end{aligned}$$

Nous avons alors

$$E_{\text{snake}} = \alpha(l - \|p_i - p_{i-1}\|)^2 + \beta\|p_{i-1} - 2p_i + p_{i+1}\|^2 - \gamma I \quad (22)$$

$$\nabla E_{\text{snake}} = 2\alpha(l - \|p_i - p_{i-1}\|) \cdot \frac{p_i - p_{i-1}}{\|p_i - p_{i-1}\|} - \beta \frac{2(p_{i-1} - 2p_i + p_{i+1})}{\|p_{i-1} - 2p_i + p_{i+1}\|} - \gamma \nabla I(p_i) \quad (23)$$

Il est à noter que le calcul de  $E_{\text{cont}}^*$  utilise la distance  $\|p_i - p_{i-1}\|$ . Pour  $i = 0$ , on utilise la distance  $\|p_i - p_{i+1}\|$ . Si tous les points de la courbe sont à une distance supérieure à  $l$ , l'optimisation poussera chacun de ces points à se rapprocher son point précédent. Le point  $p_0$ , lui, ne se déplacera très peu, donc l'ensemble de la courbe se cale vers le point  $p_0$ . En utilisant la distance vers le successeur  $\|p_i - p_{i+1}\|$ , la courbe se déplace en direction du point  $p_N$ . Il est alors possible de converger vers le point médian en alternant l'utilisation de distance avec le précédent et avec le successeur, au coût d'une convergence plus lente.

L'algorithme de modèle de contour actif est fortement sensible à l'emplacement de la courbe de départ. Dans le cas où une portion de la courbe se situe dans un endroit à très faible gradient sur  $E_{\text{image}}$ , les sommets de la courbe vont simplement optimiser  $E_{\text{internal}}$ , résultant en un segment droit, dans une zone à faible intensité, tandis que le reste de la courbe s'optimise correctement. Afin de limiter ce problème, on propose d'adapter l'algorithme Snake en Catapillar: tout au long de la descente de gradient, on réduit puis agrandit artificiellement la longueur cible  $L$ . De cette manière, une portion de courbe bloqué dans une région sans optimisation possible sur l'énergie externe sera attirée par la courbe optimisée jusqu'à retomber sur un gradient fort. La portion morte peut prendre la place des sommets optimisés. En ramenant la longueur cible  $L$  à la valeur initiale, l'optimisation est continuée avec des sommets en moins dans la zone morte. La répétition de ce procédé permet de ramener, petit à petit, tous les points en zone optimisable. Néanmoins, un changement trop rapide de la longueur cible peut empêcher les sommets d'optimiser  $E_{\text{external}}$  en amplifiant trop  $E_{\text{internal}}$ . De plus, cet algorithme peut amener à des erreurs numériques et une convergence ralentie.

---

## Computation of a metaball

---

We use the following formula to evaluate a metaball in space with a center  $c$  and of radius  $R$ :

$$g(\mathbf{p}) = 1 - \frac{\|\mathbf{p} - c\|}{R}$$

using the euclidean distance.

We have a total amount  $Q$  to define in this space, so the final metaball function  $f$  needs to satisfy the equations (24) and (25):

$$f(\mathbf{p}) = \lambda g(\mathbf{p}) \quad (24)$$

$$\int_{\mathbf{p} \in V_{3D}} f d\mathbf{p} = Q \quad (25)$$

First, let's exploit the radial symmetry of the metaball and rewrite  $g(\mathbf{p}) = 1 - r$  by using the polar coordinates of the point  $\mathbf{p} - c$ .

We can then integrate  $g$  over the volume  $V_{3D}$  as

$$\begin{aligned} & \int_0^1 \int_0^\pi \int_0^{2\pi} g(r)r^2 \sin(\theta) dr d\theta d\phi \\ &= \int_0^1 \int_0^\pi \int_0^{2\pi} (1-r)r^2 \sin(\theta) dr d\theta d\phi \\ &= \int_0^1 (1-r)r^2 dr \times \int_0^\pi \sin \theta d\theta \times \int_0^{2\pi} 1 d\phi \end{aligned}$$

We then break down the integrals one by one such as

$$\begin{aligned} \int_0^1 (1-r)r^2 dr &= \frac{1}{12} \\ \int_0^\pi \sin \theta d\theta &= 2 \\ \int_0^{2\pi} 1 d\phi &= 2\pi \end{aligned}$$

By combining all these integrals, we get  $\int g = \frac{1}{12} \times 2 \times 2\pi = \frac{\pi}{3}$ .

So given  $\int f = q_{\text{detachment}}$  and  $\int f = \lambda \int g$ , we can deduce that  $\lambda = \frac{Q}{\int g} = \frac{3}{\pi}Q$ .

From (24) we finally get

$$f(\mathbf{p}) = \frac{3Q}{\pi} \left( 1 - \frac{\|\mathbf{p} - c\|}{R} \right) \quad (26)$$

, representing the rate of change on the evaluation function of the terrain surface.

The integration in the voxel space is out of the scope of this paper and a numerical solution is instead proposed in Section 7.